Title

Studies on the effects of particulate air pollution on gut microbiome and intestinal inflammation.

Author

Chang, Candace

Publication Date

2024

Peer reviewed|Thesis/dissertation

UNIVERSITY OF CALIFORNIA

Los Angeles

Studies on the effects of particulate air pollution on gut microbiome and intestinal inflammation.

A dissertation submitted in partial satisfaction of the requirements

for the degree Doctor of Philosophy

in Molecular Toxicology

by

Candace Chang

2024

ABSTRACT OF THE DISSERTATION

Studies on the effect of inhaled particulate air pollution
on intestinal inflammation and the gut microbiome.

by

Candace Chang
Doctor of Philosophy in Molecular Toxicology
University of California, Los Angeles, 2024
Professor Jonathan P. Jacobs, Co-Chair
Professor Jesus A. Araujo, Co-Chair

It is estimated that air pollution kills 7 million people every year, and an estimated 90% of the global population live in areas with high levels of pollutants exceeding the WHO recommendations. There is a strong body of literature demonstrating the adverse effects of ambient air pollution on human health. Air pollution is a varied mix of toxic gaseous and particulate compounds, but clinical and epidemiological evidence support the particulate phase compounds as main contributors to adverse health outcomes.

Our studies investigate a novel, potential mechanism linking ultrafine particles (UFPs) with intestinal inflammation. This study would be first to report not only the kinetics of microbiome effects, but also regional and longitudinal microbiome differences caused by UFP inhalation, a more physiologically relevant route of administration. We have assessed both the small intestine and colon, as well as both the mucosal and luminal microbiome. We combined controlled exposure using UFPs, the purportedly toxic component of PM, and inhalation to investigate the impact of air pollution on the gut microflora. Furthermore, our use of controlled chambers and re-aerosolization of PM selecting for UFP-range particulate matter represents significant advances in PM toxicity research. The present study leverages physiologically relevant UFP inhalation exposure, metabolic mouse models, acute and chronic IBD models, as well as microbiome bioinformatics analysis.

In this dissertation, Chapter 1 discusses the basis for the need to study toxicological effects of ultrafine air particulates and lay the foundation for the relationship between air pollution, the microbiome, and inflammatory bowel disease. Chapter 2 describes microbiome effects from UFP exposure on hyperlipidemic and normolipidemic mice as well as in-vitro confirmation of UFP bioactivity. Chapter 3 characterizes the effect of UFP exposure on two acute chemically-induced mouse models of colitis. Chapter 4 discusses microbiome and inflammatory effects of UFP exposure in a genetically-modified, spontaneous chronic IBD mouse model, IL-$10^{-/-}$. The work is a collaborative effort between both the Jacobs and Araujo labs at UCLA, with the assistance of the Engineering students from USC led by Dr. Constantinos Sioutas.

Our studies offer insight into a potential mechanism that may explain the role of air pollution as an environmental factor contributing to rising incidence of IBD. This study is

significant because we evaluate for the first time to our knowledge the effects of pulmonary UFP exposure on gut microbiome composition in IBD murine models.

The dissertation of Candace Chang is approved.

Oliver Hankinson

Srinivasa T. Reddy

Jesus A. Araujo, Committee Co-Chair

Jonathan P. Jacobs, Committee Co-Chair

University of California, Los Angeles

2024

"If we do not find anything pleasant, at least we will find something new."

-*Voltaire*

Reflecting on the twists and turns during my time at UCLA, I cannot relate to this more. We searched, at times not finding what we expected to see, yet our discoveries are novel, and the journey, meaningful.

I express gratitude to my Araujo and Jacobs laboratory colleagues, who not only enriched my scientific development but also provided a comforting sense of camaraderie. Thank you to my parents Chang Ying-Yen and Tung Long-Chu for their support and sacrifice, and for my family members and friends who have encouraged me along the way. I not only agree that the start to this journey came as a miracle, but also believe that it was completed by every strength which God provides.

Table of Contents

List of Figures ..... *ix*

List of Tables ..... *xiii*

ACKNOWLEDGEMENTS ..... *xiv*

Vita ..... *xv*

Chapter 1-BACKGROUND *1*

Ambient PM increases morbidity and mortality **1**

UFP exposure leads to adverse health effects. **2**

UFP exposure alters gut homeostasis and metabolism. **3**

References **7**

Chapter 2-PM and the Kinetics of Gut Microbiome Alteration *15*

Abstract **15**

Introduction **16**

Materials and Methods **18**

Results **24**

Discussion **27**

Figures **35**

Supplementary Material **42**

References **45**

Chapter 3- PM Inhalation in Models of Acute Colitis *66*

Abstract **66**

Introduction **66**

Materials and Methods **69**

Results **75**

Discussion **79**

Figures **83**

References **89**

Chapter 4- PM Inhalation in a Chronic Model of Intestinal Inflammation *97*

Introduction **97**

Materials and Methods **98**

Results **103**

Discussion **106**

Figures **109**
References **116**
Chapter 5-Conclusions and Future Directions ***120***

List of Figures

Figure 1A: Experimental design, *Ldlr*$^{-/-}$, *ApoE*$^{-/-}$ and C57BL/6 mice were exposed to UFPs

Figure 1B: Schematic of aerosol generation and exposure system.

Figure 1C: Particle size distribution in the exposures of *Ldlr*$^{-/-}$ and *ApoE*$^{-/-}$ mice.

Figure 1D: Chemical profile of the PM aerosol in *Ldlr*$^{-/-}$ and *ApoE*$^{-/-}$ exposures.

Figure 1E: Chemical profile of PM aerosol in C57BL/6 exposures.

Figure 2A: Shannon Index for assessment of alpha diversity in *Ldlr*$^{-/-}$mice after PM exposure.

Figure 2B: Beta diversity analysis of *Ldlr*$^{-/-}$mice exposed to PM.

Figure 2C: Jejunal microbial alpha and beta diversity analysis of *Ldlr*$^{-/-}$ mice.

Figure 3A: Enrichment of fecal microbes in *Ldlr*$^{-/-}$ mice after 1 week of subchronic PM exposure.

Figure 3B: Enrichment of fecal microbes in *Ldlr*$^{-/-}$ mice after 5 weeks of subchronic PM exposure.

Figure 3C: Enrichment of fecal microbes in *Ldlr*$^{-/-}$ mice after 10 weeks of subchronic PM exposure.

Figure 4A: Shannon Index for assessment of alpha diversity in *ApoE*$^{-/-}$mice after PM exposure.

Figure 4B: Beta diversity analysis of *ApoE*$^{-/-}$mice exposed to PM.

Figure 4C: Jejunal microbial alpha and beta diversity analysis of *ApoE*$^{-/-}$ mice.

Figure 5A: Enrichment of fecal microbes in *ApoE*$^{-/-}$ mice after 1 week of subchronic PM exposure.

Figure 5B: Enrichment of fecal microbes in *ApoE*$^{-/-}$ mice after 5 weeks of subchronic PM exposure.

Figure 5C: Enrichment of fecal microbes in *ApoE*$^{-/-}$ mice after 10 weeks of subchronic PM exposure.

Figure 6A: Shannon Index for assessment of alpha diversity in *C57BL/6* mice after PM exposure.

Figure 6B: Beta diversity analysis of *C57BL/6* mice exposed to PM.

Figure 6C: Jejunal microbial alpha and beta diversity analysis of *C57BL/6* mice.

Figure7A: Histological scores of jejunal and colonic tissue.

Figure 7B: mRNA levels of proinflammatory cytokines IL-1β, IFNγ, and TNF-α

Supplementary Figure 1A: Shannon index for ileal samples from Ldlr$^{-/-}$ mice

Supplementary Figure 1B: Beta diversity analysis of ileum from Ldlr$^{-/-}$ mice

Supplementary Figure 1C: Shannon index for ileal samples from ApoE$^{-/-}$ mice

Supplementary Figure 1D: Beta diversity analysis of ileum from ApoE$^{-/-}$ mice

Supplementary Figure 1E: Enrichment of ileal microbes in *ApoE*$^{-/-}$ mice

Figure 8: In-vitro MTT assay for cell viability and cytotoxicity

Figure 9A: Experimental design of DSS experiment.

Figure 9B: Exposure apparatus in DSS experiment

Figure 10A: Percent weight loss in DSS mice exposed to PM

Figure 10B: Disease activity index (DAI) in DSS mice exposed to PM

Figure 10C: Colon length of DSS-treated mice exposed to UFP

Figure 11A: Representative H&E stained colon tissues from each DSS exposure

Figure 11B: Violin plots of histological scores.

Figure 12A: Schematic of PM and TNBS exposure in 3 cohorts

Figure 12B: Chemical analysis of PM in TNBS experiment

Figure 12C: Exposure apparatus in TNBS experiment.

Figure 12D: PM re-aerosolization chamber

Figure 13A: Daily average percent weight change of the three TNBS cohorts.

Figure 13B: Colon length at time of euthanasia for the three cohorts.

Figure 13C: Representative colon histology images for the PM and FA groups from TNBS cohort 1 and violin plot showing histology scores.

Figure 14A: Experimental design of *IL-10*$^{-/-}$ mice exposures to PM

Figure 14B: Schematic of aerosol generation and exposure system.

Figure 14C: Chemical profile of the PM aerosol in *IL-10*$^{-/-}$ mice experiments 1 and 2.

Figure 15A: Histology scores of experiment 1 *IL-10*$^{-/-}$ mice exposed to PM

Figure 15B: Colon weight/length with weight of *IL-10*$^{-/-}$ mice exposed to PM (exp.1)

Figure 15C: *IL-10*$^{-/-}$ colon histology images from the UFP and FA groups. (exp.1)

Figure 16A: Histology scores of experiment 2 *IL-10*$^{-/-}$ mice exposed to PM

Figure 16B: Colon weight/length with weight of *IL-10*$^{-/-}$ mice exposed to PM (exp.2)

Figure 16C: *IL-10*$^{-/-}$ colon histology images from the UFP and FA groups. (exp.2)

Figure 16D: mRNA levels of proinflammatory cytokines in *IL-10*$^{-/-}$ colons(exp.2)

Figure 17A: Alpha diversity analysis of experiment 1 *IL-10*$^{-/-}$ mice

Figure 17B: Beta diversity analysis of experiment 1 *IL-10*$^{-/-}$ mice exposed to PM.

Figure 17C: Enrichment of fecal microbes in experiment 1 *IL-10*$^{-/-}$ mice

Figure 18A: Alpha diversity analysis of experiment 2 *IL-10*$^{-/-}$ mice

Figure 18B: Beta diversity analysis of experiment 2 *IL-10*$^{-/-}$ mice exposed to PM.

Figure 18C: Enrichment of fecal microbes in experiment 2 *IL-10*$^{-/-}$ mice

Figure 19A: Cecal microbiome data from experiment 1 *IL-10*$^{-/-}$ mice

Figure 19B: Colonic microbiome data from experiment 1 *IL-10*$^{-/-}$ mice

Figure 20A: Cecal microbiome data from experiment 2 *IL-10*$^{-/-}$ mice

Figure 20B: Colonic microbiome data from experiment 2 *IL-10*$^{-/-}$ mice

List of Tables

Table 1. Collection period and dominant emission sources for each PM batch in the DSS.

Table 2. Volume and concentration of samples used in cellular assays.

Table 3. Chemical profiles of various PM used in inhalation exposure experiments.

ACKNOWLEDGEMENTS

I am grateful for the opportunity to have been a student in the Interdepartmental Molecular Toxicology program. Dr. Michael Collins, the instructor of my first toxicology course as an undergraduate student, advised me on how to pursue an opportunity as a graduate student here at UCLA. I would like to thank Dr. Michael Kleinman from the UCI for providing me a unique opportunity to gain exposure to air pollution exposures during my gap year. I would like to thank our program director, Dr. Oliver Hankinson, Dr. Jesus A. Araujo, and Dr. Jonathan P. Jacobs for taking me as an inexperienced student to participate this unique project.

I would like to thank the members of the Jacobs lab and Microbiome Core. If microbiome analysis is the bread and butter of the lab, then it was members of the Jacobs lab taught me how to use a butter knife: Dr. Tien S. Dong, William R. Katzka, and Venu Lagishetty. I thank Dr. Nerea Arias and Dr. Zhou Yi, my sources of friendship, laughter, and comfort while navigating through experiments during the COVID-19 global pandemic. I appreciate my colleague, Dr. Julianne C. Yang, for serving as my example and reminder to always press forward during challenging times. I thank my undergraduate students Ananya Eeraveni, Srihari Prabu, and Jason Ereso, for volunteering their time to assist with the project. Also, thank you to the members of the Araujo lab, especially my colleagues Rajat Gupta and Allen Louie, whose presence alongside me in the air pollution exposure room were an indispensable encouragement. I am grateful for Jocelyn Castellanos and David M. Gonzalez for their help and for being always supportive and empathetic.

Including my undergraduate years, I will have been at UCLA for nearly 8 years. I will treasure the memories made and lessons learned, looking back on these times fondly as I move forward into the next phase of discovery.

Vita

Candace Chang

EDUCATION

Cerritos College June 2015
A.A. Biology
A.A. Chemistry

University of California, Los Angeles June 2017
B.S. Environmental Science
Concentration: Environmental Health

PUBLICATIONS

Chang C, Gupta G, Sedighian F, Louie, A, Gonzalez DM, Le C, Cho JM, Park S, Castellanos J, Ting T, Dong TS, et al: Subchronic Inhalation Exposure to Ultrafine Particulate Matter Alters the Intestinal Microbiome in Various Mouse Models. Environmental Research 2024.

Dong TS, Luu K, Lagishetty V, Sedighian F, Woo SL, Dreskin BW, Katzka W, **Chang C**, Zhou Y, Arias-Jayo N, Yang J et al: A High Protein Calorie Restriction Diet Alters the Gut Microbiome in Obesity. Nutrients 2020, 12(10).

Dong TS, Luu K, Lagishetty V, Sedighian F, Woo S-L, Dreskin BW, Katzka W, **Chang C,** Zhou Y, Arias-Jayo N, Yang J et al: The Intestinal Microbiome Predicts Weight Loss on a Calorie-Restricted Diet and Is Associated With Improved Hepatic Steatosis. Frontiers in Nutrition 2021, 8(420).

Dong TS, Luu K, Lagishetty V, Sedighian F, Woo S-L, Dreskin BW, Katzka W, **Chang C**, Zhou Y, Arias-Jayo N, Yang J et al: Gut microbiome profiles associated with steatosis severity in metabolic associated fatty liver disease. Hepatoma Research 2021, 7:37.

Zhou Y, Duan L, Zeng Y, Niu L, Pu Y, Jacobs JP, **Chang C**, Wang J, Khalique A, Pan K, Fang J, Jing B, Zeng D, Ni X. The Panda-Derived Lactobacillus plantarum G201683 Alleviates the Inflammatory Response in DSS-Induced Panda Microbiota-Associated Mice. Front Immunol. 2021 Dec 8;12:747045.

Dong TS, Katzka W, Yang JC, **Chang C**, Arias-Jayo N, Lagishetty V, Balioukova A, Chen Y, Dutson E, Li Z, Mayer EA et al: Microbial changes from bariatric surgery alters glucose-dependent insulinotropic polypeptide and prevents fatty liver disease. Gut Microbes. 2023 Jan 3; 15(1).

ABSTRACTS

Chang C, Gupta R, Sedighian F, Baek K, O'Donnell RP, Hsiai, T, Reddy, S, Navab M, Sioutas C, Lagishetty V et al: A Longitudinal Study of the Fecal Microbiome of Hyperlipidemic and Normolipidemic Mice over 10 weeks of Ultrafine Particle(UFP) Inhalation.

Chang C, Gupta R, Mousavi F, O'Donnell RP, Baek K, Gonzalez D, Castellanos J, Hsiai, T, Reddy, S, Navab M et al: Particulate Matter Exposure Alters the Luminal and Mucosal Gut Microbiome of ApoE-/- and Ldlr-/- Mice

AWARDS

NIEHS Pre-doctoral Training Grant (T32) in Molecular Toxicology 2021-2023

POSTERS AND PRESENTATIONS

"Particulate Matter Exposure Alters the Luminal and Mucosal Gut Microbiome of ApoE-/- and Ldlr-/- Mice", Society of Toxicology, San Diego, CA, March 29, 2022

"Chronic Inhalation Exposure to Particulate Matter Alters the Intestinal Microbiome", Society of Toxicology, Nashville, CA, March 22, 2023

Chapter 1-BACKGROUND

Ambient PM increases morbidity and mortality

According to the National Morbidity Air Pollution Study (NMMAPS) in 2000, the relationship between mortality and particulate matter (PM) was independent of gaseous components of air pollution, including NO_2, CO, and SO_2 (Samet et al. 2000). Studies in the US and in developing areas abroad show robust associations between acute and chronic PM exposure with respiratory as well as cardiovascular morbidity and mortality(Schwartz and Dockery 1992; Ostro et al. 1999; Katsouyanni et al. 2001). In addition, researchers are discovering wider effects of PM exposure in the form of reproductive threats(Suh et al. 2009) and neurological impairments(Ranft et al. 2009) from alteration of the hypothalamic-pituitary adrenal axis. While unique characteristics of PM make it difficult to pinpoint which component is responsible for its toxicity, published literature has supported size and composition as potential characteristics contributing to toxicity (Li et al. 2003; Tong et al. 2010). PM can be subcategorized by size thresholds: PM10 (aerodynamic diameter <10 micrometer[μm]) and fine particles or PM2.5 (<2.5μm diameter) and ultrafine particles, or UFPs (aerodynamic diameter <0.10μm). Almost weightless, UFPs represent 85-90% of $PM_{2.5}$ by number and more than 80% of total of industrial and urban ambient particle numbers (Diaz et al. 2019; Hussein et al. 2004). They are mainly generated in the urban environment, from tailpipes of vehicular sources due to incomplete exhaust combustion. UFPs also display biophysical and biochemical properties contributing to increased toxicity, thus promoting disease to a greater degree than pollution particles of a larger size (e Oliveira et al. 2019; Araujo and Nel 2009; Simkhovich, Kleinman, and Kloner 2008). Their surface area-to-size ratio allows for more chemical species such as semi-organic compounds, reactive transition metals, and polycyclic aromatic hydrocarbons to

coat their carbon core (Stone et al. 2017). The small size of the particle lends to the increased surface area relative to mass, further increasing biological activity (Kumar, Verma, and Srivastava 2013). Detrimental health effects may increase with decreasing particle size (Meng et al. 2013), and surface reactivity and aspect ratio, among other properties, permit UFPs greater access to peripheral airways and uptake into circulation, leading to oxidative stress and inflammation (Miller, Shaw, and Langrish 2012).

UFP exposure leads to adverse health effects.

Air pollution has potential to harm all bodily organs(López-Feldman et al. 2020), but PM and UFPs in particular have many disease-related effects. UFPs are able to penetrate alveoli in the lung to cause pulmonary deposition and systemic translocation, reaching different systems of the body. Emerging evidence suggests that UFP exposure is associated with risks of several diseases affecting the **i)** pulmonary, **ii)** central nervous, and **iii)** cardiovascular systems. **i)** UFP exposure leads to respiratory diseases when they travel to the terminal bronchiole and accumulate, causing tissue damage characteristic of centrilobular emphysema(Schraufnagel 2020). UFPs readily contact the alveoli and travel across epithelial cells. Rats exposed to UFPs showed more inflammation in their lungs compared to those exposed to $PM_{2.5}$.(Donaldson et al. 2002) Research on the inhaled UFP exposure in healthy and asthmatic human patients showed that inhalation of carbon UFPs had effects on pulmonary vascular function (Frampton 2007). A study conducted to elucidate the respective toxicities of fine and ultrafine particles in asthma-diseased human bronchial epithelial cells showed that UFP exposures led to significant increases in different inflammatory mediators while fine particulates failed to, or did so to a lesser degree(Sotty et al. 2019). This indicates a greater human inflammatory response from UFPs compared to fine particulates. **ii)** UFPs also appear in the brain 4 to 24 hours after inhalation and

published articles have reported effects in the central nervous system. Nano-sized particles may reach the brain by traveling up the olfactory nerves leading to cell injury in the central nervous system (Block and Calderón-Garcidueñas 2009; Oberdörster et al. 2004) and impaired autonomic function. Angiogenesis, cell migration, and other mRNA alterations may predispose to adverse health outcomes. Pups of pregnant mice intranasally exposed to black carbon nanoparticles developed long-term activation of astrocytes (Onoda, Takeda, and Umezawa 2017). **iii)** UFPs have been implicated in cardiovascular disease, and even a 2-hour UFP exposure led to electrocardiographic changes and elevated levels of C-reactive protein(CRP) in middle-aged, human subjects(Devlin et al. 2014). PM count has been associated with stroke, ischemic heart disease, and hypertension. Of note, UFPs impaired microvascular function and high blood pressure, but $PM_{2.5}$ and PM_{10} did not. UFP exposure also significantly increased hypertensive crises compared to $PM_{2.5}$ or PM_{10}. Long-term exposure to UFPs was associated with heightened cardiovascular disease (CVD) risk, measured by incidents of cerebrovascular disease, ischemic cerebrovascular accidents (CVA) and hemorrhagic CVA events(Aguilera et al. 2016). UFPs have been shown to be toxic in the context of an atherosclerosis mouse model: exposure to ambient UFPs reduced high-density lipoprotein (HDL) anti-inflammatory properties and increased oxidative stress in Apolipoprotein E-knockout (*$ApoE^{-/-}$)* mice (Araujo et al. 2008). Significantly larger lesions were also observed in the UFP-exposed $ApoE^{-/-}$ mice compared to the $PM_{2.5}$-exposed mice, supporting that UFP exposure is the most proatherogenic fraction of air pollution particles(Araujo et al. 2008).

UFP exposure alters gut homeostasis and metabolism.

Inhaled UFPs could also access the gastrointestinal (GI) tract, via mucociliary clearance, in a manner akin how it has been shown for larger particulates (Kreyling et al. 1999; Moller et al.

2004) or after translocation into the systemic circulation (Nemmar et al. 2002; Nemmar et al. 2001). This may affect gut pathophysiology. In fact, particulate pollutants may exert effects on intestinal epithelial cells leading to inflammation and enhanced immune activity. PM may also modulate the gut flora composition(Fouladi et al. 2020). The complex bacterial community of the human gut consists of more than 10^{12} cells, about 1000 species, and more than 6000 functional gene groups(Zhu, Wang, and Li 2010). Their numbers match human cells in an estimated 1:1 ratio and most of them belong in the *Firmicutes* and *Bacteriodetes* phyla(Abbott 2016). Intestinal microbes also hold a major pathophysiological role and a documented capacity to metabolize environmental chemicals, to regulate host immune responses, and to maintain gut health and homeostasis(Lozupone et al. 2012). In the context of many diseases also associated with PM exposure such as cancer(Lauka et al. 2019), metabolic(Turnbaugh et al. 2006) and CV diseases(Craciun, Marks, and Balskus 2014), alterations in the gut microbiome, termed 'dysbiosis', have been shown to play a critical role. Dysbiosis modulates host metabolism, immunity, and inflammatory response. Notably, the intestines play an important role in lipid metabolism, and may therefore be involved in the dyslipidemia and hypercholesterolemia that contribute to the risks of diseases such as atherosclerosis(Vaseghi et al. 2022; Fouladi et al. 2020). *Taken together, it can be postulated that a link exists between UFP effects on the gut and associated microbiota, and the reported association between UFP inhalation and cardiovascular disease.*

Existing data supports that gastrointestinal exposure to UFPs can impact the gut microbiome. UFP administration by oral gavage altered the intestinal microbiome of low-density lipoprotein receptor deficient mice (*Ldlr*$^{-/-}$) mice on a high fat diet, supporting the notion that UFP impacts the gut microbiome (Li et al. 2017). Specifically, exposure to UFPs by oral gavage

increased abundance in *Verrucomicrobia* but decreased *Actinobacteria, Cyanobacteria, and Firmicutes*. *Ldlr*$^{-/-}$ mice exposed to UFPs by gavage had altered microbiome and atherogenic lipid metabolites, along with macrophage and neutrophil infiltration in the ileum (Li et al. 2017). The microbiome of UFP-gavaged mice was also marked by reduced diversity (Li et al. 2017). A separate study exposing *Ldlr*$^{-/-}$ mice to inhaled UFPs for 10-weeks demonstrated that UFP inhalation caused changes in intestinal villous morphology along with changes in immune cell infiltrates in the villi (Li, Navab, et al. 2015). Inhalation of UFPs by *Ldlr*$^{-/-}$ also altered lipid metabolism and caused villus shortening (Li, Navab, et al. 2015). The mice exposed to inhaled UFPs showed an increase in oxidized fatty acids and lysophosphatidic acids (LPA). These UFP-mediated alterations and microbiome shifts suggest a gut toxicity mechanism in diseases associated with increased air pollution. Evidence showing the relevance of the microbiome in many diseases, along with understanding of UFP toxicity(Beamish, Osornio-Vargas, and Wine 2011), lead us to hypothesize that inhalation of UFPs promote dysbiosis of the gut microbiome. The development of inflammatory diseases is regulated by interactions between the environment, immune responses, genetics, and the microbiome (Hacquard et al. 2015; Lynch and Hsiao 2019). Reduced diversity of normal microbial ecology, driven by environmental and genetic factors, has been characterized in diseases (Mosca, Leclerc, and Hugot 2016; Petrov et al. 2017; Kriss et al. 2018) linked to PM such as colorectal cancer (Kaplan et al. 2010), IBD (Kaplan et al. 2010), and Parkinsons's (Kasdagli et al. 2019) Thus, we suggest a link between air pollution and an aberrant microbiome, which may augment disease susceptibility.

It remains unknown whether UFP inhalation changes the gut microbiome. Thus, we exposed distinct groups of recipients to UFP (<0.20μm) at both acute and subchronic time frames. Using 16S rRNA sequencing, we will determined the profile of the bacterial community

in the fecal matter, lumen and mucosa. In Chapter 2, we expose *ApoE*$^{-/-}$, *Ldlr*$^{-/-}$ and *C57BL/6J* mice to inhaled UFP and assess chemical and histological markers of inflammation as well as changes in the gut microbiome over time. In Chapter 3, two chemically-induced acute models of colitis were exposed to inhaled UFP and observed for clinical and histological markers. Finally in Chapter 4, we determined the effects of subchronic UFP inhalation exposure on the microbiome and intestinal inflammation in a chronic, genetic model of IBD.

References

Abbott, Alison. 2016. 'Scientists bust myth that our bodies have more bacteria than human cells', *nature*, 2016: 19136.

Aguilera, Inmaculada, Julia Dratva, Seraina Caviezel, Luc Burdet, Eric de Groot, Regina E Ducret-Stich, Marloes Eeftens, Dirk Keidel, Reto Meier, and Laura Perez. 2016. 'Particulate matter and subclinical atherosclerosis: associations between different particle sizes and sources with carotid intima-media thickness in the SAPALDIA study', *Environmental health perspectives*, 124: 1700-06.

Araujo, Jesus A, Berenice Barajas, Michael Kleinman, Xuping Wang, Brian J Bennett, Ke Wei Gong, Mohamad Navab, Jack Harkema, Constantinos Sioutas, and Aldons J Lusis. 2008. 'Ambient particulate pollutants in the ultrafine range promote early atherosclerosis and systemic oxidative stress', *Circulation research*, 102: 589-96.

Araujo, Jesus A, and Andre E Nel. 2009. 'Particulate matter and atherosclerosis: role of particle size, composition and oxidative stress', *Particle and fibre toxicology*, 6: 1-19.

Beamish, Leigh A, Alvaro R Osornio-Vargas, and Eytan Wine. 2011. 'Air pollution: An environmental factor contributing to intestinal disease', *Journal of Crohn's and Colitis*, 5: 279-86.

Block, Michelle L, and Lilian Calderón-Garcidueñas. 2009. 'Air pollution: mechanisms of neuroinflammation and CNS disease', *Trends in neurosciences*, 32: 506-16.

Craciun, Smaranda, Jonathan A Marks, and Emily P Balskus. 2014. 'Characterization of choline trimethylamine-lyase expands the chemistry of glycyl radical enzymes', *ACS chemical biology*, 9: 1408-13.

Devlin, Robert B, Candice B Smith, Michael T Schmitt, Ana G Rappold, Alan Hinderliter, Don Graff, and Martha Sue Carraway. 2014. 'Controlled exposure of humans with metabolic syndrome to concentrated ultrafine ambient particulate matter causes cardiovascular effects', *Toxicological Sciences*, 140: 61-72.

Diaz, E, K Mariën, L Manahan, and J Fox. 2019. 'Summary of health research on ultrafine particles', *Washington State Department of Health, Environmental Public Health Division, Office of Environmental Public Health Science*s: 334-454.

Donaldson, Ken, David Brown, Anna Clouter, Rodger Duffin, William MacNee, Louise Renwick, Lang Tran, and Vicki Stone. 2002. 'The pulmonary toxicology of ultrafine particles', *Journal of aerosol medicine*, 15: 213-20.

e Oliveira, Juliana Regis da Costa, Luis Henrique Base, Luiz Carlos de Abreu, Celso Ferreira Filho, Celso Ferreira, and Lidia Morawska. 2019. 'Ultrafine particles and children's health: Literature review', *Paediatric respiratory reviews*, 32: 73-81.

Fouladi, Farnaz, Maximilian J Bailey, William B Patterson, Michael Sioda, Ivory C Blakley, Anthony A Fodor, Roshonda B Jones, Zhanghua Chen, Jeniffer S Kim, and Frederick Lurmann. 2020. 'Air pollution exposure is associated with the gut microbiome as revealed by shotgun metagenomic sequencing', *Environment International*, 138: 105604.

Frampton, Mark W. 2007. 'Does inhalation of ultrafine particles cause pulmonary vasular effects in humans?', *Inhalation toxicology*, 19: 75-79.

Hacquard, Stéphane, Ruben Garrido-Oter, Antonio González, Stijn Spaepen, Gail Ackermann, Sarah Lebeis, Alice C McHardy, Jeffrey L Dangl, Rob Knight, and Ruth Ley. 2015. 'Microbiota and host nutrition across plant and animal kingdoms', *Cell host & microbe*, 17: 603-16.

Hussein, Tareq, Arto Puustinen, Pasi P Aalto, Jyrki M Mäkelä, Kaarle Hämeri, and Markku Kulmala. 2004. 'Urban aerosol number size distributions', *Atmospheric Chemistry and Physics*, 4: 391-411.

Kaplan, Gilaad G, James Hubbard, Joshua Korzenik, Bruce E Sands, Remo Panaccione, Subrata Ghosh, Amanda J Wheeler, and Paul J Villeneuve. 2010. 'The inflammatory bowel diseases and ambient air pollution: a novel association', *The American journal of gastroenterology*, 105: 2412.

Kasdagli, Maria-Iosifina, Klea Katsouyanni, Konstantina Dimakopoulou, and Evangelia Samoli. 2019. 'Air pollution and Parkinson's disease: a systematic review and meta-analysis up to 2018', *International journal of hygiene and environmental health*, 222: 402-09.

Katsouyanni, Klea, Giota Touloumi, Evangelia Samoli, Alexandros Gryparis, Alain Le Tertre, Yannis Monopolis, Giuseppe Rossi, Denis Zmirou, Ferran Ballester, and Azedine Boumghar. 2001. 'Confounding and effect modification in the short-term effects of ambient particles on total mortality: results from 29 European cities within the APHEA2 project', *Epidemiology*: 521-31.

Kreyling, WG, JD Blanchard, JJ Godleski, S Haeussermann, J Heyder, P Hutzler, H Schulz, TD Sweeney, S Takenaka, and A Ziesenis. 1999. 'Anatomic localization of 24-and 96-h particle retention in canine airways', *Journal of Applied Physiology*, 87: 269-84.

Kriss, Michael, Keith Z Hazleton, Nichole M Nusbacher, Casey G Martin, and Catherine A Lozupone. 2018. 'Low diversity gut microbiota dysbiosis: drivers, functional implications and recovery', *Current opinion in microbiology*, 44: 34-40.

Kumar, Sushil, Mukesh K Verma, and Anup K Srivastava. 2013. 'Ultrafine particles in urban ambient air and their health perspectives', *Reviews on environmental health*, 28: 117-28.

Lauka, Lelde, Elisa Reitano, Maria Clotilde Carra, Federica Gaiani, Paschalis Gavriilidis, Francesco Brunetti, Gian Luigi de'Angelis, Iradj Sobhani, and Nicola de'Angelis. 2019. 'Role of the intestinal microbiome in colorectal cancer surgery outcomes', *World journal of surgical oncology*, 17: 1-12.

Li, Ning, Constantinos Sioutas, Arthur Cho, Debra Schmitz, Chandan Misra, Joan Sempf, Meiying Wang, Terry Oberley, John Froines, and Andre Nel. 2003. 'Ultrafine particulate pollutants induce oxidative stress and mitochondrial damage', *Environmental health perspectives*, 111: 455-60.

Li, Rongsong, Kaveh Navab, Greg Hough, Nancy Daher, Min Zhang, David Mittelstein, Katherine Lee, Payam Pakbin, Arian Saffari, and May Bhetraratana. 2015. 'Effect of exposure to atmospheric ultrafine particles on production of free fatty acids and lipid metabolites in the mouse small intestine', *Environmental health perspectives*, 123: 34-41.

Li, Rongsong, Jieping Yang, Arian Saffari, Jonathan Jacobs, Kyung In Baek, Greg Hough, Muriel H Larauche, Jianguo Ma, Nelson Jen, and Nabila Moussaoui. 2017. 'Ambient ultrafine particle ingestion alters gut microbiota in association with increased atherogenic lipid metabolites', *Scientific reports*, 7: 1-12.

López-Feldman, Alejandro, Carlos Chávez, María Alejandra Vélez, Hernán Bejarano, Ariaster B Chimeli, José Féres, Juan Robalino, Rodrigo Salcedo, and César Viteri. 2020. 'Environmental impacts and policy responses to Covid-19: a view from Latin America', *Environmental & resource economics*: 1.

Lozupone, Catherine A, Jesse I Stombaugh, Jeffrey I Gordon, Janet K Jansson, and Rob Knight. 2012. 'Diversity, stability and resilience of the human gut microbiota', *nature*, 489: 220-30.

Lynch, JB, and EY Hsiao. 2019. 'Microbiomes as sources of emergent host phenotypes', *Science*, 365: 1405-09.

Meng, Xia, Yanjun Ma, Renjie Chen, Zhijun Zhou, Bingheng Chen, and Haidong Kan. 2013. 'Size-fractionated particle number concentrations and daily mortality in a Chinese city', *Environmental health perspectives*, 121: 1174-78.

Miller, Mark R, Catherine A Shaw, and Jeremy P Langrish. 2012. 'From particles to patients: oxidative stress and the cardiovascular effects of air pollution', *Future cardiology*, 8: 577-602.

Moller, Winfried, Karl Haussinger, Renate Winkler-Heil, Willi Stahlhofen, Thomas Meyer, Werner Hofmann, and Joachim Heyder. 2004. 'Mucociliary and long-term particle clearance in the airways of healthy nonsmoker subjects', *Journal of Applied Physiology*, 97: 2200-06.

Mosca, Alexis, Marion Leclerc, and Jean P Hugot. 2016. 'Gut microbiota diversity and human diseases: should we reintroduce key predators in our ecosystem?', *Frontiers in microbiology*, 7: 455.

Nemmar, Abderrahim, PH Mq Hoet, B Vanquickenborne, D Dinsdale, Maarten Thomeer, MF Hoylaerts, H Vanbilloen, Luc Mortelmans, and Benoit Nemery. 2002. 'Passage of inhaled particles into the blood circulation in humans', *Circulation*, 105: 411-14.

Nemmar, Abderrahim, H Vanbilloen, MF Hoylaerts, PHM Hoet, Alfons Verbruggen, and Benoit Nemery. 2001. 'Passage of intratracheally instilled ultrafine particles from the

lung into the systemic circulation in hamster', *American journal of respiratory and critical care medicine*, 164: 1665-68.

Oberdörster, Günther, Zachary Sharp, Viorel Atudorei, Alison Elder, Robert Gelein, Wolfgang Kreyling, and Christopher Cox. 2004. 'Translocation of inhaled ultrafine particles to the brain', *Inhalation toxicology*, 16: 437-45.

Onoda, Atsuto, Ken Takeda, and Masakazu Umezawa. 2017. 'Dose-dependent induction of astrocyte activation and reactive astrogliosis in mouse brain following maternal exposure to carbon black nanoparticle', *Particle and fibre toxicology*, 14: 1-16.

Ostro, Bart, Lauraine Chestnut, Nuntavarn Vichit-Vadakan, and Adit Laixuthai. 1999. 'The impact of particulate matter on daily mortality in Bangkok, Thailand', *Journal of the Air & Waste Management Association*, 49: 100-07.

Petrov, VA, IV Saltykova, IA Zhukova, VM Alifirova, NG Zhukova, Yu B Dorofeeva, AV Tyakht, BA Kovarsky, DG Alekseev, and ES Kostryukova. 2017. 'Analysis of gut microbiota in patients with Parkinson's disease', *Bulletin of experimental biology and medicine*, 162: 734-37.

Ranft, Ulrich, Tamara Schikowski, Dorothee Sugiri, Jean Krutmann, and Ursula Krämer. 2009. 'Long-term exposure to traffic-related particulate matter impairs cognitive function in the elderly', *Environmental research*, 109: 1004-11.

Samet, Jonathan M, Scott L Zeger, Francesca Dominici, Frank Curriero, Ivan Coursac, Douglas W Dockery, Joel Schwartz, and Antonella Zanobetti. 2000. 'The national morbidity, mortality, and air pollution study', *Part II: morbidity and mortality from air pollution in the United States Res Rep Health Eff Inst*, 94: 5-79.

Schraufnagel, Dean E. 2020. 'The health effects of ultrafine particles', *Experimental & molecular medicine*, 52: 311-17.

Schwartz, Joel, and Douglas W Dockery. 1992. 'Increased mortality in Philadelphia associated with daily air pollution concentrations', *Am Rev Respir Dis*, 145: 600-04.

Simkhovich, Boris Z, Michael T Kleinman, and Robert A Kloner. 2008. 'Air pollution and cardiovascular injury: epidemiology, toxicology, and mechanisms', *Journal of the american college of cardiology*, 52: 719-26.

Sotty, Jules, Guillaume Garcon, F-O Denayer, L-Y Alleman, Yara Saleh, Esperanza Perdrix, Véronique Riffault, Pierre Dubot, J-M Lo-Guidice, and Ludivine Canivet. 2019. 'Toxicological effects of ambient fine (PM2. 5-0.18) and ultrafine (PM0. 18) particles in healthy and diseased 3D organo-typic mucocilary-phenotype models', *Environmental research*, 176: 108538.

Stone, Vicki, Mark R Miller, Martin JD Clift, Alison Elder, Nicholas L Mills, Peter Møller, Roel PF Schins, Ulla Vogel, Wolfgang G Kreyling, and Keld Alstrup Jensen. 2017. 'Nanomaterials versus ambient ultrafine particles: an opportunity to exchange toxicology knowledge', *Environmental health perspectives*, 125: 106002.

Suh, Young Ju, Ho Kim, Ju Hee Seo, Hyesook Park, Young Ju Kim, Yun Chul Hong, and Eun Hee Ha. 2009. 'Different effects of PM10 exposure on preterm birth by gestational period estimated from time-dependent survival analyses', *International archives of occupational and environmental health*, 82: 613-21.

Tong, Haiyan, Wan-Yun Cheng, James M Samet, M Ian Gilmour, and Robert B Devlin. 2010. 'Differential cardiopulmonary effects of size-fractionated ambient particulate matter in mice', *Cardiovascular toxicology*, 10: 259-67.

Turnbaugh, Peter J, Ruth E Ley, Michael A Mahowald, Vincent Magrini, Elaine R Mardis, and Jeffrey I Gordon. 2006. 'An obesity-associated gut microbiome with increased capacity for energy harvest', *nature*, 444: 1027-31.

Vaseghi, Golnaz, Shaghayegh Haghjooy Javanmard, Kiyan Heshmat-Ghahdarijani, Nizal Sarrafzadegan, and Atefeh Amerizadeh. 2022. 'Comorbidities with Familial Hypercholesterolemia (FH): A Systematic Review', *Current Problems in Cardiology*: 101109.

Zhu, Baoli, Xin Wang, and Lanjuan Li. 2010. 'Human gut microbiome: the second genome of human body', *Protein & cell*, 1: 718-25.

Chapter 2-PM and the Kinetics of Gut Microbiome Alteration

Abstract

Exposure to ultrafine particles (UFPs) has been associated with multiple adverse health effects. Inhaled UFPs could reach the gastrointestinal tract and influence the composition of the gut microbiome. We have previously shown that oral ingestion of UFPs alters the gut microbiome and promotes intestinal inflammation in hyperlipidemic *Ldlr*$^{-/-}$ mice. Particulate matter $(PM)_{2.5}$ inhalation studies have also demonstrated microbiome shifts in normolipidemic C57BL/6 mice. However, it is not known whether changes in microbiome precede or follow inflammatory effects in the intestinal mucosa. We hypothesized that inhaled UFPs modulate the gut microbiome prior to the development of intestinal inflammation. We studied the effects of UFP inhalation on the gut microbiome and intestinal mucosa in two hyperlipidemic mouse models (*ApoE*$^{-/-}$ mice and *Ldlr*$^{-/-}$ mice) and normolipidemic C57BL/6 mice. Mice were exposed to PM in the ultrafine-size range by inhalation for 6 hours a day, 3 times a week for 10 weeks at a concentration of 300-350 μg/m^3. 16S rRNA gene sequencing was performed to characterize sequential changes in the fecal microbiome during exposures, and changes in the intestinal microbiome at the end. PM exposure led to progressive differentiation of the microbiota over time, associated with increased fecal microbial richness and evenness, altered microbial composition, and differentially abundant microbes by week 10 depending on the mouse model. Cross-sectional analysis of the small intestinal microbiome at week 10 showed significant changes in α-diversity, β-diversity, and abundances of individual microbial taxa in the two hyperlipidemic models. These alterations of the intestinal microbiome were not accompanied, and therefore could not be caused, by increased intestinal inflammation as determined by histological analysis of small and large intestine, cytokine gene expression, and levels of fecal

lipocalin. In conclusion, 10-week inhalation exposures to UFPs induced taxonomic changes in the microbiome of various animal models in the absence of intestinal inflammation.

Introduction

It is estimated that 90% of the global population live in areas with high levels of pollutants exceeding the 2021 WHO recommendations, and anthropogenic air pollution exposure causes 5.5 million premature deaths each year (World Health Organization 2021; Lelieveld et al. 2019). Although some air pollution health effects are driven by gaseous components, epidemiological evidence indicates that mortality is largely driven by the particulate matter (PM) components (Samet et al. 2000). Thus, studies in the US and other countries show robust associations between acute and long-term PM exposure with respiratory as well as cardiovascular morbidity and mortality (Schwartz and Dockery 1992; Ostro et al. 1999; Katsouyanni et al. 2001; Miller et al. 2007). While it has been difficult to pinpoint the specific PM components that are responsible for its toxicity, it appears that both size and composition are important determinants of toxicity (Li et al. 2003; Tong et al. 2010; Araujo 2011). Almost weightless, ultrafine particles (UFPs), with an aerodynamic diameter <0.1 μm, constitute 85-90% of $PM_{2.5}$ (PM< 2.5μm), and more than 80% of total industrial and urban ambient particles by number (Diaz et al. 2019; Hussein et al. 2004), mainly generated in the urban environment from tailpipes of vehicular sources due to incomplete exhaust combustion.

UFPs have the potential to harm all bodily organs (López-Feldman et al. 2020). They can penetrate alveoli in the lung and translocate into the circulation to reach systemic tissues in the body. Inhaled UFPs could also access the gastrointestinal (GI) tract, via mucociliary clearance, in a manner akin to how it has been shown for larger particulates (Kreyling et al. 1999; Moller et al. 2004) or after translocation into the systemic circulation (Nemmar et al. 2002; Nemmar et al.

2001). GI exposure to UFPs may affect the complex bacterial community lining of the human gut, consisting of more than $4x10^{13}$ cells, about 5000 species, and more than 20 million functional gene groups (Pasolli et al. 2019; Sender, Fuchs, and Milo 2016). Intestinal microbes have the capacity to metabolize environmental chemicals, regulate host immune responses, modulate metabolism, and maintain gut health and homeostasis (Lozupone et al. 2012). Alterations in the gut microbiome associated with disease phenotypes, termed 'dysbiosis', have been demonstrated to play a critical role in many diseases also associated with PM exposure, including metabolic disorders (Turnbaugh et al. 2006), cardiovascular diseases (Craciun, Marks, and Balskus 2014), and cancer (Lauka et al. 2019). Li et al have reported that UFPs promote intestinal inflammation in a hyperlipidemic mouse model where exposure to ambient UFPs shortened the villi of the small intestine, and increased the average number of macrophages per villus in low-density lipoprotein null (*Ldlr*$^{-/-}$) mice (Li, Navab, et al. 2015). In addition, Li et al also showed that GI exposure to UFP by orogastric gavage altered the composition of the cecal microbiome in *Ldlr*$^{-/-}$ mice (Li et al. 2017), suggesting the development of dysbiosis of the gut microbiome with inflammatory effects in the GI tract. However, intestinal inflammation per se can induce changes in gut microbiome composition (Lupp et al. 2007), raising the possibility that gut microbiome changes could be due to intestinal inflammatory effects rather than UFP exposure.

We hypothesized that inhalation of UFPs alters gut microbiota composition prior to the development of intestinal inflammation. To test this hypothesis, we characterized the effects of subchronic inhalation exposure to UFPs on fecal microbiome profiles at 3 time points after the onset of exposures, and on the intestinal microbiome profiles at the end of the exposure protocol when we also assessed histological changes in the intestines of three distinct mouse models, two

hyperlipidemic (*Ldlr*$^{-/-}$ mice fed a high fat diet and *ApoE*$^{-/-}$ mice on a chow diet) and one normolipidemic (C57BL/6 mice fed a chow diet).

Materials and Methods

Animal Subjects

Male *Ldlr*$^{-/-}$ mice (6-8 weeks-old) and *ApoE*$^{-/-}$ mice (5-7 weeks-old) were purchased from Jackson Laboratories followed by at least 1 week of acclimation. C57BL/6 mice were from our colonies of myeloid-specific heme oxygenase 1 (HO-1) knockout (Zhang et al. 2018) and myeloid-specific nuclear factor, erythroid derived 2, like 2 (Nrf2) knockout (Bhetraratana 2018), floxed for the HO-1 and Nrf2 genes, respectively, but negative for the LysM-Cre recombined gene, and therefore, with normal expression of those genes. *Ldlr*$^{-/-}$ mice were fed an irradiated 42% high fat diet (Envigo TD.88137), high in sucrose (34% by weight), with saturated fat >60% of total fat, and 0.2% cholesterol. *ApoE*$^{-/-}$ mice and C57BL/6 mice were fed autoclaved chow diet. Food and autoclaved water were provided ad libitum except during the exposures. Mice were housed in autoclaved shoe-box type cages with cornhusk bedding. Our research protocol was conducted in compliance with the Animal Research Committee and Institutional Animal Care and Use Committee (*IACUC*) at the University of California, Los Angeles (UCLA), and performed in coordination with the Division of Laboratory Animal Medicine (DLAM) at UCLA.

Collection of Particulate Matter

Ambient $PM_{2.5}$ was collected on PTFE membrane filters (20 × 25 cm, 3.0 μm pore size, PALL Life Sciences, USA) at the University of Southern California's Particle Instrumentation Unit (PIU) using a high-volume sampler (with a flow rate of 250 lpm) connected to a $PM_{2.5}$ pre-impactor for separation and collection of $PM_{2.5}$ between February-May 2019 for exposures of

the *Ldlr*$^{-/-}$ and *ApoE*$^{-/-}$ mice, and December-January 2020 for exposures of C57BL/6 mice. Each filter was divided into 32 pieces and extracted in Milli-Q water using 1 hour of sonication. The amount of extracted PM via sonication was obtained by subtracting the pre-extraction from the post-extraction weights of the filters using a high precision (±0.001 mg) microbalance (MT5, Mettler Toledo Inc., Columbus, OH). Further details regarding PM collection and extraction have been reported by us (Soleimanian, Taghvaee, and Sioutas 2020; Taghvaee et al. 2019).

PM Inhalation Exposures

Inhalation exposures were conducted at the Air Pollution Inhalation Exposure Facility (APIEF) located within the animal vivarium (5V) in the Center for Health Sciences building at UCLA. Following at least 1 week of acclimatation, mice from the *Ldlr*$^{-/-}$, *ApoE*$^{-/-}$ and C57BL/6 groups were 12 weeks, 8 weeks and 18-20 weeks of age, respectively, at the onset of the exposure protocol, consisting of 6-hour exposure sessions, 3 days/week for 10 weeks, intercalated with non-exposure days (Fig. 1A). For the exposures, mice were placed on exposure chambers that housed up to 22 mice/cage, and subjected to exposures to re-aerosolized PM or filtered air (FA). A compressor pump built at the University of Southern California (USC) Viterbi School of Engineering pushed HEPA-filtered air into a Hope nebulizer (B&B Medical Technologies, USA) to re-aerosolize the PM-containing solutions into the ultrafine size range (Taghvaee et al. 2019) (Fig. 1B). A vacuum pump drew the stream of re-aerosolized PM through a silica gel diffusion dryer (Model 3620, TSI Inc., USA) followed by Po-210 neutralizers (Model 2U500, NRD Inc., USA) to remove the excess water content and electrical charges of the particles, respectively. This air stream entered the animal exposure chamber with a flow rate of 2.5 lpm. Before the start of each exposure session, a scanning mobility particle sizer (SMPS, Model 3936, TSI Inc., USA) was connected to a condensation particle counter (CPC, 4 Model

3022A, TSI Inc., USA) to measure the particle number concentration (PNC) distribution of re-aerosolized particle in the range of 0.013-0.76 μm as well as an optical particle sizer (OPS, Model 3330, TSI Inc., USA) for the size range of 0.3-2.5 μm (Fig. 1C). The mode diameter was ~50 nm with the total PNC of 368024 #/cm. Mass concentration was assessed by a TSI Dustrak, with a target average concentration of 300-350 □g/m^3. In parallel, the re-aerosolized particles were collected on PTFE (Teflon) and Quartz (37-mm, Pall Life Sciences, 2-μm pore, Ann Arbor, MI) filters for chemical characterization. For FA exposures, ambient air was passed through a HEPA-filter and drawn into it by a vacuum pump (Fig. 1B). Body weights and fecal pellets were recorded and collected weekly throughout the 10-week exposure. Tissues were harvested at the end of the protocol after euthanasia under isoflurane anesthesia.

PM Characterization

Aliquots of PM slurry samples were chemically analyzed to determine total organic content (Veenstra et al.), water-soluble inorganic ions, and metal elements at the Wisconsin State Laboratory of Hygiene (WSLH). One Teflon filter was extracted with a mixture of ultrapure (Milli-Q®) water and ethanol (5 mL: 0:15 mL, respectively) for analysis of inorganic anions [ammonium ($NH+$), nitrate ($NO-$), and sulfate ($SO2-$)] by ion chromatography using a Dionex Model DX-500 Ion Chromatograph (Herner, Green, and Kleeman 2006). PM-bound metals and trace elements were analyzed by magnetic-sector inductively coupled plasma mass spectroscopy in a Thermo Scientific ELEMENT2 High-Resolution ICP-MS unit using a microwave-assisted digestion employing a mixed acid made of nitric acid, hydrochloric acid, and hydrofluoric acid (Lough et al. 2005). The complete dissolution of metals present in aerosols was achieved by microwave-assisted acid digestion in Teflon bombs. An automated, temperature- and

pressure-regulated, trace analysis microwave system (Milestone Ethos+) was used for the digestion (Zhang et al. 2008).

Sample Collection, DNA Extraction and 16S rRNA Gene Sequencing

Mice were euthanized 18 hours after the last exposure, following 12 hours of fasting. Intestines were harvested and divided by region for collection of jejunal and ileal mucosal samples as previously described (Jacobs et al. 2017). Briefly, mucosal samples were obtained by incubating rinsed tissue pieces in media with dithiothreitol at 37°C in a shaker followed by centrifugation at 2000x g for 15 min at 4°C. Mucosal sample pellets were resuspended in 250-300 µl of DNA/RNA shield^{TM} and stored at-80°C until the moment of analysis. At that point, samples thawed from -80°C, underwent DNA extraction using the ZymoBIOMICS DNA Microprep Kit or ZymoBIOMICS 96 DNA Kit (Zymo Research, Irvine, CA, USA) according to the manufacturer's instructions. Sequencing of the 253 base pair V4 region of 16S ribosomal RNA gene was performed using the Illumina MiSeq for longitudinal fecal samples and cross-sectional intestine samples from C57BL/6 mice, and the Illumina NovaSeq 6000 for cross-sectional *Ldlr*$^{-/-}$ and *ApoE*$^{-/-}$ intestinal samples. Sequenced data were processed into amplicon sequence variants (ASVs), and assigned taxonomy using the DADA2 pipeline (Callahan et al. 2016) in R with the SILVA 132 database. Sequence depth ranged from 7,789 to 646,362 reads/sample with a mean of 119,457.

Microbiome Diversity Analysis

Alpha diversity was assessed using the Shannon index, a metric of species evenness and richness, with data rarefied to a sequencing depth of 5,000 in each sample subset (Jacobs et al. 2016). The data was fitted to linear mixed effects models in R studio and statistical analyses was performed using the lmer function. Exposure group, timepoint, and their interaction were

included as fixed effects in all models. Mouse ID was treated as a random effect for longitudinal fecal microbiome data and cage as a random effect for tissue microbiome data.

For beta diversity and differential abundance analysis, data were filtered to remove ASVs that were present in less than 25% of all samples. Beta diversity was assessed using the Bray-Curtis dissimilarity matrix to identify microbiome compositional differences between the different treatment groups (PM vs. FA) and in the longitudinal fecal pellet data (Week 0, 1, 5, and 10). Statistical analyses was performed using permutational multivariate analysis of variance (PERMANOVA) implemented in the Adonis package in R with treatment, timepoint (with week 0 as the baseline), and their interaction as fixed effects and cage or mouse ID as strata for permutations. Differences in taxa abundances between exposure groups were analyzed using MaAsLin2 in R (Version 1.4.1106, Vienna, Austria) with treatment and timepoint as fixed effects, and cage or mouse ID as a random effect (Mallick et al. 2021). *p*-values were adjusted for multiple comparisons using the Benjamin–Hochberg method. Significance threshold was set at *q-value<0.10.*

Histological Scoring

A ~1.5 cm piece of the middle of the jejunum and colon were cut and fixed in 10% phosphate buffered formalin and then transferred to 70% ethanol. The cassettes were sent to the Translational Pathology Core Laboratory (TPCL) at UCLA for embedding in paraffin, sectioning and staining with hematoxylin and eosin (H&E). Sections of the jejunum were scored to assess epithelial and mucosal architectural changes as well as the severity and extent of immune cell infiltration using a published scoring system with two subscales (Erben et al. 2014). Thus, inflammatory cell infiltrates were scored 0-4 based on severity ranging from mild to marked, and on extent ranging from only the mucosa to transmural involvement in the first jejunum subscale.

For the second jejunum subscale, changes in intestinal architecture were scored 0-4 based upon epithelial changes from mild to marked hyperplasia and goblet cell loss as well as mucosal architecture, from mild villous blunting to villous atrophy and ulcerations. The sum of both subscales yielded a final score 0-8 were scored separately (Erben et al. 2014). Inflammation in colons were scored from 0-12 using a scoring system with two subscales as well. A first colon subscale scored inflammation from 0-6 with severity ranging from normal to severe inflammatory cell infiltrates, and a second colon subscale (0-6) was based on extent ranging from only the mucosa to transmural involvement(Katakura et al. 2005; Jacob et al. 2018). In the first subscore, a score of 1 was assigned for hyperproliferation, irregular crypts, and goblet cell loss, 1.5 for mild crypt loss (10-25%), 2 for moderate crypt loss (25%-50%), 2.5 for severe crypt loss(50-75%), 3 severe crypt loss (75-90%), 4 for complete crypt loss, 5 for ulcers <10 crypts wide, and 6 for ulcers >10 crypts wide. For the second subscale, changes in intestinal architecture were scored from 0-6 by adding the scores from each region of the intestinal wall. The musosa was scored from 0-3 (0: Normal, 1: Mild, 2: Modest, 3: Severe), the submucosa was scored from 0-2 (0: Normal, 1: Mild to modest, 2: Severe), and the mucosa/serosa was scored 0-1 (0: Normal, 1: Moderate to severe).

Fecal Lipocalin ELISA

Fecal mouse lipocalin-2 (pg/ml) was measured in stool samples from *Ldlr*$^{-/-}$ and *ApoE*$^{-/-}$ mice at week 10 using the DuoSet® Mouse Lipocalin-2/NGAL and Ancillary Reagent Kit 2 (R&D Systems, Minneapolis, MN, USA) according to the manufacturer's instructions.

RT-qPCR

~1.5 cm pieces of the midsection of the jejunum and colon were cut and fixed in RNAlater®. The Qiagen RNAeasy Mini Kit was used to extract RNA from thawed intestinal

sections according to the manufacturer's instructions. A total of 200 nanograms of extracted RNA in each sample was used for reverse-transcribed cDNA synthesis using the Applied Biosystems High-Capacity cDNA Reverse Transcription Kit according to the manufacturer's instructions (Applied Biosystems catalog# 4368814). The mRNA expression of target genes was detected using Applied Biosystems TaqMan Fast Advanced Master Mix (catalog# 4444557) and TaqMan probes for β-actin (Mm02619580_g1), IL-1β (Mm00434228_m1), IFNγ (Mm01168134_m1), and TFNα (Mm00443258_m1). Each sample and target gene for qPCR was conducted in triplicate and each reaction was performed in a final volume of 10µL including 2.5µL of cDNA 0.5µL of the respective probe, 5µL of Master mix, and 2µL of water. TheLightCycler 480 program consisted of an initial pre-incubation warm-up cycle to 95°C for 10 minutes, followed by 45 cycles of amplification (95°C for 10 s, 60°C for 30 s, and 72°C for 1 s) and a cooling cycle at 40°C for 30 s. Quantitative PCR was performed in a LightCycler 480 (Roche Diagnostics) and gene expression was analyzed using the delta-delta Ct (DDCt or ddCt) method. TaqMan probes were validated to ensure that probes were efficiently doubling with every PCR cycle (data not shown).

Statistical Analyses

PM characterization data are shown as means. Alpha and beta diversity are shown by violin and 2D scatter plots; differential abundance is shown by dot plots. All microbiome data were analyzed as indicated above. Data from histological scoring and fecal lipocalin data were shown by violin plots and analyzed by Mann-Whitney U-test in R studio (threshold *p-value* <0.05) for comparison between PM and FA groups.

Results

Fecal microbiome changed after subchronic inhalation exposure to PM

Subchronic UFP inhalation was modeled by exposing mice to ambient PM collected at an urban site for 10 weeks, then resuspended in the ultrafine size range in a closed exposure chamber as described in the Methods. Three cohorts of mice underwent exposures for 6 hours/day, three days per week for 10 weeks, including two genetic mouse models for hyperlipidemia, *Ldlr*$^{-/-}$ mice fed a high-fat diet and *ApoE*$^{-/-}$ mice fed a chow diet, and normolipidemic C57BL/6 mice on a chow diet (Fig. 1A). The greatest fraction of extracted PM for the exposures to *Ldlr*$^{-/-}$ and *ApoE*$^{-/-}$ mice was total carbon (~48%), followed by inorganic ions (~33%), and metal elements (~19%) (Fig. 1D). In the exposure campaign with C57BL/6 mice, the chemical analysis showed inorganic ions (~43%), followed by total carbon (~39%), and metal elements (~18%) (Fig. 1E). In total, 63 mice were exposed to PM vs FA: 22 *Ldlr*$^{-/-}$ mice (n=11/group), 22 *ApoE*$^{-/-}$ mice (n=11/group), and 19 C57BL/6 mice (n=9-10/group). In all three cohorts, fecal samples were collected at baseline and weeks 1, 5, and 10 of exposures to assess the kinetics of PM effects on the microbiome. Jejunum and in some cases ileum as well, were collected after euthanasia to assess the small intestinal microbiome at the end of the protocol. All samples underwent microbiome characterization by 16S rRNA gene sequencing.

Longitudinal analysis of fecal samples from *Ldlr*$^{-/-}$ mice showed that subchronic exposure to UFPs significantly altered the microbiome. Microbial alpha diversity was significantly increased at week 10 in comparison with baseline as determined by the Shannon index ($p=0.008$) but not in the previous time points, week 1 or week 5 (Fig. 2A). Although there were no significant shifts in microbiome composition by beta diversity analysis at any time point (Fig. 2B), there were significant differences in microbial abundances at all time points by testing of differential abundance at the level of amplicon sequence variants (ASVs), which roughly corresponds to species (Fig. 3). Interestingly, there was an increase in the number of ASVs with

an increasing duration of exposures. Thus, while there was enrichment of only 1-3 ASVs at weeks 1 and 5 (Fig. 3A&B), the enrichment was of 7 ASVs at week 10, including a member of the Oscillospirales order, Lachnospirales order, and of the genus *Lachnoclostridium*.

In *ApoE*$^{-/-}$ mice, although there were no differences in microbial alpha or beta diversity (Fig. 4A&B), there were two ASVs that differed between the PM and FA groups at week 1 (Fig. 5A), four ASVs at weeks 5 and six ASVs at week 10 (Fig. 5B&C), including depletion at both timepoints of the one member of the Lachnospiraceae family in the *K4A136* group. Depletion of an ASV in the Clostridia order was also seen at both weeks 5 and 10 (Fig. 5B&C).

As microbiome changes with PM exposure could have been influenced by the hyperlipidemia in both *Ldlr*$^{-/-}$ and *ApoE*$^{-/-}$ mice, and/or high fat diet feeding in *Ldlr*$^{-/-}$ mice, we also studied PM effects on normolipidemic mice from the same C57BL/6 background. While there were no significant differences in alpha diversity (Fig. 6A) or differentially abundant ASVs at any time point, beta diversity was significantly different between PM and FA groups at week 10 ($p=0.02$) (Fig. 6B).

Cross-sectional changes in the small intestinal microbiome

Since fecal samples largely represent the colonic microbiome, we analyzed small intestinal samples from jejunum and ileum upon euthanasia at week 10 to assess whether PM exposures induced distinct effects in these regions. *Ldlr*$^{-/-}$ mice showed a significant difference in beta diversity in both jejunum ($p=0.02$, Fig. 2C) and ileum ($p=0.003$, Supplementary Fig. 1B) in spite of no significant effects on alpha diversity (Fig. 2C) or differentially abundant ASVs in either region. On the other hand, *ApoE*$^{-/-}$ mice showed a statistically significant increase in alpha diversity in the jejunum ($p=0.006$, Fig. 4C) and borderline significant changes in the ileum ($p=0.07$, Supplementary Fig. 1C) where there was a significant difference in beta diversity as

well (*p=0.008*, Supplementary Fig. 1D). In addition, PM induced significant changes in microbial abundance. Indeed, the Muribaculaceae ASV was upregulated while a Lachnospiraceae ASV was downregulated in the PM group as compared with FA group in both (Fig 4C) and ileal microbiomes (Supplementary Fig. 1E). Interestingly, while PM exposure in C57BL/6 mice led to borderline changes in jejunal beta diversity (*p=0.06*, Fig. 6C), there were no significant effects on alpha diversity (Fig. 6C) or microbial abundance.

Assessment for intestinal inflammation

Our previous studies have shown that UFP exposures by inhalation (Li, Navab, et al. 2015) or oral gavage (Li et al. 2017) led to intestinal inflammation in *Ldlr-/-* mice although we could not determine whether intestinal inflammatory effects preceded or followed changes in the composition of gut microbiota. We performed double-blind histological scoring of the jejunums and colons. To our surprise, there were no differences in mucosal architecture or extent of inflammation judged by villous blunting, goblet cell loss, and ulcerations between the PM and FA groups in none of the hyperlipidemic models or normolipidemic mice (Fig. 7A). Thus, the jejunums of *ApoE*$^{-/-}$ mice, *Ldlr*$^{-/-}$ mice, and normolipidemic C57BL/6 mice exhibited similar histological scores between the PM and FA groups. Likewise, the colon histological samples showed no differences between PM and FA groups in the *ApoE*$^{-/-}$, *Ldlr*$^{-/-}$, and C57BL/6 mice either. In addition, mRNA levels of proinflammatory cytokines (IL-1β, IFNγ, TFNα) were similar between PM and FA-exposed mice in the jejunum and colon of mice from the three cohorts (Fig. 7B). Consistently, ELISA measurement of lipocalin-2, a biomarker of intestinal inflammation, in fecal pellets collected at week 10 showed no significant differences between the PM and FA-exposed mice in the two hyperlipidemic models (Supplementary Fig. 2).

Discussion

This study is the first to report on the effects induced by inhalation of ambient ultrafine PM on the intestinal microbiome, extending our previous report where subchronic UFP oral exposure led to microbiome changes together with intestinal inflammation in *Ldlr*$^{-/-}$ mice fed a high fat diet (Li et al. 2017). In the current study, subchronic PM inhalation resulted in changes in the fecal and small intestinal microbiomes of 3 animal models, hyperlipidemic *Ldlr*$^{-/-}$ and *ApoE*$^{-/-}$mice as well as normolipidemic C57BL/6 mice that varied across mouse models and by the location of the tissue samples, in the absence of intestinal inflammation.

We found that 10-week exposure to ultrafine PM by inhalation, a physiologically relevant route of PM exposure, induced changes in the intestinal microbiome across *Ldlr*$^{-/-}$, *ApoE*$^{-/-}$, and C57BL/6 mice. Changes in fecal microbiome diversity and/or composition became consistently evident between weeks 5 and 10 in all three mouse models. This indicates that subchronic exposure was required for inhaled PM in the ultrafine-size range to induce changes in gut microbiome composition under the conditions of our experimental setup. While microbiome changes were induced across all 3 mouse models, they differed in whether they showed a microbiome effect by analysis of alpha diversity, beta diversity or differential abundance of taxa. A few individual taxa were identified as significantly altered as short as within 1 week of exposure, increasing in number as the study progressed over time (Figs. 3&5) and without plateauing, which suggests that changes in differential abundance of taxa might have further increased, had the exposures continued for additional weeks. Our data is consistent with the study of Li et al where inhalation of diesel exhaust particles (DEPs) caused changes in gut microbiome composition. However, they observed increased epithelial injury scores in the colon (Li, Sun, et al. 2019) which was absent in our study. DEPs have different chemical characteristics from ambient PM and traffic emissions (Farahani, Pirhadi, and Sioutas 2021) and while they are

enriched in UFPs, they also include particles of bigger size. Our current study demonstrates that inhalation of particles, exclusively in the ultrafine-size range, is capable of inducing changes in gut microbiota composition.

Previous studies showing UFP effects on gut microbiome and/or intestinal inflammation have not established whether dysbiosis is a driver of inflammation. The gut microbiome plays an important role in intestinal homeostasis and has been shown to produce metabolites involved in immune signaling (McHardy et al. 2013). However, the immune system is also able to shape microbiome composition and function; consequently, it is often unclear whether microbiome changes in models with increased intestinal inflammation represent a cause or consequence of inflammation (Gevers et al. 2014; Lepage et al. 2011). Importantly, our data indicates that changes in the microbiome occurred with PM inhalation exposure in the absence of intestinal inflammation and therefore, they could not be a consequence of inflammation. We cannot rule out, however, if longer exposures beyond 10 weeks could have resulted in increased intestinal inflammation in which case, microbiome changes would precede rather than follow inflammatory changes, suggesting the possibility of causality.

We did not observe evidence of increased intestinal inflammation between the PM and FA groups in either hyperlipidemic or normolipidemic mice by histological scoring, inflammatory biomarker fecal lipocalin, or cytokine gene expression. These results differ from our previous study which demonstrated UFP-induced villous shortening in the small intestine of *Ldlr*$^{-/-}$ mice, fed a HFD and exposed to UFP under similar conditions as in the current study (exposure mass 360+/- 25 μg/m^3, 5 hours/day, 3 days/week for 10 weeks) (Li, Navab, et al. 2015). Interestingly, the *Ldlr*$^{-/-}$ model was more sensitive to PM-induced changes in alpha diversity as compared to the other two mouse models but these changes observed at week 10

were not accompanied by inflammatory effects. While the PM employed in our study included a mixture of organic compounds and heavy metals (Fig 1D) that was broadly consistent with previous studies using PM collected at the same location (Li, Navab, et al. 2015; Verma et al. 2009), there were differences in PM composition which might have played a role in the ability or not to induce intestinal inflammation. Thus, while Sulfur was the 2nd most abundant PM element in the exposures for *Ldlr*$^{-/-}$ and *ApoE*$^{-/-}$ mice (Fig. 1D), it was three times less abundant by mass than in the studies by Li et al. and Verma et al. , where it was the most abundant PM element (Li, Navab, et al. 2015; Verma et al. 2009). Sulfur can be metabolized by gut bacteria to produce hydrogen sulfide which has been shown to promote intestinal inflammation (Medani et al. 2011). Therefore, the decreased amount of Sulfur in our study could be responsible, at least in part, for the lack of intestinal inflammation.

We found that although changes in microbiome composition induced by PM were different in each mouse model, hyperlipidemia appears to be an important determinant. Indeed, testing of differential abundance revealed that some taxa were significantly changed by PM inhalation in the two hyperlipidemic models but not in normolipidemic mice. The most consistent change in both *Ldlr*$^{-/-}$ and *ApoE*$^{-/-}$ models was the enrichment of a *Lachnoclostridium* ASV in PM-exposed mice at week 10. Interestingly, *Lachnoclostridium saccharolyticum* increased by choline treatment in *ApoE*$^{-/-}$ mice has been shown to promote TMAO (or trimethylamine N-oxide), a metabolite positively associated with inflammation (Cai et al. 2022). Increased *Lachnoclostridium* has also been associated with an inflammatory gene expression profile in head and neck squamous cell carcinoma samples (Yilmaz et al. 2022). On the contrary, Li et al showed that orogastric administration of UFP to *Ldlr*$^{-/-}$ mice decreased *Lachnoclostridium saccharolyticum* instead, by ~10 fold in the luminal cecum together with

increased gut inflammation (Li et al. 2017). Therefore, it is unlikely that increased *Lachnoclostridium,* in general, could have been the driver for increased inflammation then. Greater taxonomic resolution coupled with functional analyses may be required to determine the specific species of *Lachnoclostridium* that are affected by PM and which ones, if any, could exert an inflammatory role. Interestingly, microbiome analysis in our previous study (Li et al. 2017) also showed an increase in Clostridiaceae and Clostridiales, bacteria which have been associated with increased inflammation (Muñiz Pedrogo et al. 2019; Shen 2012) and were not increased in the present study. On the contrary, we noted an increase in Muribaculaceae in the jejunum of PM-exposed *ApoE*$^{-/-}$ mice, which was not seen in our previous study. Of interest, Muribaculaceae has been associated with increased propionate, a short-chain fatty acid with protective, anti-inflammatory effects (Smith et al. 2019). Therefore, an increase in its abundance might have contributed to the lack of intestinal inflammation in that group. It is possible then that inflammation or lack of it could be driven by changes in specific taxa, either individual or combinations of them. Importantly, no intestinal inflammation was induced using two different batches of PM which on the other hand limits comparisons between the hyperlipidemic models and normolipidemic mice.

Subchronic inhalation of ultrafine PM induced changes in the intestinal microbiome that were markedly different to those that have been induced by PM inhalation of other sizes. Coarse PM inhalation was shown to induce oxidative stress and increase cytokine levels in the colon (Vignal et al. 2017), and accelerated chemically induced colorectal cancer (Li, Cui, et al. 2019). In addition, two prior studies have reported effects induced by inhalation of $PM_{2.5}$ on the intestinal microbiome of normolipidemic C57BL/6 mice. Mutlu et al. showed stomach, small intestine, cecum, colon, and fecal microbiome differences in C57BL/6 mice after 3 weeks of

exposure (8hrs/day, 5 days/week) to PM2.5 collected in Chicago using the Versatile Aerosol Concentration Enrichment System (VACES) system at 135.4 ±6.4 μg/m^3 (Mutlu et al. 2018). Wang et al. reported fecal microbiome differences in C57BL/6 mice as well, following 48 weeks of exposure (8hrs/day, 6 days/week,) to $PM_{2.5}$ collected in Shanghai at a concentration of 276.2 ±170.1 μg/m^3 (Wang et al. 2018). Importantly, the specific taxa affected by PM exposures in the three mouse models studied here markedly differed from the previous $PM_{2.5}$ studies even after restricting the comparisons to the C57BL/6 mice since genetic manipulations are well known to influence the baseline microbiome. However, dissecting the contribution of particle size for differences among these studies is extremely difficult since there were marked differences in several factors that are likely to influence intestinal microbiome such as age, particle mass concentration, length of exposure and particle composition, all of which could be factors, among many others, contributing to the differences observed among the various studies. Indeed, Mutlu et al. exposed 8 to 12-week-old mice for a shorter exposure length but larger number of hours/session and sessions/week. On the other hand, Wang et al. exposed much younger 4-week-old mice for a much longer duration. Aging has been shown to alter the taxonomic composition of the microbiome and can individually drive microbiome aggregation (Langille et al. 2014; Miyoshi et al. 2018). Therefore, our C57BL/6 mice reflecting a mouse microbiome that was 28-30-weeks old at the end of the study were largely different to the 11 to 15-week-old mice (Mutlu et al. 2018) or 52-week-old mice (Wang et al. 2018) in the previous studies. In addition, there were marked differences in particle composition. For example, Wang et al. reported a high percentage of Si due to nearby construction, which was not present in our study, and conditions known to influence particle composition such as seasonal differences at the time of PM

collection as well as locational differences are markedly different between Los Angeles, Chicago (Mutlu et al. 2018) and Shanghai (Wang et al. 2018).

Strengths of our study include use of exposure to inhaled PM and longitudinal analysis of microbiome response across three different mouse models. A potential limitation is the use of a narrow dose range of particles for all experiments. In addition, we could not expose all three mouse cohorts concurrently and to the same batch of PM due to limitations in the availability of particles, thus we cannot make direct comparisons between hyperlipidemic mice and wild-type mice. Our exposure experiments only represent the PMs within the period when they were collected, albeit from the same location and within the span of a year. In spite of this, we consistently observed that UFPs induced microbiome changes in the absence of intestinal inflammation in both hyperlipidemic and normolipidemic mouse models even after using different batches of PM. Other limitations are the variation in age across the three groups of mice and the differences in PM administered to hyperlipidemic compared to normolipidemic mice. While we are unable to establish dose response of ultrafine PM effects on the microbiome, the exposures were a reasonable approximation of human exposure. The PM dosage employed in the exposure aerosols was 300-350 $\mu g/m^3$, resulting in a mouse PM exposure ~ 35 $\mu g/m^3$ typical of human PM exposures in Los Angeles and other urban areas of the US over about 1 year (Hasheminassab et al. 2014).

Conclusion

Subchronic inhalation exposures to ultrafine PM induced varied changes in the gut microbiomes of hyperlipidemic and normolipidemic mouse models. These microbiome shifts were not accompanied by and therefore, not attributable to increased intestinal inflammation.

Further studies are warranted to investigate whether microbiome shifts causally contribute to the health effects induced by subchronic PM inhalation exposure.

Figures

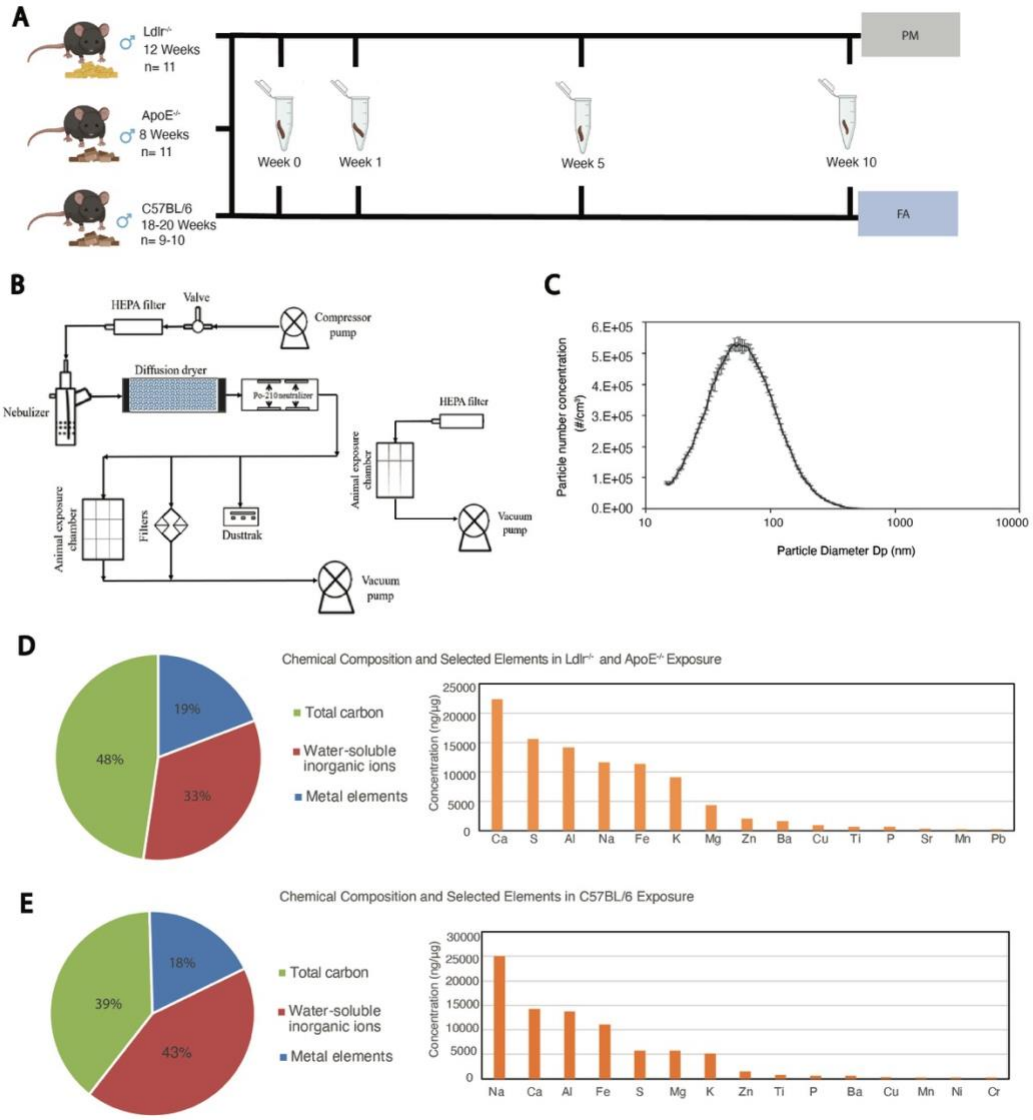

Figure 1. Exposure protocol and PM characterization. (A) Experimental design, *Ldlr*$^{-/-}$, *ApoE*$^{-/-}$ and C57BL/6 mice were exposed to UFPs by inhalation 3 times per week for 10 weeks. Fecal pellet samples were collected at weeks 0 (baseline), 1, 5, and 10 to evaluate longitudinal changes. Jejunal and ileal samples were collected at the end after euthanasia. Figure1A was created with Biorender.com. (B) Schematic of aerosol generation and exposure system. (C) Particle size distribution in the exposures of *Ldlr*$^{-/-}$ and *ApoE*$^{-/-}$ mice; distribution that was similar in the exposures of C57BL/6 mice. (D) Chemical profile of the PM aerosol in *Ldlr*$^{-/-}$ and *ApoE*$^{-/-}$ exposures. (E) Chemical profile of PM aerosol in C57BL/6 exposures.

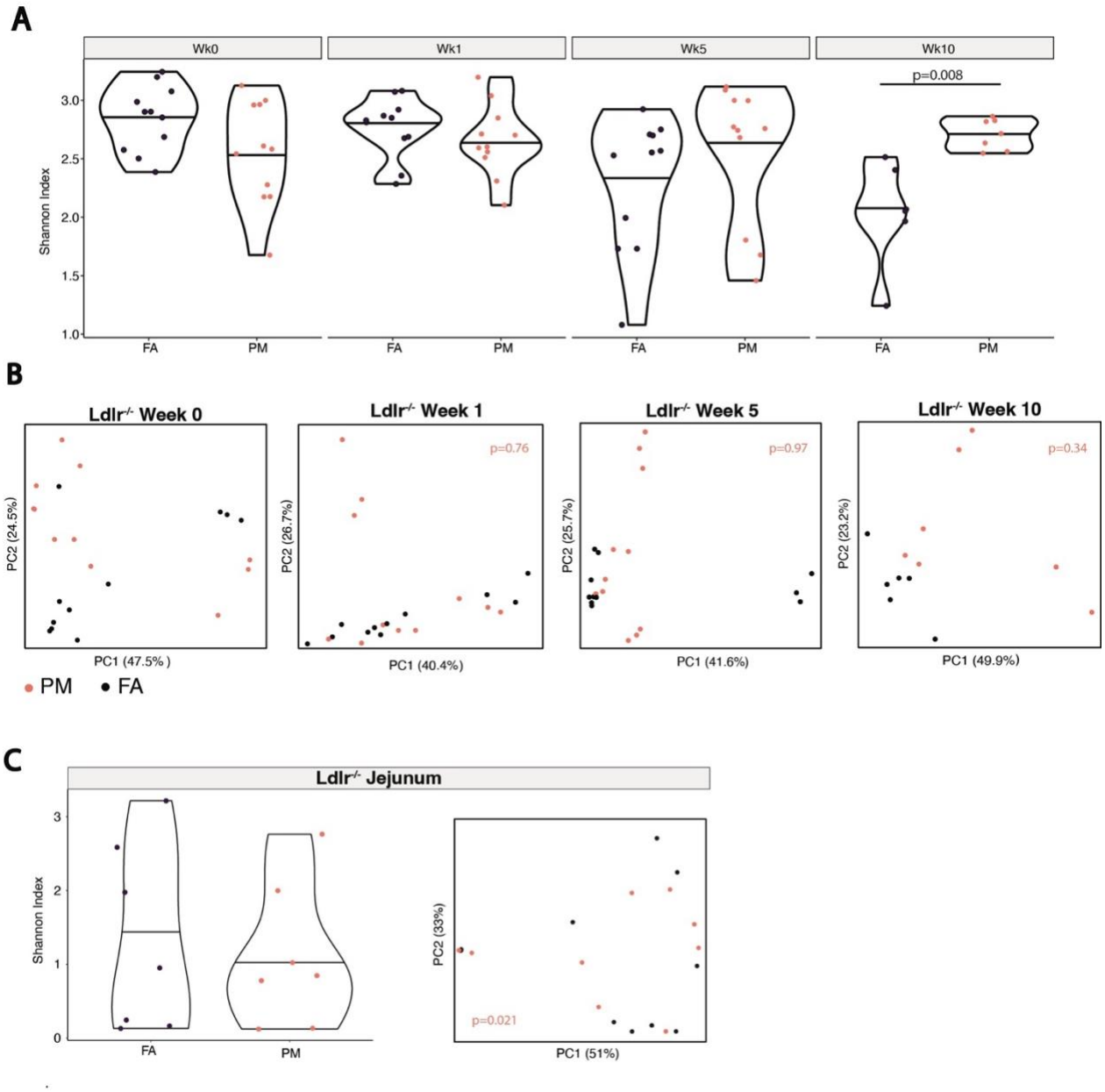

Figure 2. PM exposure altered gut microbial diversity and composition in *Ldlr*$^{-/-}$mice. (A) Shannon Index for assessment of alpha diversity, shown as separate violin plots for each time point. Significance was determined by a linear mixed effects model. (B) Beta diversity analysis, by principal coordinates analysis (PCoA) of Bray-Curtis dissimilarity. Significance was assessed by PERMANOVA. Each dot represents one sample with color representing exposure group (UFP or FA). (C) Jejunal microbial alpha and beta diversity analysis of *Ldlr*$^{-/-}$ mice at week 10.

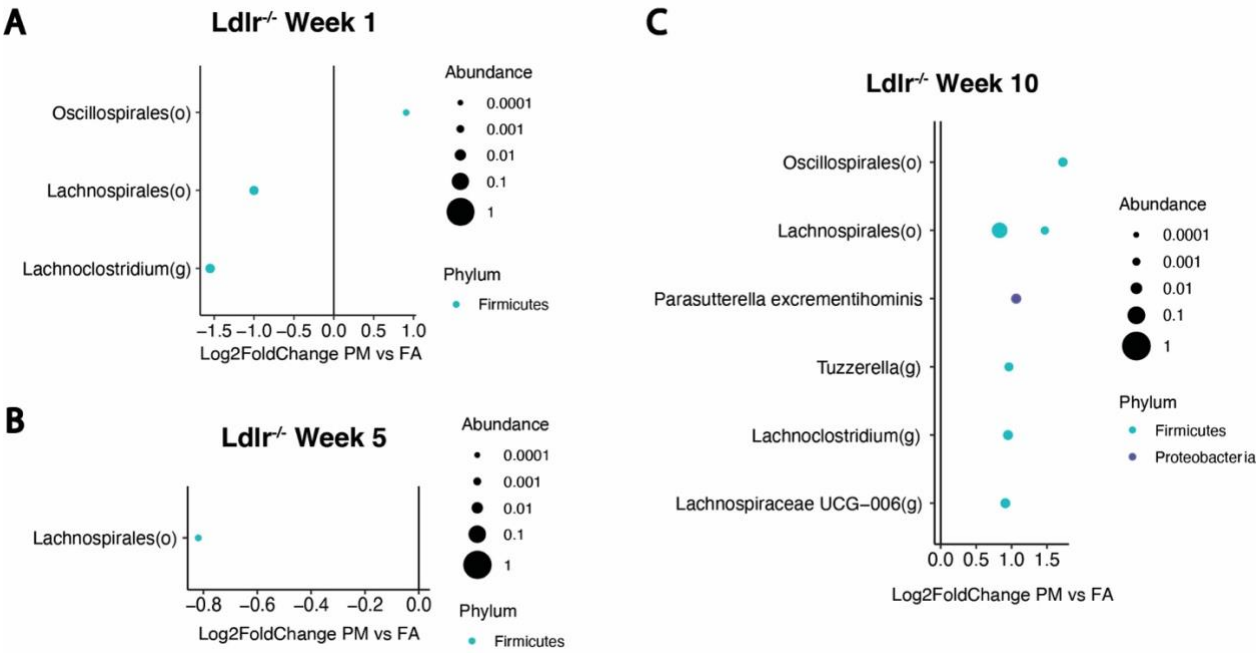

Figure 3. Enrichment of fecal microbes in *Ldlr*$^{-/-}$ mice after subchronic PM exposure. Enriched microbes include members of the *Lachnoclostridium* genus, *Oscillospirales* order, and *Lachnospirales* order. Plots showing differentially abundant amplicon sequence variants (ASVs) between UFP and FA exposure groups at weeks 1(A), 5(B), and 10(C). Each dot represents one ASV, displayed with its lowest taxonomic classification which could be at the species, genus (g), family (f), or order (o) level, when species was not available. Multiple differentially abundant ASVs with the same taxonomic classification are shown in the same row. Dot size is proportional to relative abundance of the ASV and color represents phylum. Magnitude of effect is shown as the log2 of the fold change (Log2FoldChange) between the UFP and FA groups in MaAsLin2 models.

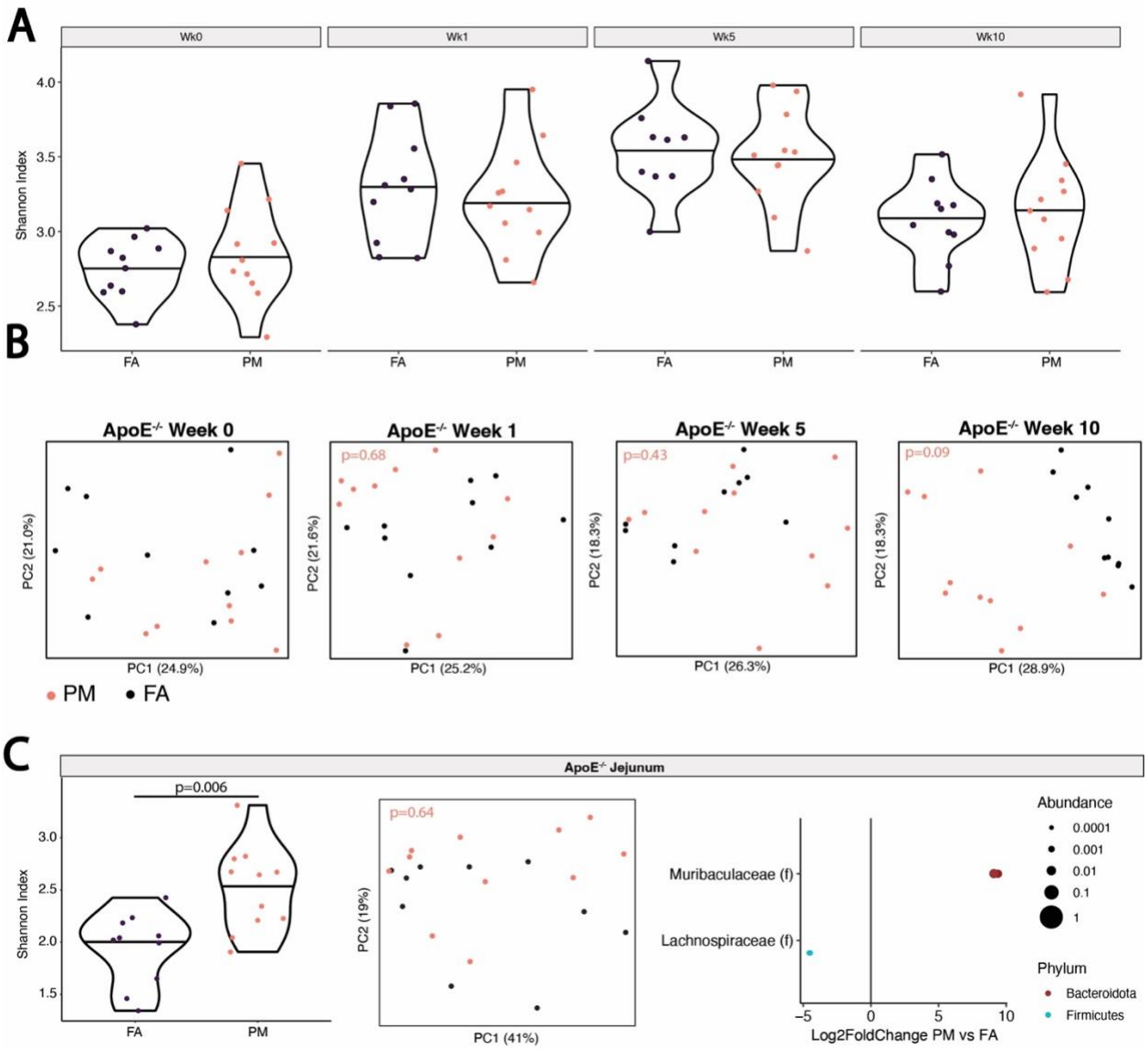

Figure 4. Subchronic UFP exposure induces shifts in fecal microbial composition of *ApoE*$^{-/-}$ mice. (A) Violin plots of fecal microbial alpha diversity *ApoE*$^{-/-}$ mice, measured by the Shannon index at weeks 0, 1, 5, and 10. (B) PCoA plots of Bray-Curtis dissimilarity, showing microbial composition of UFP and FA groups. Significance determined by PERMANOVA. (C) *ApoE*$^{-/-}$ jejunal microbial alpha and beta diversity analyses. Differentially abundant jejunal taxa between UFP and FA are also shown.

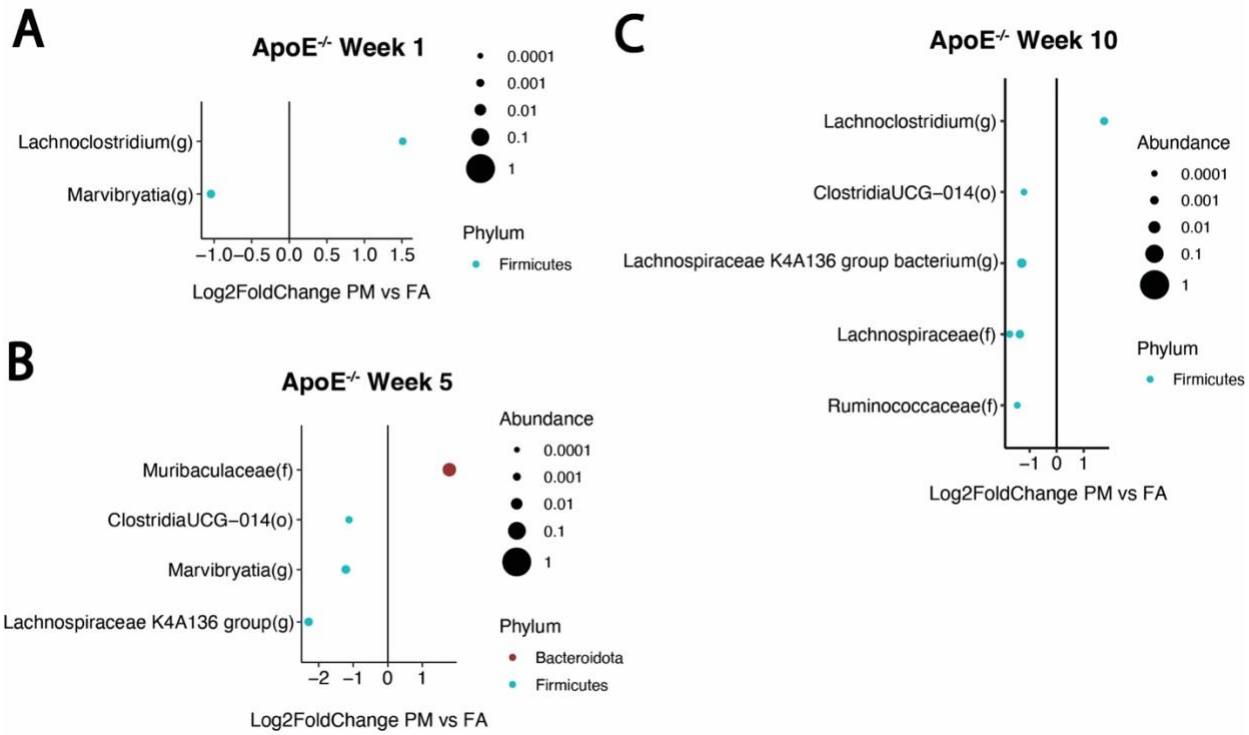

Figure 5. Differentially abundant fecal microbes in *ApoE*$^{-/-}$ mice exposed to UFPs. Log2FoldChange plots showing differential taxa in the UFP group compared to FA group at weeks 1(A), 5(B), and 10(C). Each dot represents one ASV, displayed with its lowest taxonomic classification which could be at the species, genus (g), family (f), or order (o) level, when species was not available.

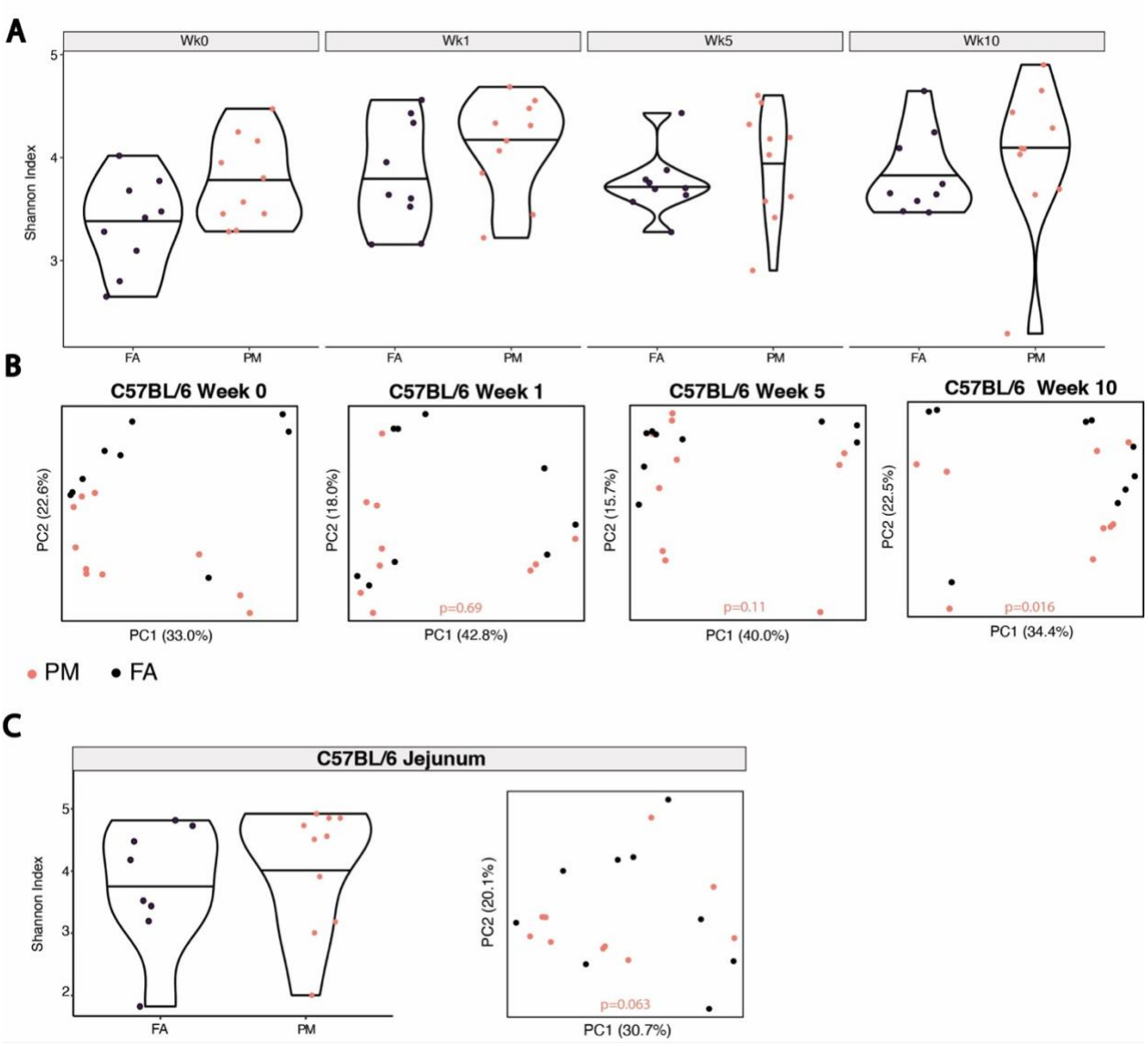

Figure 6. Subchronic UFP exposure alters fecal microbial composition in C57BL/6 mice. (A) Violin plots displaying alpha diversity (Shannon index) of fecal samples collected at weeks 0, 1, 5, and 10. (B) PCoA plots showing microbial compositional differences between the UFP and FA groups over 10 weeks of exposure. (C) Alpha and beta diversity analysis of the jejunal microbiome at week 10.

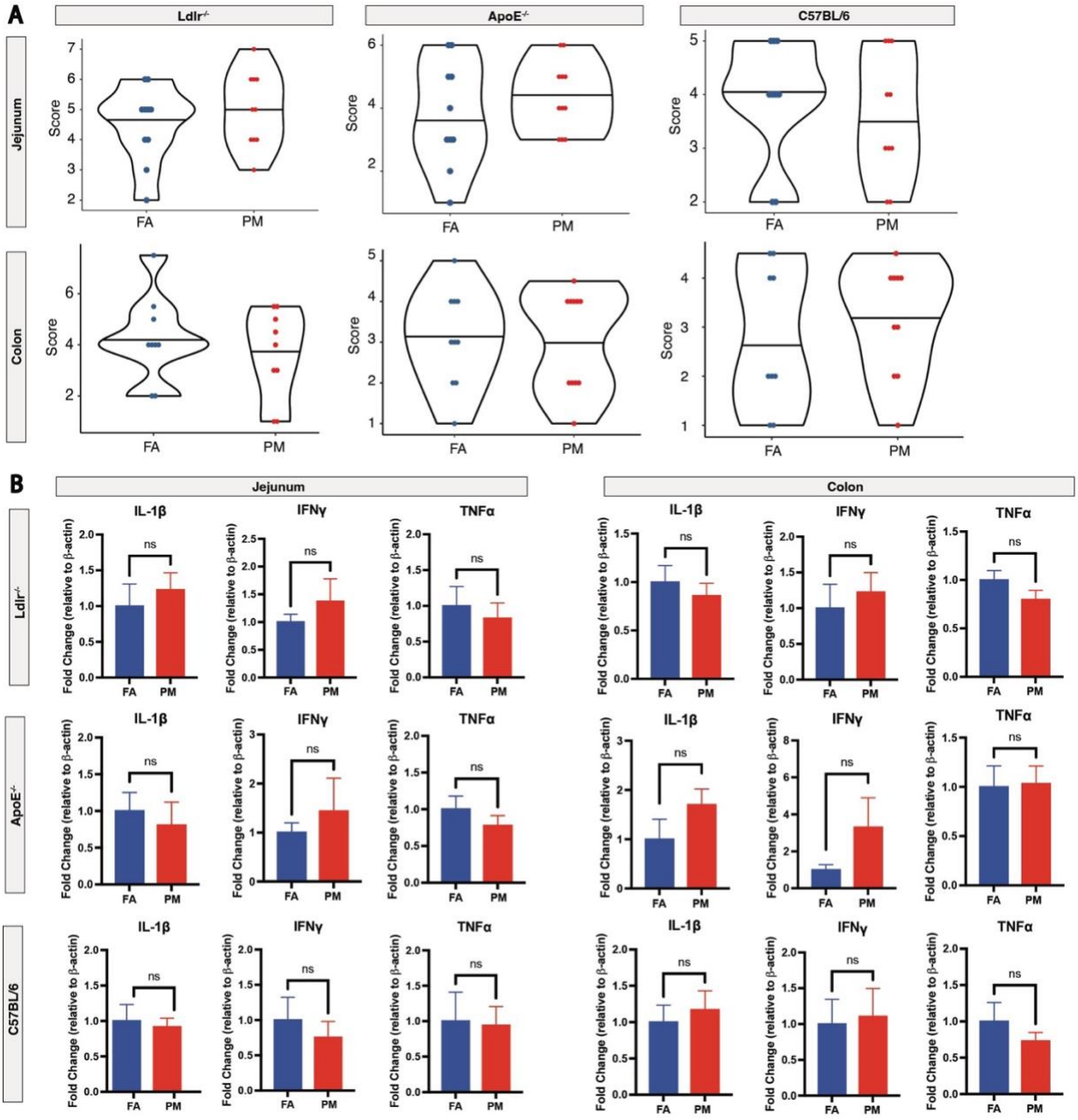

Figure 7. Assessment of intestinal inflammation in PM-exposed *Ldlr*$^{-/-}$, *ApoE*$^{-/-}$, and C57BL/6 mice by histological scoring and RT-qPCR. (A) Violin plots displaying histological scores of jejunal and colonic tissue based on severity and extent of immune infiltration, epithelial change and mucosal architecture. Significance was assessed by the Kruskal-Wallis rank sum test in R studio. (B) mRNA levels of proinflammatory cytokines IL-1β, IFNγ, and TNF-α measured by RT-qPCR. ns= not significant.

Supplementary Material

Subchronic Inhalation Exposure to Ultrafine Particulate Matter Alters the Intestinal Microbiome in Various Mouse Models

Candace Chang[1-5], Rajat Gupta[2,3,5], Farzaneh Sedighian[1], Allen Louie[2,3,5], David Gonzalez[2,5], Collin Le[1], Jae Min Cho[2], Seul-Ki Park[2], Jocelyn Castellanos[2,3], To-Wei Ting[3], Tien S. Dong[1,4,8], Nerea Arias-Jayo[1], Venu Lagishetty[1], Mohamad Navab[2], Srinivasa Reddy[2,5,9], Constantinos Sioutas[7], Tzung Hsiai[2,6], Jonathan P. Jacobs[1,4,5,8*], Jesus A. Araujo[2,3,5,10*]

[1] Vatche and Tamar Manoukian Division of Digestive Diseases, David Geffen School of Medicine, University of California Los Angeles, Los Angeles, California.

[2] Division of Cardiology, David Geffen School of Medicine, University of California Los Angeles, Los Angeles, California.

[3] Department of Environmental Health Sciences, Fielding School of Public Health, University of California Los Angeles, Los Angeles, California.

[4] Goodman-Luskin Microbiome Center, University of California Los Angeles, Los Angeles, California.

[5] Molecular Toxicology Interdepartmental Program, University of California Los Angeles, Los Angeles, California.

[6] Henry Samueli School of Engineering, University of California Los Angeles, Los Angeles, California.

[7] University of Southern California (USC) Viterbi School of Engineering, Los Angeles, California.

[8] Division of Gastroenterology, Hepatology and Parenteral Nutrition, Veterans Administration Greater Los Angeles Healthcare System, Los Angeles, California, Los Angeles, California.

[9] Molecular & Medical Pharmacology, University of California Los Angeles, Los Angeles, California.

[10] Molecular Biology Institute, University of California Los Angeles, Los Angeles, California.

*Equal contribution

Corresponding author: Jesus A. Araujo, MD, PhD. Division of Cardiology, Department of Medicine, David Geffen School of Medicine, University of California Los Angeles, 10833 Le Conte Avenue, CHS 43-264, Los Angeles, CA 90095. P.O. Box 951679. Phone number (310) 825-3222, Fax number (310) 206-9133. E-mail address: JAraujo@mednet.ucla.edu

Co-corresponding author: Jonathan P. Jacobs, MD, PhD. Vatche and Tamar Manoukian Division of Digestive Diseases, Department of Medicine, David Geffen School of Medicine, University of California Los Angeles, 10945 Le Conte Avenue, CHS 44-139, Los Angeles, CA 90095-6949. Phone number (310) 825-9333, Fax number (310) 267-1861 E-mail address: JJacobs@mednet.ucla.edu

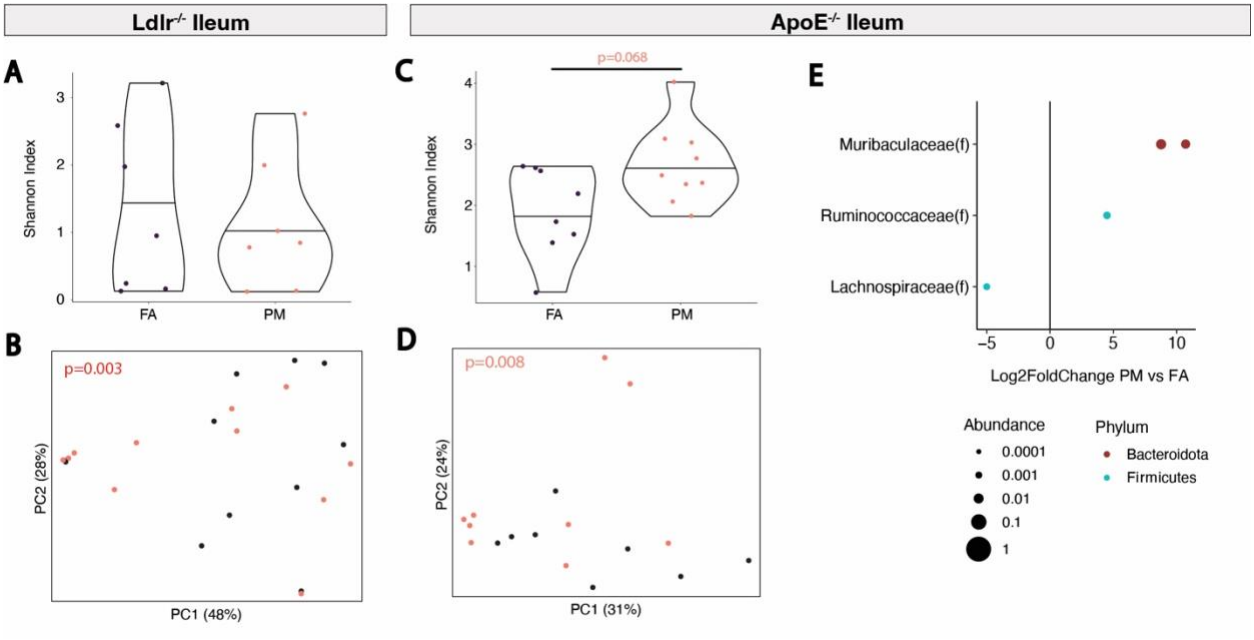

Supplementary Figure 1. Chronic UFP inhalation alters ileal microbial composition in hyperlipidemic mice. (A,C) Violin plots showing Shannon index for ileal samples from Ldlr$^{-/-}$ mice (A) and ApoE$^{-/-}$ (C). (B,D) Beta diversity analysis, by principal coordinates analysis (PCoA) of Bray-Curtis dissimilarity in Ldlr$^{-/-}$ mice (B) and ApoE$^{-/-}$ mice (D). Significance was assessed by PERMANOVA. Each point represents one sample with color representing exposure group (PM or FA). (E) Log2FoldChange plot show differentially abundant taxa identified in the ileum of ApoE$^{-/-}$ mice.

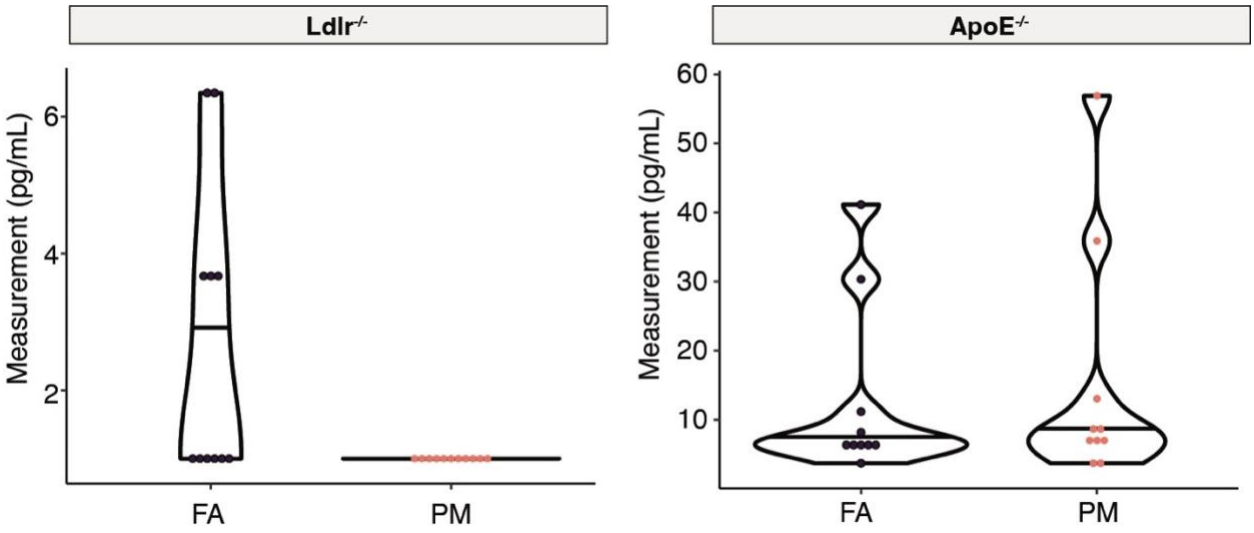

Supplementary Figure 2. No evidence of increased intestinal inflammation in PM-exposed *Ldlr*$^{-/-}$ and *ApoE*$^{-/-}$ mice by fecal lipocalin measurement. Violin plots of fecal lipocalin-2 levels obtained by ELISA. Measurements below the lower limit of detection were imputed to the lower limit of the assay (6.344 pg/mL). All fecal samples from *Ldlr*$^{-/-}$ mice treated with UFP were below the lower limit of the assay.

References

Abbott, Alison. 2016. 'Scientists bust myth that our bodies have more bacteria than human cells', *nature*, 2016: 19136.

Aguilera, Inmaculada, Julia Dratva, Seraina Caviezel, Luc Burdet, Eric de Groot, Regina E Ducret-Stich, Marloes Eeftens, Dirk Keidel, Reto Meier, and Laura Perez. 2016. 'Particulate matter and subclinical atherosclerosis: associations between different particle sizes and sources with carotid intima-media thickness in the SAPALDIA study', *Environmental health perspectives*, 124: 1700-06.

Alatab, Sudabeh, Sadaf G Sepanlou, Kevin Ikuta, Homayoon Vahedi, Catherine Bisignano, Saeid Safiri, Anahita Sadeghi, Molly R Nixon, Amir Abdoli, and Hassan Abolhassani. 2020. 'The global, regional, and national burden of inflammatory bowel disease in 195 countries and territories, 1990–2017: a systematic analysis for the Global Burden of Disease Study 2017', *The Lancet gastroenterology & hepatology*, 5: 17-30.

Aldekheel, Mohammad, Vahid Jalali Farahani, Ramin Tohidi, Abdulmalik Altuwayjiri, and Constantinos Sioutas. 2023. 'Development and performance evaluation of a two-stage cascade impactor equipped with gelatin filter substrates for the collection of multi-sized particulate matter', *Atmospheric Environment*, 294: 119493.

Ananthakrishnan, A. N., E. L. McGinley, D. G. Binion, and K. Saeian. 2011. 'Ambient air pollution correlates with hospitalizations for inflammatory bowel disease: an ecologic analysis', *Inflamm Bowel Dis*, 17: 1138-45.

Araujo, Jesus A. 2011. 'Particulate air pollution, systemic oxidative stress, inflammation, and atherosclerosis', *Air Quality, Atmosphere & Health*, 4: 79-93.

Araujo, Jesus A, Berenice Barajas, Michael Kleinman, Xuping Wang, Brian J Bennett, Ke Wei Gong, Mohamad Navab, Jack Harkema, Constantinos Sioutas, and Aldons J Lusis. 2008. 'Ambient particulate pollutants in the ultrafine range promote early atherosclerosis and systemic oxidative stress', *Circulation research*, 102: 589-96.

Araujo, Jesus A, and Andre E Nel. 2009. 'Particulate matter and atherosclerosis: role of particle size, composition and oxidative stress', *Particle and fibre toxicology*, 6: 1-19.

Beamish, Leigh A, Alvaro R Osornio-Vargas, and Eytan Wine. 2011. 'Air pollution: An environmental factor contributing to intestinal disease', *Journal of Crohn's and Colitis*, 5: 279-86.

Berg, Daniel J, Natalie Davidson, Ralf Kühn, Werner Müller, Satish Menon, Gina Holland, LuAnn Thompson-Snipes, Michael W Leach, and Donna Rennick. 1996. 'Enterocolitis and colon cancer in interleukin-10-deficient mice are associated with aberrant cytokine production and CD4 (+) TH1-like responses', *The Journal of clinical investigation*, 98: 1010-20.

Bhetraratana, May. 2018. 'Studies on the role of macrophagesin the toxicity induced by diesel exhaust particles,and on cardiovascular effects triggered by electronic cigarettes', University of California, Los Angeles

Block, Michelle L, and Lilian Calderón-Garcidueñas. 2009. 'Air pollution: mechanisms of neuroinflammation and CNS disease', *Trends in neurosciences*, 32: 506-16.

Britto, Savini Lanka, Mahesh Krishna, and Richard Kellermayer. 2019. 'Weight loss is a sufficient and economical single outcome measure of murine dextran sulfate sodium colitis', *FASEB BioAdvances*, 1: 493.

Britton, Graham J, Eduardo J Contijoch, Matthew P Spindler, Varun Aggarwala, Belgin Dogan, Gerold Bongers, Lani San Mateo, Andrew Baltus, Anuk Das, and Dirk Gevers.

2020. 'Defined microbiota transplant restores Th17/RORγt+ regulatory T cell balance in mice colonized with inflammatory bowel disease microbiotas', *Proceedings of the National Academy of Sciences*, 117: 21536-45.

Cai, Yuan-Yuan, Feng-Qing Huang, Xingzhen Lao, Yawen Lu, Xuejiao Gao, Raphael N Alolga, Kunpeng Yin, Xingchen Zhou, Yun Wang, and Baolin Liu. 2022. 'Integrated metagenomics identifies a crucial role for trimethylamine-producing Lachnoclostridium in promoting atherosclerosis', *NPJ biofilms and microbiomes*, 8: 11.

Callahan, Benjamin J, Paul J McMurdie, Michael J Rosen, Andrew W Han, Amy Jo A Johnson, and Susan P Holmes. 2016. 'DADA2: High-resolution sample inference from Illumina amplicon data', *Nature methods*, 13: 581-83.

Chang, Candace, Rajat Gupta, Farzaneh Sedighian, Allen Louie, David Gonzalez, Collin Le, Jae Min Cho, Seul-Ki Park, Jocelyn Castellanos, and To-Wei Ting. 2024. 'Subchronic inhalation exposure to ultrafine particulate matter alters the intestinal microbiome in various mouse models', *Environmental research*: 118242.

Craciun, Smaranda, Jonathan A Marks, and Emily P Balskus. 2014. 'Characterization of choline trimethylamine-lyase expands the chemistry of glycyl radical enzymes', *ACS chemical biology*, 9: 1408-13.

D'amico, G, G Frascaroli, G Bianchi, P Transidico, A Doni, A Vecchi, S Sozzani, P Allavena, and A Mantovani. 2000. 'Uncoupling of inflammatory chemokine receptors by IL-10: generation of functional decoys', *Nature immunology*, 1: 387-91.

Devlin, Robert B, Candice B Smith, Michael T Schmitt, Ana G Rappold, Alan Hinderliter, Don Graff, and Martha Sue Carraway. 2014. 'Controlled exposure of humans with

metabolic syndrome to concentrated ultrafine ambient particulate matter causes cardiovascular effects', *Toxicological Sciences*, 140: 61-72.

Diaz, E, K Mariën, L Manahan, and J Fox. 2019. 'Summary of health research on ultrafine particles', *Washington State Department of Health, Environmental Public Health Division, Office of Environmental Public Health Sciences*: 334-454.

Donaldson, Ken, David Brown, Anna Clouter, Rodger Duffin, William MacNee, Louise Renwick, Lang Tran, and Vicki Stone. 2002. 'The pulmonary toxicology of ultrafine particles', *Journal of aerosol medicine*, 15: 213-20.

e Oliveira, Juliana Regis da Costa, Luis Henrique Base, Luiz Carlos de Abreu, Celso Ferreira Filho, Celso Ferreira, and Lidia Morawska. 2019. 'Ultrafine particles and children's health: Literature review', *Paediatric respiratory reviews*, 32: 73-81.

Elson, Charles O, R Balfour Sartor, Gary S Tennyson, and Robert H Riddell. 1995. 'Experimental models of inflammatory bowel disease', *Gastroenterology*, 109: 1344-67.

Elten, M, E Benchimol, D Fell, and E Lavigne. 2019. 'Air pollution and greenness, and their associated risk with pediatric inflammatory bowel disease', *Environmental Epidemiology*, 3: 111.

Erben, Ulrike, Christoph Loddenkemper, Katja Doerfel, Simone Spieckermann, Dirk Haller, Markus M Heimesaat, Martin Zeitz, Britta Siegmund, and Anja A Kühl. 2014. 'A guide to histomorphological evaluation of intestinal inflammation in mouse models', *International journal of clinical and experimental pathology*, 7: 4557.

Farahani, Vahid Jalali, Abdulmalik Altuwayjiri, Milad Pirhadi, Vishal Verma, Ario Alberto Ruprecht, Evangelia Diapouli, Konstantinos Eleftheriadis, and Constantinos Sioutas. 2022. 'The oxidative potential of particulate matter (PM) in different regions around the world and its relation to air pollution sources', *Environmental Science: Atmospheres*, 2: 1076-86.

Farahani, Vahid Jalali, Milad Pirhadi, and Constantinos Sioutas. 2021. 'Are standardized diesel exhaust particles (DEP) representative of ambient particles in air pollution toxicological studies?', *Science of the Total Environment*, 788: 147854.

Fouladi, Farnaz, Maximilian J Bailey, William B Patterson, Michael Sioda, Ivory C Blakley, Anthony A Fodor, Roshonda B Jones, Zhanghua Chen, Jeniffer S Kim, and Frederick Lurmann. 2020. 'Air pollution exposure is associated with the gut microbiome as revealed by shotgun metagenomic sequencing', *Environment International*, 138: 105604.

Frampton, Mark W. 2007. 'Does inhalation of ultrafine particles cause pulmonary vasular effects in humans?', *Inhalation toxicology*, 19: 75-79.

Gevers, Dirk, Subra Kugathasan, Lee A Denson, Yoshiki Vázquez-Baeza, Will Van Treuren, Boyu Ren, Emma Schwager, Dan Knights, Se Jin Song, and Moran Yassour. 2014. 'The treatment-naive microbiome in new-onset Crohn's disease', *Cell host & microbe*, 15: 382-92.

Grahame, Thomas J, and Richard B Schlesinger. 2007. 'Health effects of airborne particulate matter: do we know enough to consider regulating specific particle types or sources?', *Inhalation toxicology*, 19: 457-81.

Hacquard, Stéphane, Ruben Garrido-Oter, Antonio González, Stijn Spaepen, Gail Ackermann, Sarah Lebeis, Alice C McHardy, Jeffrey L Dangl, Rob Knight, and Ruth Ley. 2015. 'Microbiota and host nutrition across plant and animal kingdoms', *Cell host & microbe*, 17: 603-16.

Hakimzadeh, Maryam, Ehsan Soleimanian, Amirhosein Mousavi, Alessandro Borgini, Cinzia De Marco, Ario A Ruprecht, and Constantinos Sioutas. 2020. 'The impact of biomass burning on the oxidative potential of PM2. 5 in the metropolitan area of Milan', *Atmospheric Environment*, 224: 117328.

Halfvarson, Jonas, Lennart Bodin, Curt Tysk, EVA Lindberg, and Gunnar Järnerot. 2003. 'Inflammatory bowel disease in a Swedish twin cohort: a long-term follow-up of concordance and clinical characteristics', *Gastroenterology*, 124: 1767-73.

Hart, Jaime E, Francine Laden, Robin C Puett, Karen H Costenbader, and Elizabeth W Karlson. 2009. 'Exposure to traffic pollution and increased risk of rheumatoid arthritis', *Environmental health perspectives*, 117: 1065-69.

Hasheminassab, Sina, Nancy Daher, Martin M Shafer, James J Schauer, Ralph J Delfino, and Constantinos Sioutas. 2014. 'Chemical characterization and source apportionment of indoor and outdoor fine particulate matter (PM2. 5) in retirement communities of the Los Angeles Basin', *Science of the Total Environment*, 490: 528-37.

Herner, Jorn D, Peter G Green, and Michael J Kleeman. 2006. 'Measuring the trace elemental composition of size-resolved airborne particles', *Environmental science & technology*, 40: 1925-33.

Hussein, Tareq, Arto Puustinen, Pasi P Aalto, Jyrki M Mäkelä, Kaarle Hämeri, and Markku Kulmala. 2004. 'Urban aerosol number size distributions', *Atmospheric Chemistry and Physics*, 4: 391-411.

Jacob, Noam, Jonathan P Jacobs, Kotaro Kumagai, Connie WY Ha, Yoshitake Kanazawa, Venu Lagishetty, Katherine Altmayer, Ariel M Hamill, Aimee Von Arx, and R Balfour Sartor. 2018. 'Inflammation-independent TL1A-mediated intestinal fibrosis is dependent on the gut microbiome', *Mucosal immunology*, 11: 1466-76.

Jacobs, Jonathan P, Maryam Goudarzi, Namita Singh, Maomeng Tong, Ian H McHardy, Paul Ruegger, Miro Asadourian, Bo-Hyun Moon, Allyson Ayson, and James Borneman. 2016. 'A disease-associated microbial and metabolomics state in

relatives of pediatric inflammatory bowel disease patients', *Cellular and molecular gastroenterology and hepatology*, 2: 750-66.

Jacobs, Jonathan P, Lin Lin, Maryam Goudarzi, Paul Ruegger, Dermot PB McGovern, Albert J Fornace Jr, James Borneman, Lijun Xia, and Jonathan Braun. 2017. 'Microbial, metabolomic, and immunologic dynamics in a relapsing genetic mouse model of colitis induced by T-synthase deficiency', *Gut microbes*, 8: 1-16.

Kaplan, Gilaad, Elijah Dixon, Remo Panaccione, Steven Heitman, Andrew Fong, Li Chen, Mietek Szyszkowicz, Anthony MacLean, Donald Buie, and Paul Villeneuve. 2008. 'Air Pollution and Appendicitis: a Novel Association: 292', *Official journal of the American College of Gastroenterology| ACG*, 103: S113.

Kaplan, Gilaad G, James Hubbard, Joshua Korzenik, Bruce E Sands, Remo Panaccione, Subrata Ghosh, Amanda J Wheeler, and Paul J Villeneuve. 2010. 'The inflammatory bowel diseases and ambient air pollution: a novel association', *The American journal of gastroenterology*, 105: 2412.

Kasdagli, Maria-Iosifina, Klea Katsouyanni, Konstantina Dimakopoulou, and Evangelia Samoli. 2019. 'Air pollution and Parkinson's disease: a systematic review and meta-analysis up to 2018', *International journal of hygiene and environmental health*, 222: 402-09.

Katakura, Kyoko, Jongdae Lee, Daniel Rachmilewitz, Gloria Li, Lars Eckmann, and Eyal Raz. 2005. 'Toll-like receptor 9–induced type I IFN protects mice from experimental colitis', *The Journal of clinical investigation*, 115: 695-702.

Katsouyanni, Klea, Giota Touloumi, Evangelia Samoli, Alexandros Gryparis, Alain Le Tertre, Yannis Monopolis, Giuseppe Rossi, Denis Zmirou, Ferran Ballester, and Azedine Boumghar. 2001. 'Confounding and effect modification in the short-

term effects of ambient particles on total mortality: results from 29 European cities within the APHEA2 project', *Epidemiology*: 521-31.

Keubler, Lydia M, Manuela Buettner, Christine Häger, and André Bleich. 2015. 'A multihit model: colitis lessons from the interleukin-10–deficient mouse', *Inflammatory bowel diseases*, 21: 1967-75.

Kish, Lisa, Naomi Hotte, Gilaad G Kaplan, Renaud Vincent, Robert Tso, Michael Gänzle, Kevin P Rioux, Aducio Thiesen, Herman W Barkema, and Eytan Wine. 2013. 'Environmental particulate matter induces murine intestinal inflammatory responses and alters the gut microbiome', *PloS one*, 8: e62220.

Kreyling, WG, JD Blanchard, JJ Godleski, S Haeussermann, J Heyder, P Hutzler, H Schulz, TD Sweeney, S Takenaka, and A Ziesenis. 1999. 'Anatomic localization of 24-and 96-h particle retention in canine airways', *Journal of Applied Physiology*, 87: 269-84.

Kriss, Michael, Keith Z Hazleton, Nichole M Nusbacher, Casey G Martin, and Catherine A Lozupone. 2018. 'Low diversity gut microbiota dysbiosis: drivers, functional implications and recovery', *Current opinion in microbiology*, 44: 34-40.

Kumar, Sushil, Mukesh K Verma, and Anup K Srivastava. 2013. 'Ultrafine particles in urban ambient air and their health perspectives', *Reviews on environmental health*, 28: 117-28.

Langille, Morgan GI, Conor J Meehan, Jeremy E Koenig, Akhilesh S Dhanani, Robert A Rose, Susan E Howlett, and Robert G Beiko. 2014. 'Microbial shifts in the aging mouse gut', *Microbiome*, 2: 1-12.

Lauka, Lelde, Elisa Reitano, Maria Clotilde Carra, Federica Gaiani, Paschalis Gavriilidis, Francesco Brunetti, Gian Luigi de’Angelis, Iradj Sobhani, and Nicola

de'Angelis. 2019. 'Role of the intestinal microbiome in colorectal cancer surgery outcomes', *World journal of surgical oncology*, 17: 1-12.

Lelieveld, J, K Klingmüller, A Pozzer, RT Burnett, A Haines, and V Ramanathan. 2019. 'Effects of fossil fuel and total anthropogenic emission removal on public health and climate', *Proceedings of the National Academy of Sciences*, 116: 7192-97.

Lepage, Patricia, Robert Häsler, Martina E Spehlmann, Ateequr Rehman, Aida Zvirbliene, Alexander Begun, Stephan Ott, Limas Kupcinskas, Joël Doré, and Andreas Raedler. 2011. 'Twin study indicates loss of interaction between microbiota and mucosa of patients with ulcerative colitis', *Gastroenterology*, 141: 227-36.

Li, Bofeng, Prajwal Gurung, RK Subbarao Malireddi, Peter Vogel, Thirumala-Devi Kanneganti, and Terrence L Geiger. 2015. 'IL-10 engages macrophages to shift Th17 cytokine dependency and pathogenicity during T-cell-mediated colitis', *Nature communications*, 6: 1-13.

Li, Ning, Constantinos Sioutas, Arthur Cho, Debra Schmitz, Chandan Misra, Joan Sempf, Meiying Wang, Terry Oberley, John Froines, and Andre Nel. 2003. 'Ultrafine particulate pollutants induce oxidative stress and mitochondrial damage', *Environmental health perspectives*, 111: 455-60.

Li, Rongsong, Kaveh Navab, Greg Hough, Nancy Daher, Min Zhang, David Mittelstein, Katherine Lee, Payam Pakbin, Arian Saffari, and May Bhetraratana. 2015. 'Effect of exposure to atmospheric ultrafine particles on production of free fatty acids and lipid metabolites in the mouse small intestine', *Environmental health perspectives*, 123: 34-41.

Li, Rongsong, Jieping Yang, Arian Saffari, Jonathan Jacobs, Kyung In Baek, Greg Hough, Muriel H Larauche, Jianguo Ma, Nelson Jen, and Nabila Moussaoui. 2017. 'Ambient

ultrafine particle ingestion alters gut microbiota in association with increased atherogenic lipid metabolites', *Scientific reports*, 7: 1-12.

Li, Xiaobo, Jian Cui, Hongbao Yang, Hao Sun, Runze Lu, Na Gao, Qingtao Meng, Shenshen Wu, Jiong Wu, and Michael Aschner. 2019. 'Colonic injuries induced by inhalational exposure to particulate-matter air pollution', *Advanced Science*, 6: 1900180.

Li, Xiaobo, Hao Sun, Bin Li, Xinwei Zhang, Jian Cui, Jun Yun, Yiping Yang, Li'e Zhang, Qingtao Meng, and Shenshen Wu. 2019. 'Probiotics ameliorate Colon epithelial injury induced by ambient ultrafine particles exposure', *Advanced Science*, 6: 1900972.

López-Feldman, Alejandro, Carlos Chávez, María Alejandra Vélez, Hernán Bejarano, Ariaster B Chimeli, José Féres, Juan Robalino, Rodrigo Salcedo, and César Viteri. 2020. 'Environmental impacts and policy responses to Covid-19: a view from Latin America', *Environmental & resource economics*: 1.

Lough, Glynis C, James J Schauer, June-Soo Park, Martin M Shafer, Jeffrey T DeMinter, and Jason P Weinstein. 2005. 'Emissions of metals associated with motor vehicle roadways', *Environmental science & technology*, 39: 826-36.

Lozupone, Catherine A, Jesse I Stombaugh, Jeffrey I Gordon, Janet K Jansson, and Rob Knight. 2012. 'Diversity, stability and resilience of the human gut microbiota', *nature*, 489: 220-30.

Lupp, Claudia, Marilyn L Robertson, Mark E Wickham, Inna Sekirov, Olivia L Champion, Erin C Gaynor, and B Brett Finlay. 2007. 'Host-mediated inflammation disrupts the intestinal microbiota and promotes the overgrowth of Enterobacteriaceae', *Cell host & microbe*, 2: 119-29.

Lynch, JB, and EY Hsiao. 2019. 'Microbiomes as sources of emergent host phenotypes', *Science*, 365: 1405-09.

Mallick, Himel, Ali Rahnavard, Lauren J McIver, Siyuan Ma, Yancong Zhang, Long H Nguyen, Timothy L Tickle, George Weingart, Boyu Ren, and Emma H Schwager. 2021. 'Multivariable association discovery in population-scale meta-omics studies', *PLoS computational biology*, 17: e1009442.

McHardy, Ian H, Maryam Goudarzi, Maomeng Tong, Paul M Ruegger, Emma Schwager, John R Weger, Thomas G Graeber, Justin L Sonnenburg, Steve Horvath, and Curtis Huttenhower. 2013. 'Integrative analysis of the microbiome and metabolome of the human intestinal mucosal surface reveals exquisite inter-relationships', *Microbiome*, 1: 1-19.

Medani, Mekki, Danielle Collins, Neil G Docherty, Alan W Baird, Patrick R O'Connell, and Des C Winter. 2011. 'Emerging role of hydrogen sulfide in colonic physiology and pathophysiology', *Inflammatory bowel diseases*, 17: 1620-25.

Meng, Xia, Yanjun Ma, Renjie Chen, Zhijun Zhou, Bingheng Chen, and Haidong Kan. 2013. 'Size-fractionated particle number concentrations and daily mortality in a Chinese city', *Environmental health perspectives*, 121: 1174-78.

Miller, Kristin A, David S Siscovick, Lianne Sheppard, Kristen Shepherd, Jeffrey H Sullivan, Garnet L Anderson, and Joel D Kaufman. 2007. 'Long-term exposure to air pollution and incidence of cardiovascular events in women', *New England Journal of Medicine*, 356: 447-58.

Miller, Mark R, Catherine A Shaw, and Jeremy P Langrish. 2012. 'From particles to patients: oxidative stress and the cardiovascular effects of air pollution', *Future cardiology*, 8: 577-602.

Miyoshi, Jun, Vanessa Leone, Kentaro Nobutani, Mark W Musch, Kristina Martinez-Guryn, Yunwei Wang, Sawako Miyoshi, Alexandria M Bobe, A Murat Eren, and

Eugene B Chang. 2018. 'Minimizing confounders and increasing data quality in murine models for studies of the gut microbiome', *PeerJ*, 6: e5166.

Moller, Winfried, Karl Haussinger, Renate Winkler-Heil, Willi Stahlhofen, Thomas Meyer, Werner Hofmann, and Joachim Heyder. 2004. 'Mucociliary and long-term particle clearance in the airways of healthy nonsmoker subjects', *Journal of Applied Physiology*, 97: 2200-06.

Mosca, Alexis, Marion Leclerc, and Jean P Hugot. 2016. 'Gut microbiota diversity and human diseases: should we reintroduce key predators in our ecosystem?', *Frontiers in microbiology*, 7: 455.

Muñiz Pedrogo, David A, Jun Chen, Benjamin Hillmann, Patricio Jeraldo, Gabriel Al-Ghalith, Veena Taneja, John M Davis III, Dan Knights, Heidi Nelson, and William A Faubion. 2019. 'An increased abundance of Clostridiaceae characterizes arthritis in inflammatory bowel disease and rheumatoid arthritis: a cross-sectional study', *Inflammatory bowel diseases*, 25: 902-13.

Mutlu, Ece A, Işın Y Comba, Takugo Cho, Phillip A Engen, Cemal Yazıcı, Saul Soberanes, Robert B Hamanaka, Recep Niğdelioğlu, Angelo Y Meliton, and Andrew J Ghio. 2018. 'Inhalational exposure to particulate matter air pollution alters the composition of the gut microbiome', *Environmental pollution*, 240: 817-30.

Mutlu, Ece A, Phillip A Engen, Saul Soberanes, Daniela Urich, Christopher B Forsyth, Recep Nigdelioglu, Sergio E Chiarella, Kathryn A Radigan, Angel Gonzalez, and Shriram Jakate. 2011. 'Particulate matter air pollution causes oxidant-mediated increase in gut permeability in mice', *Particle and fibre toxicology*, 8: 1-13.

Nemmar, Abderrahim, PH Mq Hoet, B Vanquickenborne, D Dinsdale, Maarten Thomeer, MF Hoylaerts, H Vanbilloen, Luc Mortelmans, and Benoit Nemery. 2002. 'Passage

of inhaled particles into the blood circulation in humans', *Circulation*, 105: 411-14.

Nemmar, Abderrahim, H Vanbilloen, MF Hoylaerts, PHM Hoet, Alfons Verbruggen, and Benoit Nemery. 2001. 'Passage of intratracheally instilled ultrafine particles from the lung into the systemic circulation in hamster', *American journal of respiratory and critical care medicine*, 164: 1665-68.

Oberdörster, Günther, Zachary Sharp, Viorel Atudorei, Alison Elder, Robert Gelein, Wolfgang Kreyling, and Christopher Cox. 2004. 'Translocation of inhaled ultrafine particles to the brain', *Inhalation toxicology*, 16: 437-45.

Onoda, Atsuto, Ken Takeda, and Masakazu Umezawa. 2017. 'Dose-dependent induction of astrocyte activation and reactive astrogliosis in mouse brain following maternal exposure to carbon black nanoparticle', *Particle and fibre toxicology*, 14: 1-16.

Opstelten, Jorrit L, Rob MJ Beelen, Max Leenders, Gerard Hoek, Bert Brunekreef, Fiona DM van Schaik, Peter D Siersema, Kirsten T Eriksen, Ole Raaschou-Nielsen, and Anne Tjønneland. 2016. 'Exposure to ambient air pollution and the risk of inflammatory bowel disease: a European nested case–control study', *Digestive diseases and sciences*, 61: 2963-71.

Organization, World Health. 2021. 'WHO global air quality guidelines: particulate matter (PM2. 5 and PM10), ozone, nitrogen dioxide, sulfur dioxide and carbon monoxide: executive summary'.

Ostro, Bart, Lauraine Chestnut, Nuntavarn Vichit-Vadakan, and Adit Laixuthai. 1999. 'The impact of particulate matter on daily mortality in Bangkok, Thailand', *Journal of the Air & Waste Management Association*, 49: 100-07.

Pasolli, Edoardo, Francesco Asnicar, Serena Manara, Moreno Zolfo, Nicolai Karcher, Federica Armanini, Francesco Beghini, Paolo Manghi, Adrian Tett, and Paolo Ghensi.

2019. 'Extensive unexplored human microbiome diversity revealed by over 150,000 genomes from metagenomes spanning age, geography, and lifestyle', *Cell*, 176: 649-62. e20.

Peters, Annette, Douglas W Dockery, James E Muller, and Murray A Mittleman. 2001. 'Increased particulate air pollution and the triggering of myocardial infarction', *Circulation*, 103: 2810-15.

Petrov, VA, IV Saltykova, IA Zhukova, VM Alifirova, NG Zhukova, Yu B Dorofeeva, AV Tyakht, BA Kovarsky, DG Alekseev, and ES Kostryukova. 2017. 'Analysis of gut microbiota in patients with Parkinson's disease', *Bulletin of experimental biology and medicine*, 162: 734-37.

Piovani, Daniele, Silvio Danese, Laurent Peyrin-Biroulet, Georgios K Nikolopoulos, Theodore Lytras, and Stefanos Bonovas. 2019. 'Environmental risk factors for inflammatory bowel diseases: an umbrella review of meta-analyses', *Gastroenterology*, 157: 647-59. e4.

Pirhadi, Milad, Amirhosein Mousavi, Sina Taghvaee, Martin M Shafer, and Constantinos Sioutas. 2020. 'Semi-volatile components of PM2. 5 in an urban environment: volatility profiles and associated oxidative potential', *Atmospheric Environment*, 223: 117197.

Ranft, Ulrich, Tamara Schikowski, Dorothee Sugiri, Jean Krutmann, and Ursula Krämer. 2009. 'Long-term exposure to traffic-related particulate matter impairs cognitive function in the elderly', *Environmental research*, 109: 1004-11.

Saleh, Maya, and Giorgio Trinchieri. 2011. 'Innate immune mechanisms of colitis and colitis-associated colorectal cancer', *Nature Reviews Immunology*, 11: 9-20.

Salim, Saad Y, Juan Jovel, Eytan Wine, Gilaad G Kaplan, Renaud Vincent, Aducio Thiesen, Herman W Barkema, and Karen L Madsen. 2014. 'Exposure to Ingested

Airborne Pollutant Particulate Matter Increases Mucosal Exposure to Bacteria and Induces Early Onset of Inflammation in Neonatal IL-10–Deficient Mice', *Inflammatory bowel diseases*, 20: 1129-38.

Samet, Jonathan M, Scott L Zeger, Francesca Dominici, Frank Curriero, Ivan Coursac, Douglas W Dockery, Joel Schwartz, and Antonella Zanobetti. 2000. 'The national morbidity, mortality, and air pollution study', *Part II: morbidity and mortality from air pollution in the United States Res Rep Health Eff Inst*, 94: 5-79.

San Román, Antonio López, and Fernando Muñoz. 2011. 'Comorbidity in inflammatory bowel disease', *World journal of gastroenterology: WJG*, 17: 2723.

Schraufnagel, Dean E. 2020. 'The health effects of ultrafine particles', *Experimental & molecular medicine*, 52: 311-17.

Schwartz, Joel, and Douglas W Dockery. 1992. 'Increased mortality in Philadelphia associated with daily air pollution concentrations', *Am Rev Respir Dis*, 145: 600-04.

Sellon, Rance K, Susan Tonkonogy, Michael Schultz, Levinus A Dieleman, Wetonia Grenther, ED Balish, Donna M Rennick, and R Balfour Sartor. 1998. 'Resident enteric bacteria are necessary for development of spontaneous colitis and immune system activation in interleukin-10-deficient mice', *Infection and immunity*, 66: 5224-31.

Sender, Ron, Shai Fuchs, and Ron Milo. 2016. 'Revised estimates for the number of human and bacteria cells in the body', *PLoS biology*, 14: e1002533.

Shen, Aimee. 2012. 'Clostridium difficile toxins: mediators of inflammation', *Journal of innate immunity*, 4: 149-58.

Simkhovich, Boris Z, Michael T Kleinman, and Robert A Kloner. 2008. 'Air pollution and cardiovascular injury: epidemiology, toxicology, and mechanisms', *Journal of the american college of cardiology*, 52: 719-26.

Skapenko, Alla, Jan Leipe, Peter E Lipsky, and Hendrik Schulze-Koops. 2005. 'The role of the T cell in autoimmune inflammation', *Arthritis research & therapy*, 7: 1-11.

Smith, Byron J, Richard A Miller, Aaron C Ericsson, David C Harrison, Randy Strong, and Thomas M Schmidt. 2019. 'Changes in the gut microbiome and fermentation products concurrent with enhanced longevity in acarbose-treated mice', *BMC microbiology*, 19: 1-16.

Soleimanian, Ehsan, Sina Taghvaee, and Constantinos Sioutas. 2020. 'Characterization of organic compounds and oxidative potential of aqueous PM2. 5 suspensions collected via an aerosol-into-liquid collector for use in toxicology studies', *Atmospheric Environment*, 241: 117839.

Song, Conghua, Jinpu Yang, Wen Ye, Yuting Zhang, Chunyan Tang, Xiaomei Li, Xiaojiang Zhou, and Yong Xie. 2019. 'Urban–rural environmental exposure during childhood and subsequent risk of inflammatory bowel disease: A meta-analysis', *Expert Review of Gastroenterology & Hepatology*, 13: 591-602.

Soon, Ing Shian, Natalie A Molodecky, Doreen M Rabi, William A Ghali, Herman W Barkema, and Gilaad G Kaplan. 2012. 'The relationship between urban environment and the inflammatory bowel diseases: a systematic review and meta-analysis', *BMC gastroenterology*, 12: 1-14.

Sotty, Jules, Guillaume Garcon, F-O Denayer, L-Y Alleman, Yara Saleh, Esperanza Perdrix, Véronique Riffault, Pierre Dubot, J-M Lo-Guidice, and Ludivine Canivet. 2019. 'Toxicological effects of ambient fine (PM2. 5-0.18) and ultrafine (PM0. 18)

particles in healthy and diseased 3D organo-typic mucocilary-phenotype models', *Environmental research*, 176: 108538.

Steerenberg, PA, CET Withagen, WJ Van Dalen, JAMA Dorma, SH Heisterkamp, H van Loveren, and FR Cassee. 2005. 'Dose dependency of adjuvant activity of particulate matter from five european sites in three seasons in an ovalbumin–mouse model', *Inhalation toxicology*, 17: 133-45.

Stone, Vicki, Mark R Miller, Martin JD Clift, Alison Elder, Nicholas L Mills, Peter Møller, Roel PF Schins, Ulla Vogel, Wolfgang G Kreyling, and Keld Alstrup Jensen. 2017. 'Nanomaterials versus ambient ultrafine particles: an opportunity to exchange toxicology knowledge', *Environmental health perspectives*, 125: 106002.

Suh, Young Ju, Ho Kim, Ju Hee Seo, Hyesook Park, Young Ju Kim, Yun Chul Hong, and Eun Hee Ha. 2009. 'Different effects of PM10 exposure on preterm birth by gestational period estimated from time-dependent survival analyses', *International archives of occupational and environmental health*, 82: 613-21.

Taghvaee, Sina, Amirhosein Mousavi, Mohammad H Sowlat, and Constantinos Sioutas. 2019. 'Development of a novel aerosol generation system for conducting inhalation exposures to ambient particulate matter (PM)', *Science of the Total Environment*, 665: 1035-45.

Tong, Haiyan, Wan-Yun Cheng, James M Samet, M Ian Gilmour, and Robert B Devlin. 2010. 'Differential cardiopulmonary effects of size-fractionated ambient particulate matter in mice', *Cardiovascular toxicology*, 10: 259-67.

Turnbaugh, Peter J, Ruth E Ley, Michael A Mahowald, Vincent Magrini, Elaine R Mardis, and Jeffrey I Gordon. 2006. 'An obesity-associated gut microbiome with increased capacity for energy harvest', *nature*, 444: 1027-31.

van EEDEN, STEPHAN F, Wan C Tan, Tatsushi Suwa, Hiroshi Mukae, Takeshi Terashima, Takeshi Fujii, Diwen Qui, Renaud Vincent, and James C Hogg. 2001. 'Cytokines involved in the systemic inflammatory response induced by exposure to particulate matter air pollutants (PM10)', *American journal of respiratory and critical care medicine*, 164: 826-30.

Vaseghi, Golnaz, Shaghayegh Haghjooy Javanmard, Kiyan Heshmat-Ghahdarijani, Nizal Sarrafzadegan, and Atefeh Amerizadeh. 2022. 'Comorbidities with Familial Hypercholesterolemia (FH): A Systematic Review', *Current Problems in Cardiology*: 101109.

Veenstra, Jacob P, Bhaskar Vemu, Restituto Tocmo, Mirielle C Nauman, and Jeremy J Johnson. 2021. 'Pharmacokinetic analysis of carnosic acid and carnosol in standardized rosemary extract and the effect on the disease activity index of DSS-induced colitis', *Nutrients*, 13: 773.

Verma, Vishal, Zhi Ning, Arthur K Cho, James J Schauer, Martin M Shafer, and Constantinos Sioutas. 2009. 'Redox activity of urban quasi-ultrafine particles from primary and secondary sources', *Atmospheric Environment*, 43: 6360-68.

Vidgren, M, JC Waldrep, J Arppe, M Black, JA Rodarte, W Cole, and V Knight. 1995. 'A study of 99mtechnetium-labelled beclomethasone dipropionate dilauroylphosphatidylcholine liposome aerosol in normal volunteers', *International Journal of Pharmaceutics*, 115: 209-16.

Vignal, Cécile, Muriel Pichavant, Laurent Y Alleman, Madjid Djouina, Florian Dingreville, Esperanza Perdrix, Christophe Waxin, Adil Ouali Alami, Corinne Gower-Rousseau, and Pierre Desreumaux. 2017. 'Effects of urban coarse particles inhalation on oxidative and inflammatory parameters in the mouse lung and colon', *Particle and fibre toxicology*, 14: 1-13.

Volk, Heather E, Fred Lurmann, Bryan Penfold, Irva Hertz-Picciotto, and Rob McConnell. 2013. 'Traffic-related air pollution, particulate matter, and autism', *JAMA psychiatry*, 70: 71-77.

Wang, Huaijun, Jose G Vilches-Moure, Samir Cherkaoui, Isabelle Tardy, Charline Alleaume, Thierry Bettinger, Amelie Lutz, and Ramasamy Paulmurugan. 2019. 'Chronic Model of Inflammatory Bowel Disease in IL-10-/-Transgenic Mice: Evaluation with Ultrasound Molecular Imaging', *Theranostics*, 9: 6031.

Wang, Shaoxuan, JinXuan Wang, Ran Ma, Shaofeng Yang, Tingting Fan, Jing Cao, Yang Wang, Wenbin Ma, Wenxiu Yang, and Fulai Wang. 2020. 'IL-10 enhances T cell survival and is associated with faster relapse in patients with inactive ulcerative colitis', *Molecular immunology*, 121: 92-98.

Wang, Ting, Lichun Wang, Liliana Moreno-Vinasco, Gabriel D Lang, Jessica H Siegler, Biji Mathew, Peter V Usatyuk, Jonathan M Samet, Alison S Geyh, and Patrick N Breysse. 2012. 'Particulate matter air pollution disrupts endothelial cell barrier via calpain-mediated tight junction protein degradation', *Particle and fibre toxicology*, 9: 1-12.

Wang, Wanjun, Ji Zhou, Minjie Chen, Xingke Huang, Xiaoyun Xie, Weihua Li, Qi Cao, Haidong Kan, Yanyi Xu, and Zhekang Ying. 2018. 'Exposure to concentrated ambient PM 2.5 alters the composition of gut microbiota in a murine model', *Particle and fibre toxicology*, 15: 1-13.

Watanabe, Tomohiro, Naoki Asano, Peter J Murray, Keiko Ozato, Prafullakumar Tailor, Ivan J Fuss, Atsushi Kitani, and Warren Strober. 2008. 'Muramyl dipeptide activation of nucleotide-binding oligomerization domain 2 protects mice from experimental colitis', *The Journal of clinical investigation*, 118: 545-59.

Wirtz, Stefan, Clemens Neufert, Benno Weigmann, and Markus F Neurath. 2007. 'Chemically induced mouse models of intestinal inflammation', *Nature protocols*, 2: 541-46.

Wirtz, Stefan, Vanessa Popp, Markus Kindermann, Katharina Gerlach, Benno Weigmann, Stefan Fichtner-Feigl, and Markus F Neurath. 2017. 'Chemically induced mouse models of acute and chronic intestinal inflammation', *Nature protocols*, 12: 1295-309.

Xie, Shanshan, Caihong Zhang, Jinzhuo Zhao, Dan Li, and Jianmin Chen. 2022. 'Exposure to concentrated ambient PM2. 5 (CAPM) induces intestinal disturbance via inflammation and alternation of gut microbiome', *Environment International*, 161: 107138.

Yan, Fang, Lihong Wang, Yan Shi, Hanwei Cao, Liping Liu, M Kay Washington, Rupesh Chaturvedi, Dawn A Israel, Hailong Cao, and Bangmao Wang. 2012. 'Berberine promotes recovery of colitis and inhibits inflammatory responses in colonic macrophages and epithelial cells in DSS-treated mice', *American Journal of Physiology-Gastrointestinal and Liver Physiology*, 302: G504-G14.

Yilmaz, Emrullah, Anirudh Yalamanchali, Mohammed E Dwidar, Jessica L Geiger, S Koyfman, Timothy A Chan, and Natalie Silver. 2022. 'Lachnoclostridium and Immune Inflamed Gene Expression Signature Association in Head & Neck Cancers', *International Journal of Radiation Oncology, Biology, Physics*, 112: e37.

Zhang, Min, Kojiro Nakamura, Shoichi Kageyama, Akeem O Lawal, Ke Wei Gong, May Bhetraratana, Takehiro Fujii, Dawoud Sulaiman, Hirofumi Hirao, and Subhashini Bolisetty. 2018. 'Myeloid HO-1 modulates macrophage polarization and protects against ischemia-reperfusion injury', *JCI insight*, 3.

Zhang, Yuanxun, James J Schauer, Martin M Shafer, Michael P Hannigan, and Steven J Dutton. 2008. 'Source apportionment of in vitro reactive oxygen species bioassay

activity from atmospheric particulate matter', *Environmental science & technology*, 42: 7502-09.

Zhu, Baoli, Xin Wang, and Lanjuan Li. 2010. 'Human gut microbiome: the second genome of human body', *Protein & cell*, 1: 718-25.

Zuo, Tao, and Siew C Ng. 2018. 'The gut microbiota in the pathogenesis and therapeutics of inflammatory bowel disease', *Frontiers in microbiology*, 9: 2247.

Chapter 3- PM Inhalation in Models of Acute Colitis

Abstract

Inflammatory bowel disease (IBD) is an immunologically complex disorder involving genetic, microbial, and environmental risk factors. Its global burden has continued to rise since industrialization, with epidemiological studies suggesting that ambient particulate matter (PM) in air pollution could be a contributing factor. Prior animal studies have shown that oral PM_{10} exposure promotes intestinal inflammation in a genetic IBD model of IBD and that $PM_{2.5}$ inhalation exposure can increase intestinal levels of pro-inflammatory cytokines. PM_{10} and $PM_{2.5}$ include ultrafine particles (UFP), which have an aerodynamic diameter <0.10μm and biophysical and biochemical properties that promote toxicity. UFP inhalation, however, has not been previously studied in the context of murine models of IBD. Here, we demonstrated that ambient PM is toxic to cultured Caco-2 intestinal epithelial cells and examined whether UFP inhalation affected acute colitis induced by dextran sodium sulfate and 2,4,6-trinitrobenzenesulfonic acid. C57BL/6 mice were exposed to filtered air (FA) or various sources of ambient PM reaerosolized in the ultrafine size range at ~300 $\mu g/m^3$, 6 hours/day, 3-5 days/week, starting 7-10 days before disease induction. No differences in weight change, clinical disease activity, or histology were observed between the PM and FA exposed groups. In conclusion, UFP inhalation exposure did not exacerbate intestinal inflammation in acute, chemically-induced colitis models.

Introduction

Between 1990 and 2017, the incidence of inflammatory bowel disease (IBD), a debilitating condition characterized by chronic inflammation in the gastrointestinal tract, increased by 31% globally(Alatab et al. 2020). IBD encompasses two clinical diagnoses – Crohn's disease and ulcerative colitis – with pathogenesis involving an interplay between genetic susceptibility and

environmental factors such as diet. Environmental triggers may be the cause for increasing prevalence of IBD in industrialized countries, with more than 3.6 million people in the United States affected by IBD (Piovani et al. 2019). Intriguingly, urban living has been associated with increased risk of IBD compared to rural living in studies throughout the world(Song et al. 2019; Soon et al. 2012). Among the potential risk factors associated with urban living, increased air particulate matter levels have been linked to IBD diagnosis and exacerbation in epidemiological studies (Kaplan et al. 2010; Opstelten et al. 2016; Elten et al. 2019). Long-term exposure to high concentrations of nitrogen dioxide and particulate matter (PM) have been associated with an increased risk of early-onset Crohn's disease (Kaplan et al. 2010; Halfvarson et al. 2003). Studies have also correlated increased density of ambient air pollution with IBD hospitalizations (Ananthakrishnan et al. 2011; Kaplan et al. 2010). It is possible air pollutants promote IBD based on their ability to trigger inflammation in other non-pulmonary diseases such as myocardial infarction (Peters et al. 2001), appendicitis (Kaplan et al. 2008), and arthritis (Hart et al. 2009). These studies suggest that air pollution may be an environmental factor contributing to the development of IBD.

PM can be categorized by size into PM10 (aerodynamic diameter <10μm), fine particles or PM2.5 (<2.5μm diameter), and ultrafine particles or UFPs (aerodynamic diameter <0.10μm). UFP represent 85-90% of $PM_{2.5}$ by number and more than 80% of total industrial and urban ambient particle numbers (Diaz et al. 2019; Hussein et al. 2004). Detrimental health effects may increase with decreasing particle size (Meng et al. 2013). Surface reactivity and aspect ratio, among other properties, enable their greater access to peripheral airways and potential uptake into the circulation (Miller, Shaw, and Langrish 2012). Their small size results in increased surface area relative to mass, further increasing their biological activity (Kumar, Verma, and

Srivastava 2013). Cumulative evidence indicates that UFP exposure is associated with risk of diseases affecting the pulmonary (Schraufnagel 2020), central nervous(Block and Calderón-Garcidueñas 2009), and cardiovascular systems (Devlin et al. 2014). This may occur by various mechanisms including increased oxidative stress and permeability (Mutlu et al. 2011; Wang et al. 2012) . Particulate matter also alters levels of cytokines capable of inducing systemic response. Alveolar macrophages exposed to PM exhibited increased levels of IL-6, IL-1β, and GM-CSF, which were also found elevated in the serum of human subjects after exposure to an acute air pollution episode (van EEDEN et al. 2001).

PM has the potential to reach the gastrointestinal tract after inhalation via mucociliary transport and systemic absorption. Particles > 6μm have been shown to translocate via mucociliary clearance(Moller et al. 2004; Vidgren et al. 1995). Smaller particles such as ultrafine particles may gain access to organs via mucociliary clearance as it has been shown for larger particulates (Kreyling et al. 1999; Moller et al. 2004), or after dissemination via the systemic circulation (Nemmar et al. 2002; Nemmar et al. 2001). Once in the gastrointestinal tract, ambient particles have the potential to promote intestinal inflammation through effects on the intestinal epithelium, intestinal immune cells, and gut microbiota (Beamish, Osornio-Vargas, and Wine 2011). Oral ingestion of PM_{10} altered the microbiome and generated inflammatory responses in IL-$10^{-/-}$ mice – a genetic model of spontaneous colitis – 7 and 14 days after gavage (Kish et al. 2013). Elevated inflammatory markers in IL-$10^{-/-}$ mice were also reported after 10 and 14 weeks on a chow diet containing PM_{10} (Salim et al. 2014). Orogastric administration of UFPs has been reported to induce subclinical intestinal inflammation in *Ldlr-/-* mice, a model of hyperlipidemia (Li et al. 2017). A study using wild-type C57BL/6 mice reported that inhalation exposure to concentrated $PM_{2.5}$ for three weeks resulted in increased colonic mRNA expression of TNF-α

(Xie et al. 2022). In contrast, we found that mRNA levels of proinflammatory cytokines (IL-1β, IFNγ, TFNα) were similar between PM and FA-exposed mice in the jejunum and colon of *ApoE*$^{-/-}$, *Ldlr*$^{-/-}$, and C57BL/6 mice exposed to PM for 10 weeks and there was no histological evidence of inflammation(Chang et al. 2024). The existing literature collectively suggests that inhalation exposure to PM may promote inflammation in specific contexts, potentially in the setting of existing triggers of colitis.

Thus, we hypothesized that PM inhalation promotes intestinal inflammation in acute mouse models of IBD. To test our hypothesis, we assessed the effects of inhalation exposure to PM reaerosolized in the UFP size range on two distinct models of acute colitis, induced by dextran sodium sulfate (DSS) and 2,4,6-trinitrobenzenesulfonic acid (TNBS).

Materials and Methods

Animal Subjects

Male C56BL/6 (4-7 weeks-old) were purchased from Jackson Laboratories and were acclimated in our facilities until reaching 8 weeks of age. The C57BL/6 mice were fed autoclaved chow diet ad libitum expect during exposures. Mice were housed in autoclaved shoe-box type cages with cornhusk bedding. Our research protocol was conducted in compliance with the Animal Research Committee and Institutional Animal Care and Use Committee (*IACUC*) at the University of California, Los Angeles (UCLA), and performed in coordination with the Division of Laboratory Animal Medicine (DLAM) at UCLA.

Collection of Particulate Matter

Four different PM sources collected between August 2020 and January 2021 were tested, employing different collection methods and geographic sources. Our study included $PM_{2.5}$ collected from filters, $PM_{2.5}$ collected into liquid slurries, and UFP collected from filters.

Suspended particulate matter (sPM) represents particulate matter collected directly as slurries via the versatile aerosol concentration enrichment system (VACES)/aerosol-into-liquid-collector tandem technology. Nanosize class of PM (nPM) was collected in Los Angeles on filters and extracted into Milli-Q water. PM samples pertaining to Los Angeles sPM, Athens PMs and Milan PMs were collected as $PM_{2.5}$, whereas Los Angeles nPMs were collected as UFP. Both Athens and Milan were collected as $PM_{2.5}$ from filters. The PM batch of Los Angeles sPM was collected as $PM_{2.5}$ as slurries via versatile aerosol concentration enrichment system (VACES)/aerosol-into-liquid-collector tandem technology. Los Angeles nPM, Athens PM, and Milan PM were collected on PTFE membrane filters (20 × 25 cm, 3.0 μm pore size, PALL Life Sciences, USA) using a high-volume sampler (with a flow rate of 250 lpm) connected to a PM pre-impactor for separation. Collection of PMs for the DSS experiments and the first TNBS cohort occurred between December 2020 and January 2021 (Table 1). PM samples used in the second and third TNBS experiments were LA - nPM and were collected between December 2020 and February 2021. Each filter was divided into 32 pieces and extracted in Milli-Q water using 1 hour of sonication. The amount of extracted PM via sonication was obtained by subtracting the pre-extraction from the post-extraction weights of the filters using a high precision (±0.001 mg) microbalance (MT5, Mettler Toledo Inc., Columbus, OH). Further details regarding PM collection and extraction have been reported by us (Soleimanian, Taghvaee, and Sioutas 2020; Taghvaee et al. 2019).

Table 1. Collection period and dominant emission sources for each PM batch in the DSS exposures.

Period	Location	Dominant emission source	Collection period
Campaign I	Los Angeles (sPM)	Vehicular emissions	Dec 2020 – Jan 2021
	Los Angeles (nPM)	Vehicular emissions	Sept 2020 – Oct 2020
Campaign II	Athens PM	Secondary aerosols	Aug 2020 – Sept 2020
	Milan PM	Residential heating (biomas burning)	Dec 2020 – Jan 2021

In vitro experiments

Caco-2 cells, a human colon adenocarcinoma cell line, were cultured in Dulbecco's minimum essential medium (DMEM) with 20% filtered, heat-inactivated fetal bovine serum (FBS), 1% MEM non-essential amino acids and 1% Penicillin-Streptomycin at 37°C, 5% CO_2, 100% relative humidity. Cells were seeded in growth media in a 96-well plate for 24 hours before PM treatment, which was performed with 3 biological replicates per PM sample. All PM samples were thawed by sonicating in a water bath for 10 minutes and diluted to a concentration of 25µg/mL in the treatment media (DMEM). For LA- nPM , Milan and Athens PMs, the stock concentration was 200 µg/mL (Table 2); a blank of 125µL MilliQ water and 875 µL of media was used to compare cell viability. For LA- sPM, the stock concentration was 65 µg/mL, and a corresponding blank of 384.61µL MilliQ water and 615.39 µL media was used. At time of seeding, there were 1.51 x 10^6 cells/mL and the live count was 7.39 x 10^5 (49% live cells). Cell viability was assessed by the MTT assay; average absorbance at 560 nm was calculated between three experimental well triplicates. Cell viability for each PM sample type was calculated using this formula: (average absorbance of each PM treatment/average absorbance of experimental blank)*100.

Table 2. Volume and Concentration of samples used in cellular assays.

Sample ID	Location	Concentration (µg/ml)	Volume (ml)	Mass (mg)
1	Los Angeles - sPM	65	355	23
2	Los Angeles - nPM	200	115	23
3	Athens PM	200	115	23
4	Milan PM	200	115	23

DSS PM Inhalation Exposures

Inhalation exposures were conducted at the Air Pollution Inhalation Exposure Facility (APIEF) located within the animal vivarium (5V) in the Center for Health Sciences (Sender,

Fuchs, and Milo) building at UCLA. Following at least 1 week of acclimatation, the C57BL/6 were 8 weeks of age at the start of the experiment. The exposure protocol consisted of 6-hour exposure sessions to filtered air (FA) or ambient ultrafine PM at 300 μg/m^3, 3 days/week for a total of 9 sessions over 20 days (Fig. 9A). Exposed mice were placed in exposure chambers that housed up to 22 mice/cage. A compressor pump built at the University of Southern California (USC) Viterbi School of Engineering pushed HEPA-filtered air into a Hope nebulizer (B&B Medical Technologies, USA) to re-aerosolize the different PM-containing solutions into the ultrafine size range (Taghvaee et al. 2019) as previously described (Chang et al. 2024) (Fig. 9B). Two parallel exposure lines were running for LA- nPM and LA - sPM in our first exposure campaign, and Milan and Athens PM exposures were conducted in a subsequent campaign following the first. The re-aerosolized PM was drawn through a silica gel diffusion dryer (Model 3620, TSI Inc., USA) followed by Po-210 neutralizers (Model 2U500, NRD Inc., USA) to remove the excess water content and electrical charges of the particles, respectively. The air stream entered the animal exposure chamber with a flow rate of 2.5 lpm for in vivo inhalation exposure assessments. In parallel, the re-aerosolized particles were collected on PTFE (Teflon) and Quartz (37-mm, Pall Life Sciences, 2-μm pore, Ann Arbor, MI) filters to investigate the chemical characterization of particles in the system. Furthermore, variations in PM mass concentration were measured by TSI DustTrak during operation, where the average PM concentration was set at about 300 μg/m^3. An adjacent control chamber was used in exposure experiments in which ambient air was passed through a HEPA-filter and drawn into the chamber via a vacuum pump.

On day 11 of the PM exposure, the drinking water was replaced with 2% DSS in de-ionized water and provided ad libitum to induce acute colitis. DSS exposure occurred

concurrently with UFP inhalation exposure until the end of 18 days from the first exposure. DSS water was then replaced with regular water for 2 days before euthanasia on day 20 (Wirtz et al. 2007). Weight, stool consistency and rectal bleeding were monitored daily after initiation of DSS to assess colitis severity. The mice were euthanized under isoflurane anesthesia 18 hours after the last exposure. Colon tissue was harvested after euthanasia as previously described (Jacobs et al. 2017). Colon length excluding the cecum was measured in centimeters. Colon length was assessed after euthanasia as a morphological assessment of intestinal inflammation, with shorter colon length indicating greater colitis severity.

DSS PM Characterization

The particles collected on filters and slurries were chemically analyzed for their constituents, including carbonaceous content, water-soluble inorganic ions, and metal elements by Wisconsin State Laboratory of Hygiene (WSLH) (Taghvaee et al. 2019).

TNBS PM Exposures

Exposures for the TNBS experiments were conducted at the same location and using the same exposure apparatus set-up and concentrations as described for DSS. Cohort 1 was exposed for 7 sessions over ten days, while cohorts 2 and 3 were exposed for 9 sessions over 12 days. All three cohorts of 8-week C57BL/6 male mice were pre-sensitized to TNBS on the morning before their first PM exposure session. This involved shaving the skin on the back of the neck then administering a pre-sensitization solution containing 4 parts acetone/olive oil with 1 part 5% TNBS solution for a final concentration of 1% TNBS as described in the literature (Wirtz et al. 2017). Cohort 1 received intrarectal administration of 150 μL of 5% TNBS solution under anesthesia by isoflurane vapor on Day 8 of PM exposure. Cohort 2 also received the same

volume of 5% TNBS solution. Cohort 3 received intrarectal administration of 150 μL of 2.5% TNBS solution (1 volume of 5% TNBS mixed in water with 1 volume of absolute ethanol).

Clinical Measures of Inflammation Analysis

Daily body weights were measured from the onset of the DSS or TNBS regimen (day 11 and day 8, respectively). Fecal pellets were also collected daily from DSS mice starting from day 11. Percent weight change on each day was calculated using this formula: % weight change = 100 * (baseline weight*100)/(baseline weight), where baseline weight is measured at the time of initial administration of DSS or intrarectal TNBS administration. Disease activity index (DAI, 0-12 point scale) was calculated by adding together subscales for percent weight change, stool consistency, and stool blood (fecal occult blood test). Each of the three elements was scored from 0-4 points. Fecal occult blood test was scored as follows: 0 for no color development, 1 for flecks of color reaction, 2 for consistent blue color, 3 for rust color stools with blue reaction, and 4 for wet blood with dark blue reaction. Stool consistency received a score of 0 for small, firm, dry, nonadherent and friable stool, 1 for small firm, moist, and adherent stool, 2 for larger, soft, very adherent stool, 3 for larger, soft, and pliable stool, and 4 for liquid stool. Weight change was also scored from 0-4 where % weight loss less than 1% was scored 0, % weight loss between 1% and 5% was scored 1, % weight loss between 5% and 10% was scored 2, % weight loss between 10% and 15% was scored 3, and daily % weight loss greater than 15% was scored 4.

Histological Scoring

A ~1.5 cm piece of the middle of the colon was cut and fixed in 10% phosphate buffered formalin then transferred to 70% ethanol. The cassettes were sent to the Translational Pathology Core Laboratory (TPCL) at UCLA for embedding in paraffin, sectioning, and staining with hematoxylin and eosin (H&E). Sections were scored to assess epithelial and mucosal

architectural changes as well as the severity and extent of immune cell infiltration using a scoring system from 0-12 with two subscales (Erben et al. 2014). For the first subscale, inflammatory cell infiltrates were scored 0-6 based on severity ranging from normal to severe, and the second subscale was based on extent ranging from only the mucosa to transmural involvement. In the first subscore, a score of 1 was assigned for hyperproliferation, irregular crypts, and goblet cell loss, 1.5 for mild crypt loss (10-25%), 2 for moderate crypt loss (25%-50%), 2.5 for severe crypt loss(50-75%), 3 for severe crypt loss (75-90%), 4 for complete crypt loss, 5 for ulcers <10 crypts wide, and 6 for ulcers >10 crypts wide. For the second subscale, changes in intestinal architecture were scored from 0-6 by adding the scores from each region of the intestinal wall. The mucosa was scored from 0-3 (0: Normal, 1: Mild, 2: Modest, 3: Severe), the submucosa was scored from 0-2 (0: Normal, 1: Mild to modest, 2: Severe), and the mucosa/serosa was scored 0-1 (0: Normal, 1: Moderate to severe).

Statistical Analyses

Data from histological scoring were shown by violin plots and analyzed by the Mann-Whitney U-test in R studio (threshold *p-value* <0.05). Colon length is shown in bar plots and significance was also assessed by the Mann-Whitney U-test in R studio. Significance of percent weight loss and DAI scores was determined by linear mixed effects models using the lme4 package in R studio.

Results

In-vitro exposure PM increased toxicity in intestinal cells.

In-vitro experiments were performed to evaluate PM toxicity on the Caco-2 intestinal cell line. Four different sources of PM were tested spanning different collection methods and geographic

origin: Athens, Milan, and Los Angeles (LA, collected as either suspended or nanosized PM as described in the Methods). Caco-2 cells were seeded in 24-well plates and exposed to PM samples, each diluted to a concentration of 25 μg/mL in the treatment media for 24 hours. Cell viability was assessed by mitochondrial dehydrogenase conversion of MTT reagent (3-(4,5-dimethylthiazol-2-yl)-2,5-diphenyl-2H-tetrazolium bromide) to purple formazan, and average absorbance at 560 nm was calculated between three biological triplicates. *In-vitro* experiments validated biological toxicity in intestinal cells, where exposure to LA nPM, Athens PM, and Milan PM statistically decreased ($p<0.05$) cell viability compared to the blank (Fig. 8). Our re-aerosolized ultrafine particles showed comparable *in-vitro* activity to 25 μg/mL of UFP treatment previously shown to increase permeability to Streptavidin-HRP(Li et al. 2017).

Analysis of the PM used in our experiment showed that the main observed differences were less organic matter in the LA- nPM compared to the other three PMs, as well as reduced metal elements in Milan compared to the other PMs. Water-soluble inorganic ions were the dominant fraction of Los Angeles sPM (~43%), followed by organic matter (~39%) and metal elements (~18%), while Los Angeles nPM sample included a similar proportion of inorganic ions (44%), less organic matter (28%) and more metal elements (27%). Milan PM samples exhibited high levels of inorganic ions (45%) and organic matter (46%), while Athens showed high levels of organic matter (44%) and moderate loading of inorganic ions and metal elements (36% and 20%, respectively) (Table 3).

Table 3. Chemical profiles of various PM aerosol used for inhalation exposure experiments.

Composition (μg/mg)				
	LA- sPM	**LA-nPM**	**Milan PM**	**Athens PM**
Total carbon	186	119	392	35

Metal elements	86	109	80	195
Water-soluble inorganic ions	206	178	382	360

Selected Metals (µg/mg)

	LA- sPM	**LA-nPM**	**Milan PM**	**Athens PM**
Ca	12462.87	20980.27	10754.79	31979.41
Al	13462.87	17648.89	5424.49	9856.5
Fe	9886.88	22602.19	5973.15	13183.55
Mg	6222.17	6384.25	4964.33	4888.91
Zn	1550.92	1378.97	618.18	1092.9
Ba	487.30	1155.79	214.18	404.88
Cu	331.28	596.59	241.26	226.55
Ti	774.31	1308.46	119.48	562.11
Mn	283.90	445.07	158.37	301.56
Pb	131.21	235.81	293.95	241.13
Ni	262.81	179.99	37.14	115.26
Sn	48.11	216.82	147.62	135.52
Cr	225.22	345.39	111.43	155.79
V	20.58	40.73	6.6	90.33
Li	12.95	23.93	4.17	8.51
Cd	1.38	4.13	4.84	6.61
Pd	0.80	1.64	4.52	0.56

Water Soluble Inorganic Ions (µg/mg)

	LA- sPM	**LA-nPM**	**Milan PM**	**Athens PM**
Cl	33.2	19.2	9.7	1.1
NO3	105.6	78.8	224.8	3.9
PO4	0.0	1.7	0.8	BDL
SO4	24.8	39.0	40.3	264.2
Na	34.4	27.3	3.0	15.2
NH4	4.7	7.6	91.1	69.6
K	3.5	4.0	11.9	5.8

Inhalation exposure to PM from four distinct sources did not exacerbate DSS colitis severity

DSS chemically induces colitis by exerting toxicity on the epithelial cells of the basal crypts in the colon (Yan et al. 2012). Colitis severity after acute DSS exposure model is driven by several factors including epithelial barrier integrity, innate immune responses, and tissue repair

mechanisms(Saleh and Trinchieri 2011). Subacute PM inhalation exposure was modeled by exposing C57BL/6 mice for 6-hour sessions to filtered air (FA) or resuspended, ambient PM at 300 μg/m^3, 3 days/week for a total of 9 sessions over 20 days (Fig. 9A,B). Two cohorts were used, each comparing two PM samples with FA. On day 11 of the PM exposure, the drinking water was replaced with 2% DSS in de-ionized (DI) water and provided ad libitum to induce acute colitis. DSS exposure occurred concurrently with PM inhalation exposure until the end of 18 days from the first PM exposure, when DSS water was replaced with regular water. Mice were euthanized and tissues collected at day 20 from the first PM exposure. Colitis severity after initiation of DSS treatment was assessed by weight change and Disease Activity Index (DAI), which was calculated by adding together subscales for percent weight change, stool consistency, and stool blood (fecal occult blood test)(Britto, Krishna, and Kellermayer 2019). There were no significant differences in percent weight change between the PM and FA groups with the exception of the Athens PM group, which showed reduced weight loss compared to FA on day 7 ($p=0.035$) and to a lesser extent on day 8 ($p=0.054$) (Fig. 10A). Similarly, there were no significant differences in DAI between the PM and FA groups other than the Athens PM group, which demonstrated reduced DAI scores compared to FA on days 7 ($p=0.035$) and 8 ($p=0.015$) (Fig. 10B). Colon length was measured as a morphological assessment of inflammation, and no differences between PM and FA were observed (Fig. 10C). We further performed double-blind histological scoring of the colon, which did not demonstrate differences in mucosal architecture or extent of inflammation between the PM and FA groups (Fig. 11).

TNBS colitis severity is unaffected by PM inhalation exposure

To further investigate the effect of PM inhalation on acute colitis, we utilized a second model driven by distinct immunological mechanisms. The TNBS model functions by induction of a Th1

response to an antigen (TNBS) administered into the colon after initial sensitization by skin exposure (Elson et al. 1995). This model is believed to be relevant to Crohn's disease based on its histological features and dependence on NOD2, which has been strongly implicated in the pathogenesis of Crohn's (Watanabe et al. 2008). Ethanol is typically added in TNBS protocols to disturb the epithelial layer, allowing TNBS to interact with the intestinal wall to increase severity. Since there were no differences found between animals exposed to the different types of PM used in our DSS experiments, we decided to focus on a single particle type. Only the true UFP source, LA -nPM, was used for the TNBS experiments, which were divided into three cohorts with different induction regimens or experiment duration. Two experiments were performed with moderate TNBS severity (intrarectal TNBS administration without ethanol), one in which mice were sacrificed after 2 days for histology and one in which mice were followed for 4 days until clinical resolution (Fig. 12). A third experiment was conducted with greater disease severity due to the introduction of ethanol with rectal TNBS administration. Mice were exposed for 6-hour exposure sessions to filtered air (FA) or resuspended, ambient PM at 300 $\mu g/m^3$, every 1-2 days for a total of 7 sessions over 10 days for cohort 1 and 9 sessions over 12 days for cohorts 2 and 3. No differences were observed in average percent weight loss between PM and FA groups in any of the experiments (Fig. 13A). There were also no significant differences in colon length between the two groups in all three experiments (Fig. 13B). Mean histological scores obtained from cohort 1 (sacrificed at peak disease severity on day 2) showed no differences in histological measures of inflammation between the PM and FA groups ($p=0.56$) (Fig. 13C).

Discussion

This study is the first to report on the *in vitro* toxicity of PM to intestinal epithelial cells and the effects of PM inhalation on acute models of chemically-induced colitis. PM inhalation exposures represent a physiological route of administration in contrast to prior PM colitis experiments which have used oral administration. Our rigorous, controlled exposures are a suitable representation of exposure to real air pollution. Our study utilized two distinct models of acute colitis with differing disease mechanisms to capture varying aspects of potential IBD pathophysiology. The DSS model works primarily via intestinal epithelial injury, disrupting the barrier and thereby exposing mucosal immune cells to luminal antigens thereby inciting an inflammatory response. The TNBS model promotes IBD via a T-cell driven process. We found that exposure to ultrafine PM by inhalation did not exacerbate inflammation in either acute DSS or TNBS colitis despite the *in vitro* toxicity of the various PM sources to cultured intestinal epithelial cells.

Multiple PM sources were used for the DSS model to assess the possibility of varying biological effects of PM based upon their source and method of collection. The PMs tested in our study were collected from 3 locations: Milan, Athens, and LA. PM from Milan, Athens were collected on filters and resuspended in liquid. PMs from LA included PMs collected from aerosol into liquid (LA- sPM) as well as PMs from filters and resuspended in liquid (LA- nPM). Comparisons on toxicological characteristics and constituents of particles collected from these two methods have been previously published and it was found that sPMs showed a nonsignificant increased capture of semi-volatile organic compounds (Soleimanian, Taghvaee, and Sioutas 2020). Collections conducted during different seasons caused greater variation in n-alkanes than between PMs from the different collection methods. Similar oxidative potential between the PMs collected on ambient filters and in liquid suspension demonstrate that both

methods are representative of ambient PM. The dominant source for Athens PM was secondary aerosols(Farahani et al. 2022), formed by gas phase precursors emitted mainly by traffic and biomass combustion that react with ozone and hydroxyl radicals to form lower volatility products that partition in the particle phase. The dominant source for Milan PM was biomass burning for residential heating (Hakimzadeh et al. 2020), while vehicular emissions were the dominant source of LA PMs (Pirhadi et al. 2020). Although the atmospheric PM across the four cities originated from a variety of sources, the PM collected in each city represents the impact of the dominant emission sources in the area. Differences in where PM is collected have previously been associated with variation in the effects of PM on immune activation (Steerenberg et al. 2005). While we did not observe statistical differences in intestinal inflammation between vehicular emissions, biomass burning, and secondary aerosols in this context, previous studies have also generally supported that PM sourced from vehicular emissions and industrial activity are more harmful than secondary organic aerosols (Grahame and Schlesinger 2007). PM primarily derived from automobile emissions, secondary aerosols, and biomass burning all had no effect on DSS colitis, suggesting that the source of UFP does not explain the lack of effect.

It is possible that higher doses during inhalation exposure may be required to increase colitis severity. However, the exposures were a reasonable approximation of human exposure. The PM dosage employed in the exposure aerosols was 300-350 $\mu g/m^3$, resulting in a mouse PM exposure ~35 $\mu g/m^3$ typical of human PM exposures in Los Angeles and other urban areas of the US over 1 year (Alatab et al. 2020). Alternatively, the lack of effect of inhaled UFP may reflect differential transport of larger-sized PM compared to ultrafine PM to the gastrointestinal tract by mucociliary transport, which has been suggested to primarily act upon particles above 6 μm (Beamish, Osornio-Vargas, and Wine 2011). Experiments testing PM2.5 and PM10 inhalation

exposures at equivalent doses as used for UFP would be required to further investigate this possibility. In addition, longer duration of PM exposure prior to DSS or TNBS administration may be required to significantly modulate inflammation in these models.

We did not test chronic models of colitis, which may respond differently to UFP inhalation, particularly if they involve distinct mechanisms compared to acute DSS and TNBS colitis. This could explain previous reports that PM10 administered via gavage or feeding affected severity of IL-10$^{-/-}$ colitis, a genetic mouse model that develops over several months (Kish et al. 2013; Salim et al. 2014). Kish et al. 2013 showed increased histological damage and proinflammatory cytokine expression following gavage of PM_{10}, while Salim et al. 2014 found increases in IFN-γ and TNFα, as well as decreases in IL-17 and IL-1β in IL-10$^{-/-}$ mice fed PM_{10}. Interestingly, we reported that 10-week PM inhalation exposure of hyperlipidemic and normolipidemic mice did not induce changes in proinflammatory cytokines (Chang et al. 2024). This suggests that inflammatory effects of chronic PM inhalation may be more visible in models predisposed to IBD, such as IL-10$^{-/-}$ mice. Future studies are warranted with chronic models of colitis and chronic PM inhalation exposure to further investigate the impact of air pollution inhalation on IBD.

Figures

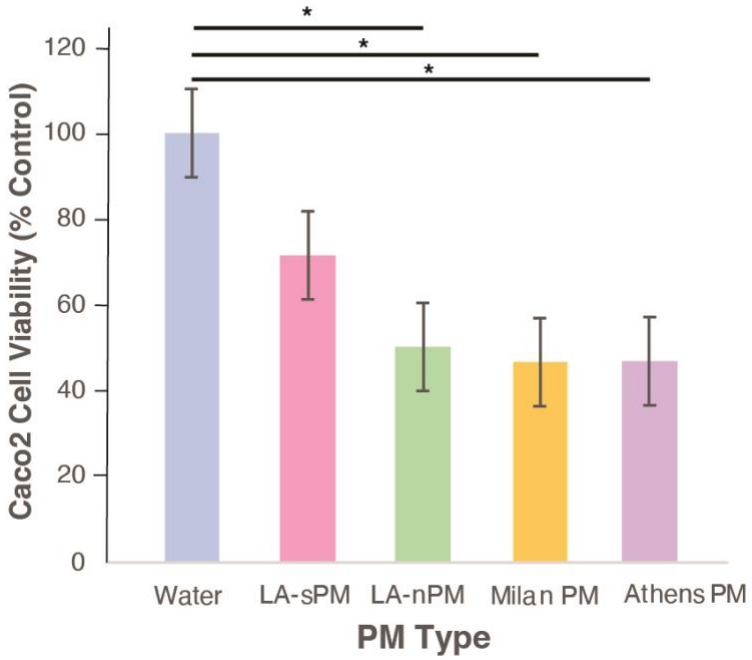

Figure 8. Diverse PM sources demonstrated toxicity to cultured Caco-2 intestinal epithelial cells. (A) In-vitro MTT assay for cell viability and cytotoxicity. Each PM sample was diluted to 25 ug/mL in the treatment media. *p<0.05

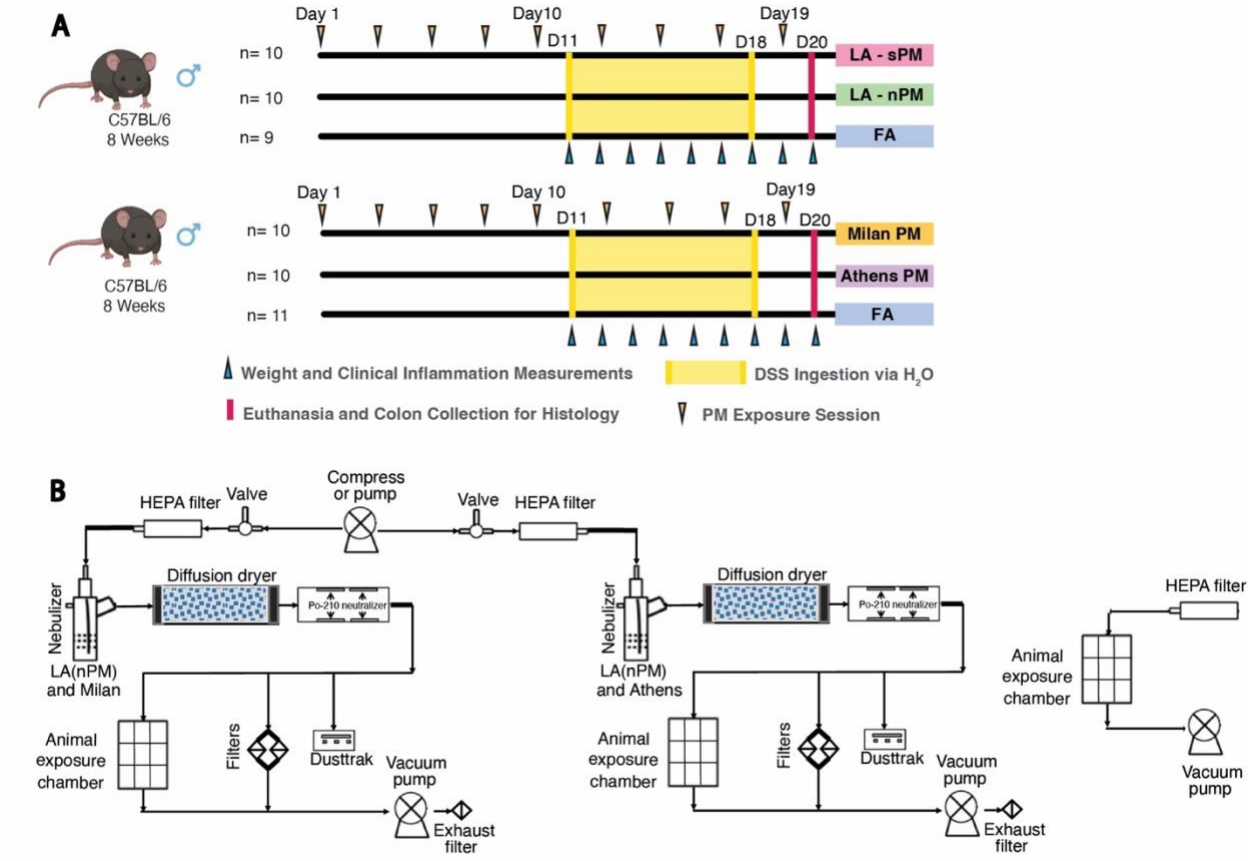

Figure 9. DSS experimental design(A) Experimental design. C57BL/6 mice were exposed to UFPs 3 times per week for a total of 9 sessions over 3 weeks. Daily weight measurements and fecal pellet collections were performed from Day 11-20, and fecal pellets were collected to assess stool consistency and blood. Mice were euthanized on Day 20 for colon tissue collection. Schematics were created with Biorender. (B) Exposure apparatus. PM re-aerosolization chambers (LEFT) Filtered air exposure chambers (RIGHT).

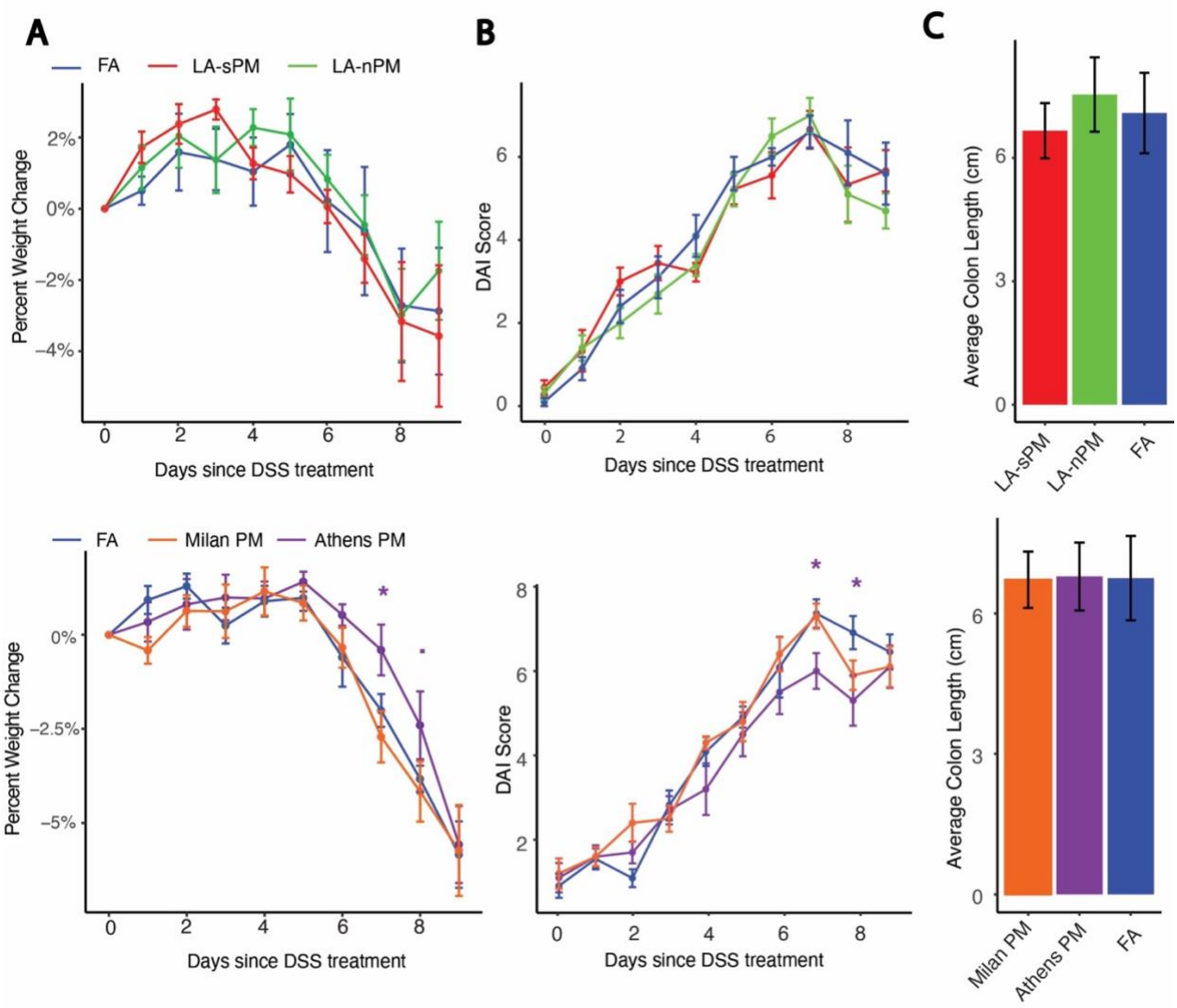

Figure 10. UFP inhalation exposure did not increase clinical severity of DSS colitis. (A) Percent weight loss, (B) disease activity index (DAI), and (C) colon length measured in centimeters of DSS-treated mice exposed to UFP or FA in the two experimental cohorts. (▪p<0.1, *p<0.05)

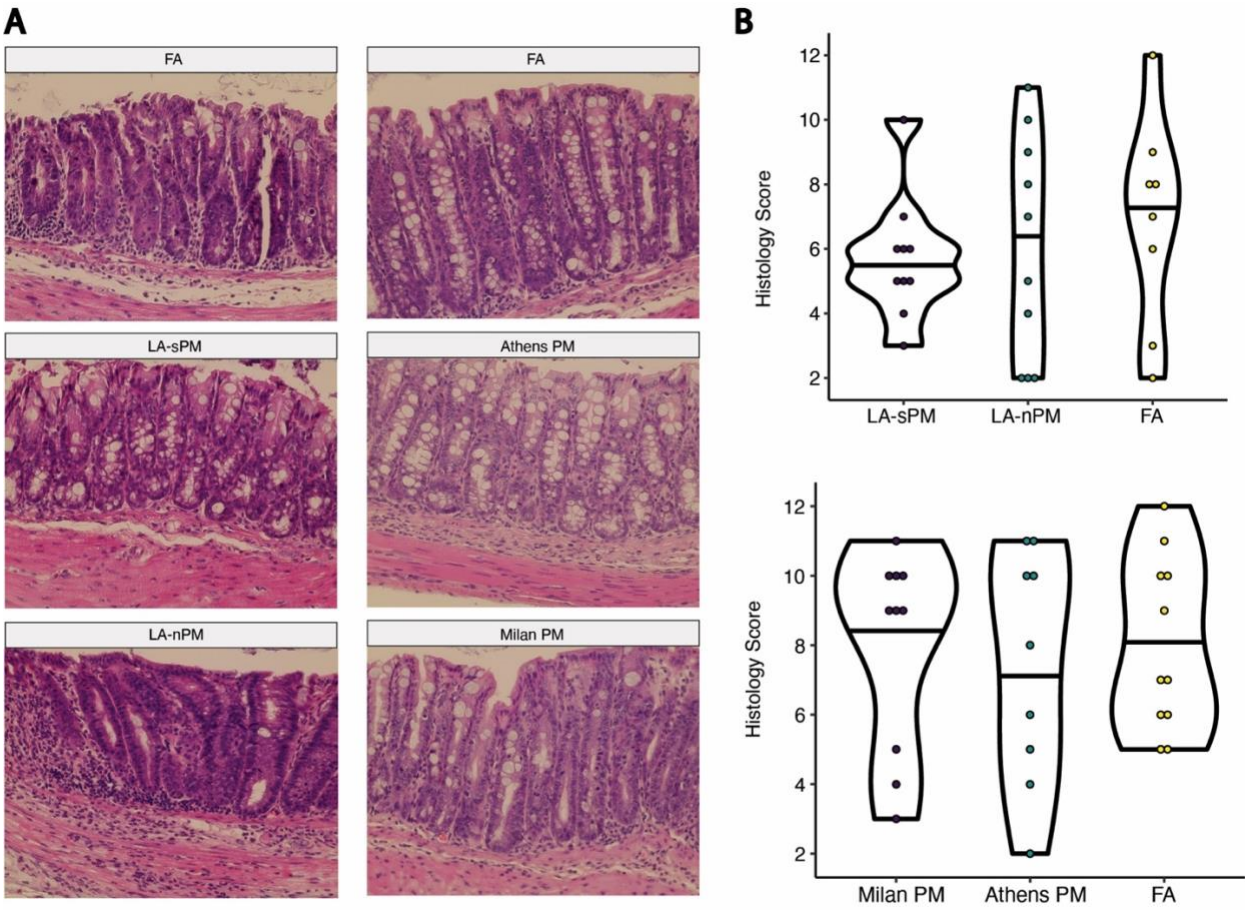

Figure 11. No effect of UFP exposure on histological severity of DSS colitis. (A) Representative H&E stained colon tissues (40X magnification) from each exposure group. (B) Violin plots of histological scores.

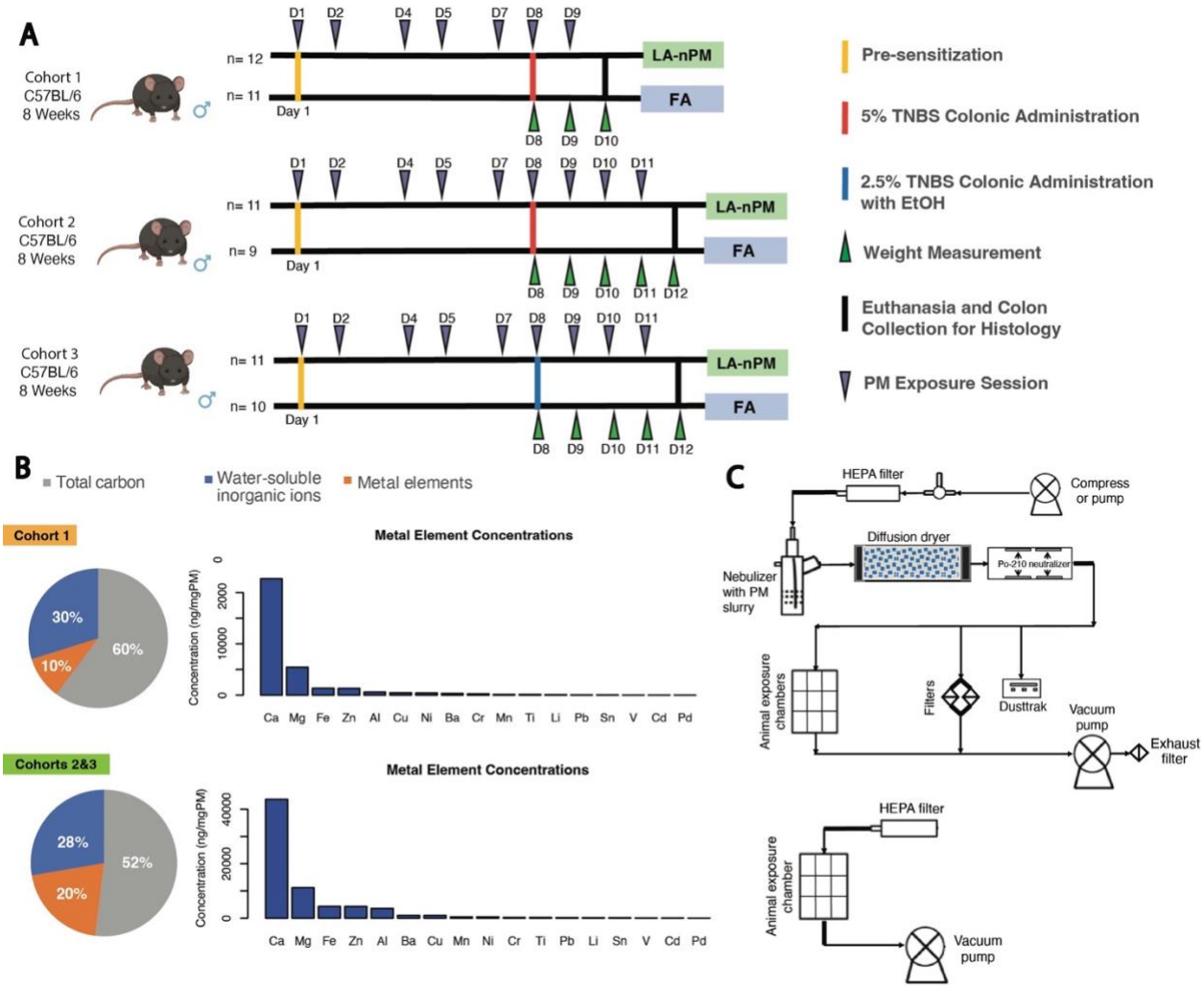

Figure 12. TNBS experimental design and PM characterization. (A) Schematic of PM and TNBS exposure in 3 cohorts. (B) Chemical analysis of PM. (C) Exposure apparatus. PM re-aerosolization chamber (TOP). Filtered air exposure chamber (BOTTOM).

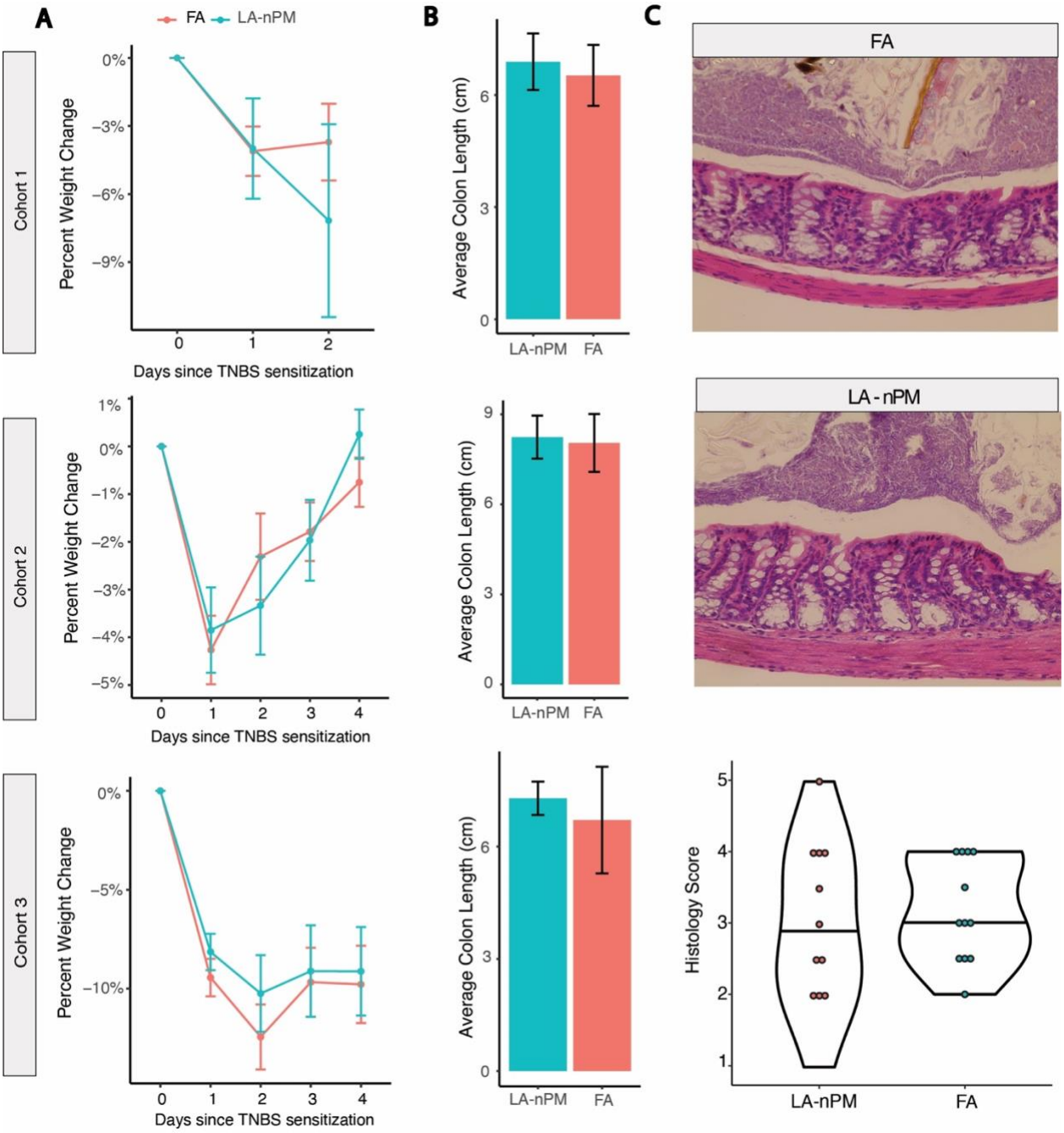

Figure 13. No effect of UFP exposure on TNBS colitis severity. (A) Daily average percent weight change of the three TNBS cohorts. (B) Colon length at time of euthanasia for the three cohorts. (C) Representative colon histology images for the LA-nPM and FA groups from TNBS cohort 1 and violin plot showing histology scores.

References

Alatab, Sudabeh, Sadaf G Sepanlou, Kevin Ikuta, Homayoon Vahedi, Catherine Bisignano, Saeid Safiri, Anahita Sadeghi, Molly R Nixon, Amir Abdoli, and Hassan Abolhassani. 2020. 'The global, regional, and national burden of inflammatory bowel disease in 195 countries and territories, 1990–2017: a systematic analysis for the Global Burden of Disease Study 2017', *The Lancet gastroenterology & hepatology*, 5: 17-30.

Ananthakrishnan, A. N., E. L. McGinley, D. G. Binion, and K. Saeian. 2011. 'Ambient air pollution correlates with hospitalizations for inflammatory bowel disease: an ecologic analysis', *Inflamm Bowel Dis*, 17: 1138-45.

Beamish, Leigh A, Alvaro R Osornio-Vargas, and Eytan Wine. 2011. 'Air pollution: An environmental factor contributing to intestinal disease', *Journal of Crohn's and Colitis*, 5: 279-86.

Block, Michelle L, and Lilian Calderón-Garcidueñas. 2009. 'Air pollution: mechanisms of neuroinflammation and CNS disease', *Trends in neurosciences*, 32: 506-16.

Britto, Savini Lanka, Mahesh Krishna, and Richard Kellermayer. 2019. 'Weight loss is a sufficient and economical single outcome measure of murine dextran sulfate sodium colitis', *FASEB BioAdvances*, 1: 493.

Chang, Candace, Rajat Gupta, Farzaneh Sedighian, Allen Louie, David Gonzalez, Collin Le, Jae Min Cho, Seul-Ki Park, Jocelyn Castellanos, and To-Wei Ting. 2024. 'Subchronic inhalation exposure to ultrafine particulate matter alters the intestinal microbiome in various mouse models', *Environmental research*: 118242.

Devlin, Robert B, Candice B Smith, Michael T Schmitt, Ana G Rappold, Alan Hinderliter, Don Graff, and Martha Sue Carraway. 2014. 'Controlled exposure of humans with

metabolic syndrome to concentrated ultrafine ambient particulate matter causes cardiovascular effects', *Toxicological Sciences*, 140: 61-72.

Diaz, E, K Mariën, L Manahan, and J Fox. 2019. 'Summary of health research on ultrafine particles', *Washington State Department of Health, Environmental Public Health Division, Office of Environmental Public Health Sciences*: 334-454.

Elson, Charles O, R Balfour Sartor, Gary S Tennyson, and Robert H Riddell. 1995. 'Experimental models of inflammatory bowel disease', *Gastroenterology*, 109: 1344-67.

Elten, M, E Benchimol, D Fell, and E Lavigne. 2019. 'Air pollution and greenness, and their associated risk with pediatric inflammatory bowel disease', *Environmental Epidemiology*, 3: 111.

Erben, Ulrike, Christoph Loddenkemper, Katja Doerfel, Simone Spieckermann, Dirk Haller, Markus M Heimesaat, Martin Zeitz, Britta Siegmund, and Anja A Kühl. 2014. 'A guide to histomorphological evaluation of intestinal inflammation in mouse models', *International journal of clinical and experimental pathology*, 7: 4557.

Farahani, Vahid Jalali, Abdulmalik Altuwayjiri, Milad Pirhadi, Vishal Verma, Ario Alberto Ruprecht, Evangelia Diapouli, Konstantinos Eleftheriadis, and Constantinos Sioutas. 2022. 'The oxidative potential of particulate matter (PM) in different regions around the world and its relation to air pollution sources', *Environmental Science: Atmospheres*, 2: 1076-86.

Grahame, Thomas J, and Richard B Schlesinger. 2007. 'Health effects of airborne particulate matter: do we know enough to consider regulating specific particle types or sources?', *Inhalation toxicology*, 19: 457-81.

Hakimzadeh, Maryam, Ehsan Soleimanian, Amirhosein Mousavi, Alessandro Borgini, Cinzia De Marco, Ario A Ruprecht, and Constantinos Sioutas. 2020. 'The impact of

biomass burning on the oxidative potential of PM2. 5 in the metropolitan area of Milan', *Atmospheric Environment*, 224: 117328.

Halfvarson, Jonas, Lennart Bodin, Curt Tysk, EVA Lindberg, and Gunnar Järnerot. 2003. 'Inflammatory bowel disease in a Swedish twin cohort: a long-term follow-up of concordance and clinical characteristics', *Gastroenterology*, 124: 1767-73.

Hart, Jaime E, Francine Laden, Robin C Puett, Karen H Costenbader, and Elizabeth W Karlson. 2009. 'Exposure to traffic pollution and increased risk of rheumatoid arthritis', *Environmental health perspectives*, 117: 1065-69.

Hussein, Tareq, Arto Puustinen, Pasi P Aalto, Jyrki M Mäkelä, Kaarle Hämeri, and Markku Kulmala. 2004. 'Urban aerosol number size distributions', *Atmospheric Chemistry and Physics*, 4: 391-411.

Jacobs, Jonathan P, Lin Lin, Maryam Goudarzi, Paul Ruegger, Dermot PB McGovern, Albert J Fornace Jr, James Borneman, Lijun Xia, and Jonathan Braun. 2017. 'Microbial, metabolomic, and immunologic dynamics in a relapsing genetic mouse model of colitis induced by T-synthase deficiency', *Gut microbes*, 8: 1-16.

Kaplan, Gilaad, Elijah Dixon, Remo Panaccione, Steven Heitman, Andrew Fong, Li Chen, Mietek Szyszkowicz, Anthony MacLean, Donald Buie, and Paul Villeneuve. 2008. 'Air Pollution and Appendicitis: a Novel Association: 292', *Official journal of the American College of Gastroenterology| ACG*, 103: S113.

Kaplan, Gilaad G, James Hubbard, Joshua Korzenik, Bruce E Sands, Remo Panaccione, Subrata Ghosh, Amanda J Wheeler, and Paul J Villeneuve. 2010. 'The inflammatory bowel diseases and ambient air pollution: a novel association', *The American journal of gastroenterology*, 105: 2412.

Kish, Lisa, Naomi Hotte, Gilaad G Kaplan, Renaud Vincent, Robert Tso, Michael Gänzle, Kevin P Rioux, Aducio Thiesen, Herman W Barkema, and Eytan Wine. 2013.

'Environmental particulate matter induces murine intestinal inflammatory responses and alters the gut microbiome', *PloS one*, 8: e62220.

Kreyling, WG, JD Blanchard, JJ Godleski, S Haeussermann, J Heyder, P Hutzler, H Schulz, TD Sweeney, S Takenaka, and A Ziesenis. 1999. 'Anatomic localization of 24-and 96-h particle retention in canine airways', *Journal of Applied Physiology*, 87: 269-84.

Kumar, Sushil, Mukesh K Verma, and Anup K Srivastava. 2013. 'Ultrafine particles in urban ambient air and their health perspectives', *Reviews on environmental health*, 28: 117-28.

Li, Rongsong, Jieping Yang, Arian Saffari, Jonathan Jacobs, Kyung In Baek, Greg Hough, Muriel H Larauche, Jianguo Ma, Nelson Jen, and Nabila Moussaoui. 2017. 'Ambient ultrafine particle ingestion alters gut microbiota in association with increased atherogenic lipid metabolites', *Scientific reports*, 7: 1-12.

Meng, Xia, Yanjun Ma, Renjie Chen, Zhijun Zhou, Bingheng Chen, and Haidong Kan. 2013. 'Size-fractionated particle number concentrations and daily mortality in a Chinese city', *Environmental health perspectives*, 121: 1174-78.

Miller, Mark R, Catherine A Shaw, and Jeremy P Langrish. 2012. 'From particles to patients: oxidative stress and the cardiovascular effects of air pollution', *Future cardiology*, 8: 577-602.

Moller, Winfried, Karl Haussinger, Renate Winkler-Heil, Willi Stahlhofen, Thomas Meyer, Werner Hofmann, and Joachim Heyder. 2004. 'Mucociliary and long-term particle clearance in the airways of healthy nonsmoker subjects', *Journal of Applied Physiology*, 97: 2200-06.

Mutlu, Ece A, Phillip A Engen, Saul Soberanes, Daniela Urich, Christopher B Forsyth, Recep Nigdelioglu, Sergio E Chiarella, Kathryn A Radigan, Angel Gonzalez, and

Shriram Jakate. 2011. 'Particulate matter air pollution causes oxidant-mediated increase in gut permeability in mice', *Particle and fibre toxicology*, 8: 1-13.

Nemmar, Abderrahim, PH Mq Hoet, B Vanquickenborne, D Dinsdale, Maarten Thomeer, MF Hoylaerts, H Vanbilloen, Luc Mortelmans, and Benoit Nemery. 2002. 'Passage of inhaled particles into the blood circulation in humans', *Circulation*, 105: 411-14.

Nemmar, Abderrahim, H Vanbilloen, MF Hoylaerts, PHM Hoet, Alfons Verbruggen, and Benoit Nemery. 2001. 'Passage of intratracheally instilled ultrafine particles from the lung into the systemic circulation in hamster', *American journal of respiratory and critical care medicine*, 164: 1665-68.

Opstelten, Jorrit L, Rob MJ Beelen, Max Leenders, Gerard Hoek, Bert Brunekreef, Fiona DM van Schaik, Peter D Siersema, Kirsten T Eriksen, Ole Raaschou-Nielsen, and Anne Tjønneland. 2016. 'Exposure to ambient air pollution and the risk of inflammatory bowel disease: a European nested case–control study', *Digestive diseases and sciences*, 61: 2963-71.

Peters, Annette, Douglas W Dockery, James E Muller, and Murray A Mittleman. 2001. 'Increased particulate air pollution and the triggering of myocardial infarction', *Circulation*, 103: 2810-15.

Piovani, Daniele, Silvio Danese, Laurent Peyrin-Biroulet, Georgios K Nikolopoulos, Theodore Lytras, and Stefanos Bonovas. 2019. 'Environmental risk factors for inflammatory bowel diseases: an umbrella review of meta-analyses', *Gastroenterology*, 157: 647-59. e4.

Pirhadi, Milad, Amirhosein Mousavi, Sina Taghvaee, Martin M Shafer, and Constantinos Sioutas. 2020. 'Semi-volatile components of PM2. 5 in an urban environment: volatility

profiles and associated oxidative potential', *Atmospheric Environment*, 223: 117197.

Saleh, Maya, and Giorgio Trinchieri. 2011. 'Innate immune mechanisms of colitis and colitis-associated colorectal cancer', *Nature Reviews Immunology*, 11: 9-20.

Salim, Saad Y, Juan Jovel, Eytan Wine, Gilaad G Kaplan, Renaud Vincent, Aducio Thiesen, Herman W Barkema, and Karen L Madsen. 2014. 'Exposure to Ingested Airborne Pollutant Particulate Matter Increases Mucosal Exposure to Bacteria and Induces Early Onset of Inflammation in Neonatal IL-10–Deficient Mice', *Inflammatory bowel diseases*, 20: 1129-38.

Schraufnagel, Dean E. 2020. 'The health effects of ultrafine particles', *Experimental & molecular medicine*, 52: 311-17.

Sender, Ron, Shai Fuchs, and Ron Milo. 2016. 'Revised estimates for the number of human and bacteria cells in the body', *PLoS biology*, 14: e1002533.

Soleimanian, Ehsan, Sina Taghvaee, and Constantinos Sioutas. 2020. 'Characterization of organic compounds and oxidative potential of aqueous PM2. 5 suspensions collected via an aerosol-into-liquid collector for use in toxicology studies', *Atmospheric Environment*, 241: 117839.

Song, Conghua, Jinpu Yang, Wen Ye, Yuting Zhang, Chunyan Tang, Xiaomei Li, Xiaojiang Zhou, and Yong Xie. 2019. 'Urban–rural environmental exposure during childhood and subsequent risk of inflammatory bowel disease: A meta-analysis', *Expert Review of Gastroenterology & Hepatology*, 13: 591-602.

Soon, Ing Shian, Natalie A Molodecky, Doreen M Rabi, William A Ghali, Herman W Barkema, and Gilaad G Kaplan. 2012. 'The relationship between urban environment and the inflammatory bowel diseases: a systematic review and meta-analysis', *BMC gastroenterology*, 12: 1-14.

Steerenberg, PA, CET Withagen, WJ Van Dalen, JAMA Dorma, SH Heisterkamp, H van Loveren, and FR Cassee. 2005. 'Dose dependency of adjuvant activity of particulate matter from five european sites in three seasons in an ovalbumin–mouse model', *Inhalation toxicology*, 17: 133-45.

Taghvaee, Sina, Amirhosein Mousavi, Mohammad H Sowlat, and Constantinos Sioutas. 2019. 'Development of a novel aerosol generation system for conducting inhalation exposures to ambient particulate matter (PM)', *Science of the Total Environment*, 665: 1035-45.

van EEDEN, STEPHAN F, Wan C Tan, Tatsushi Suwa, Hiroshi Mukae, Takeshi Terashima, Takeshi Fujii, Diwen Qui, Renaud Vincent, and James C Hogg. 2001. 'Cytokines involved in the systemic inflammatory response induced by exposure to particulate matter air pollutants (PM10)', *American journal of respiratory and critical care medicine*, 164: 826-30.

Vidgren, M, JC Waldrep, J Arppe, M Black, JA Rodarte, W Cole, and V Knight. 1995. 'A study of 99mtechnetium-labelled beclomethasone dipropionate dilauroylphosphatidylcholine liposome aerosol in normal volunteers', *International Journal of Pharmaceutics*, 115: 209-16.

Wang, Ting, Lichun Wang, Liliana Moreno-Vinasco, Gabriel D Lang, Jessica H Siegler, Biji Mathew, Peter V Usatyuk, Jonathan M Samet, Alison S Geyh, and Patrick N Breysse. 2012. 'Particulate matter air pollution disrupts endothelial cell barrier via calpain-mediated tight junction protein degradation', *Particle and fibre toxicology*, 9: 1-12.

Watanabe, Tomohiro, Naoki Asano, Peter J Murray, Keiko Ozato, Prafullakumar Tailor, Ivan J Fuss, Atsushi Kitani, and Warren Strober. 2008. 'Muramyl dipeptide activation of nucleotide-binding oligomerization domain 2 protects mice from experimental colitis', *The Journal of clinical investigation*, 118: 545-59.

Wirtz, Stefan, Clemens Neufert, Benno Weigmann, and Markus F Neurath. 2007. 'Chemically induced mouse models of intestinal inflammation', *Nature protocols*, 2: 541-46.

Wirtz, Stefan, Vanessa Popp, Markus Kindermann, Katharina Gerlach, Benno Weigmann, Stefan Fichtner-Feigl, and Markus F Neurath. 2017. 'Chemically induced mouse models of acute and chronic intestinal inflammation', *Nature protocols*, 12: 1295-309.

Xie, Shanshan, Caihong Zhang, Jinzhuo Zhao, Dan Li, and Jianmin Chen. 2022. 'Exposure to concentrated ambient PM2. 5 (CAPM) induces intestinal disturbance via inflammation and alternation of gut microbiome', *Environment International*, 161: 107138.

Yan, Fang, Lihong Wang, Yan Shi, Hanwei Cao, Liping Liu, M Kay Washington, Rupesh Chaturvedi, Dawn A Israel, Hailong Cao, and Bangmao Wang. 2012. 'Berberine promotes recovery of colitis and inhibits inflammatory responses in colonic macrophages and epithelial cells in DSS-treated mice', *American Journal of Physiology-Gastrointestinal and Liver Physiology*, 302: G504-G14.

Chapter 4- PM Inhalation in a Chronic Model of Intestinal Inflammation

Introduction

Around 6.8 million people in the world suffer from Inflammatory Bowel Disease (IBD) (Alatab et al. 2020). With no curative therapies, understanding the various factors involved in disease development becomes increasingly important as the prevalence of IBD continues to rise in developing nations (Alatab et al. 2020). IL-10 is an immunoregulatory cytokine and its suppression leads to overblown immune response via an abundance of proinflammatory cell secretion (Keubler et al. 2015). The IL-$10^{-/-}$ mouse is a widely studied immune-mediated, microbiota-dependent mouse model of colitis that may also manifest with enteritis. IL-$10^{-/-}$ colitis involves induction by microbial signals of pathogenic Th17 activity (Wang et al. 2019; Wang et al. 2020; Li, Gurung, et al. 2015; Sellon et al. 1998; Berg et al. 1996). This is consistent with studies in other settings supporting a link between the composition of the intestinal microbiota and Th17 responses (Skapenko et al. 2005). Oral administration of air pollution (PM_{10}) to IL-$10^{-/-}$ mice induces inflammation and increases mucosal exposure to bacteria in neonatal mice (Salim et al. 2014). This was associated with decreased *Bifidobacterium* and significantly elevated levels of the pro-inflammatory cytokines, IFN-γ and TNF-α (Salim et al. 2014). Ingested air particulate matter has also been shown to increase gut permeability and exacerbate colonic inflammation (Kish et al. 2013). Oral PM_{10} treatment of IL-$10^{-/-}$ mice for 35 days resulted in increased colonic epithelial hyperplasia, mononuclear infiltrate, and neutrophilic infiltrate ($p < 0.05$) compared to colons from WT control, WT PM_{10}, and IL-$10^{-/-}$ control groups (Kish et al. 2013). Furthermore, significant increases in IL-17, IL-1β, TNFα, and IL-12 were seen in the colons of IL-$10^{-/-}$ mice treated with PM_{10} for 35 days daily (Kish et al. 2013). These publications have shown the inflammatory and microbiome-modifying effects of ingested PMs in the context

of IL-10$^{-/-}$ mice. However, the effects of inhaled UFP on the IL-10$^{-/-}$ has yet to be elucidated, and it remains uncertain whether inhaled particles exacerbate inflammation in this murine model of spontaneous, genetic IBD. We hypothesize that inhaled UFP will similarly exacerbate IL-10$^{-/-}$ severity and that this will be mediated by effects of UFP on the intestinal microbiome.

In this chapter, we aimed at determining longitudinal and cross-sectional changes in the IL-10$^{-/-}$ microbiome after exposure to inhaled UFP. We conducted 2 separate experiments with PMs that were collected using 2 different methods and an increased number of mice in the second experiment to increase power to detect differences between UFP and FA.

Materials and Methods

Animal Subjects

Male B6.129P2-*Il10*^{tm1Cgn}/J mice from The Jackson Laboratory (JAX) were acclimated in our facilities for at least 1 week before the start of exposures. The mice were fed autoclaved chow diet ad libitum expect during exposures. Mice were housed in autoclaved shoe-box type cages with cornhusk bedding. Our research protocol was conducted in compliance with the Animal Research Committee and Institutional Animal Care and Use Committee (*IACUC*) at the University of California, Los Angeles (UCLA), and performed in coordination with the Division of Laboratory Animal Medicine (DLAM) at UCLA.

PM Inhalation Exposure

In the first experiment, 6-week-old IL-10$^{-/-}$ mice (n=10-11) were exposed to UFP for 6hr/session, 3/wk for 10 wks, at 350μg/m^3 in the Air Pollution Inhalation Exposure Facility (APIEF) in the animal vivarium (5V) in the Center for Health Sciences building at UCLA. A compressor pump built at the University of Southern California (USC) Viterbi School of Engineering pushed HEPA-filtered air into a Hope nebulizer (B&B Medical Technologies, USA)

to re-aerosolize the different PM-containing solutions into the ultrafine size range (Taghvaee et al. 2019) as previously described (Chang et al. 2024) (Fig. 14B). Re-aerosolized PM was drawn through a silica gel diffusion dryer (Model 3620, TSI Inc., USA) followed by Po-210 neutralizers (Model 2U500, NRD Inc., USA) to remove the excess water content and electrical charges of the particles, respectively. The air stream entered the animal exposure chamber with a flow rate of 2.5 lpm. Concurrently, re-aerosolized particles were collected on PTFE (Teflon) and Quartz (37-mm, Pall Life Sciences, 2-μm pore, Ann Arbor, MI) filters to chemically characterize particles in the system. In addition, variations in PM mass concentration were measured by TSI DustTrak during operation, where the average PM concentration was set at about 350 $\mu g/m^3$. In the same room, ambient air was passed through a HEPA-filter and drawn into an adjacent chamber by a vacuum pump as the experimental control chamber. In the second experiment, 6-week-old male IL-$10^{-/-}$ (n=20-22) were exposed to UFP for 5hr/session, 3/wk for 10 wks, at 450$\mu g/m^3$ as described above in the same facility.

Collection of Particulate Matter

Both PMs used in this study were collected from Los Angeles as UFP and re-aerosolized as UFP by collaborators from the University of Southern California (USC). Particles used for the first experiment were collected on PTFE membrane filters (20 × 25 cm, 3.0 μm pore size, PALL Life Sciences, USA) using a high-volume sampler (with a flow rate of 250 lpm) connected to a PM pre-impactor for separation. Particles from the second experiment were collected using a gelatin cascade impactor consisting of an air inlet and pump separated by 2 impaction states and a filter holder at the end. Gelatin filters were placed at each impaction step diameters 47mm and 80mm, and the impactor was operated at a flow rate of 100 lpm. Particles collected in this

manner have been previously demonstrated to retain redox-active constituents of particulates (Aldekheel et al. 2023).

Sample Collection, DNA Extraction and 16S rRNA Gene Sequencing

All mice were euthanized under isoflurane anesthesia 18 hours after the last exposure. Colon and cecal tissue was harvested post-mortem as previously described (Jacobs et al. 2017). Colon length excluding the cecum was measured in centimeters and weighed in milligrams. Samples were thawed from -80°C and underwent DNA extraction using the ZymoBIOMICS DNA Microprep Kit or ZymoBIOMICS 96 DNA Kit (Zymo Research, Irvine, CA, USA) according to the manufacturer's instructions. Sequencing of the 253 base pair V4 region of 16S ribosomal RNA gene was performed using the Illumina MiSeq. Sequenced data were processed into amplicon sequence variants (ASVs), and assigned taxonomy using the DADA2 pipeline (Callahan et al. 2016) in R with the SILVA 132 database.

Microbiome Diversity Analysis

Alpha diversity was assessed using the Shannon index, a metric of species evenness and richness, with data rarefied to a sequencing depth of 5,000 in each sample subset (Jacobs et al. 2016). The data was fitted to linear mixed effects models in R studio and statistical analyses was performed using the lmer function. Exposure group, timepoint, and their interaction were included as fixed effects in all models. Mouse ID was treated as a random effect for longitudinal fecal microbiome data and cage as a random effect for tissue microbiome data.

For beta diversity and differential abundance analysis, data were filtered to remove ASVs that were present in less than 25% of all samples. Beta diversity was assessed using the Bray-Curtis dissimilarity matrix to identify microbiome compositional differences between the different treatment groups (PM vs. FA) and in the longitudinal fecal pellet data (Week 0, 1, 5, and 10).

Statistical analyses was performed using permutational multivariate analysis of variance (PERMANOVA) implemented in the Adonis package in R with treatment, timepoint (with week 0 as the baseline), and their interaction as fixed effects and cage or mouse ID as strata for permutations. Differences in taxa abundances between exposure groups were analyzed using MaAsLin2 in R (Version 1.4.1106, Vienna, Austria) with treatment and timepoint as fixed effects, and cage or mouse ID as a random effect (Mallick et al. 2021). P-values were adjusted for multiple comparisons using the Benjamin–Hochberg method. Significance threshold was set at q-value<0.10.

Histological Scoring

A 1.0 cm piece of the distal colon was cut and fixed in 10% phosphate buffered formalin before being transferred to 70% ethanol. Cassettes containing the samples were sent to the Translational Pathology Core Laboratory (TPCL) at UCLA to be embedded in paraffin, sectioned, and stained with hematoxylin and eosin (H&E). A first colon subscale scored inflammation from 0-6 with severity ranging from normal to severe inflammatory cell infiltrates, and a second colon subscale (0-6) was based on extent ranging from only the mucosa to transmural involvement (Katakura et al. 2005; Jacob et al. 2018). In the first subscore, a score of 1 was assigned for hyperproliferation, irregular crypts, and goblet cell loss, 1.5 for mild crypt loss (10-25%), 2 for moderate crypt loss (25%-50%), 2.5 for severe crypt loss(50-75%), 3 severe crypt loss (75-90%), 4 for complete crypt loss, 5 for ulcers <10 crypts wide, and 6 for ulcers >10 crypts wide. For the second subscale, changes in intestinal architecture were scored from 0-6 by adding the scores from each layer of the intestinal wall. The mucosa was scored from 0-3 (0: Normal, 1: Mild, 2: Modest, 3: Severe), the submucosa was scored from 0-2 (0: Normal, 1: Mild to modest, 2: Severe), and the serosa was scored 0-1 (0: Normal, 1: Moderate to severe).

Microbiome Diversity Analysis

Assessment of alpha diversity was conducted using the Shannon index, a metric of species evenness and richness, with data rarefied to a sequencing depth of 5,000 in each sample subset (Jacobs et al. 2016). The data was fitted to linear mixed effects models in R studio and statistical analyses was performed using the lmer function. Exposure group, timepoint, and their interaction were included as fixed effects in all models. Mouse ID was treated as a random effect for longitudinal fecal microbiome data and cage as a random effect for tissue microbiome data. In the beta diversity and differential abundance analysis, data were filtered to remove ASVs that were present in less than 25% of all samples. Beta diversity analysis was conducted with the Bray-Curtis dissimilarity matrix to identify microbiome compositional differences between the different treatment groups (PM vs. FA) and in the longitudinal fecal pellet data (Week 0, 1, 5, and 10) from the first experiment, with the addition of Week 3 timepoint in the second experiment. Statistical analyses was performed using permutational multivariate analysis of variance (PERMANOVA) implemented in the Adonis package in R with treatment, timepoint (with week 0 as the baseline), and their interaction as fixed effects and cage or mouse ID as strata for permutations. Differences in taxa abundances between exposure groups were analyzed using MaAsLin2 in R (Version 1.4.1106, Vienna, Austria) with treatment and timepoint as fixed effects, and cage or mouse ID as a random effect (Mallick et al. 2021). P-values were adjusted for multiple comparisons using the Benjamin–Hochberg method. Significance threshold was set at q-value<0.10.

RT-qPCR

~1.5 cm pieces of the midsection of the colon were cut and fixed in RNAlater®. The Qiagen RNAeasy Mini Kit was used to extract RNA from thawed intestinal sections according to

the manufacturer's instructions. A total of 200 nanograms of extracted RNA in each sample was used for reverse-transcribed cDNA synthesis using the Applied Biosystems High-Capacity cDNA Reverse Transcription Kit according to the manufacturer's instructions (Applied Biosystems catalog# 4368814). The mRNA expression of target genes was detected using Applied Biosystems TaqMan Fast Advanced Master Mix (catalog# 4444557) and TaqMan probes for β-actin (Mm02619580_g1), IL-1β (Mm00434228_m1), IFNγ (Mm01168134_m1), and TFNα (Mm00443258_m1). qPCR for target genes was conducted for each sample in triplicate and each reaction was performed in a final volume of 10µL including 2.5µL of cDNA 0.5µL of the respective probe, 5µL of Master mix, and 2µL of water. TheLightCycler 480 program consisted of an initial pre-incubation warm-up cycle to 95°C for 10 minutes, followed by 45 cycles of amplification (95°C for 10 s, 60°C for 30 s, and 72°C for 1 s) and a cooling cycle at 40°C for 30 s. Quantitative PCR was performed in a LightCycler 480 (Roche Diagnostics) and gene expression was analyzed using the delta-delta Ct (DDCt or ddCt) method.

Statistical Analyses

Colon weight/length ratio and histological scores were shown by violin plots and analyzed by the Mann-Whitney U-test in R studio (threshold *p-value* <0.05).

Results

Increased inflammation severity in IL-10$^{-/-}$ mice exposed to inhaled PM

Subchronic UFP inhalation was modeled by exposing mice to ambient PM collected at an urban site for 10 weeks, then resuspended in the ultrafine size range in a closed exposure chamber as described in previous chapters. The mice from experiment 1 underwent UFP exposures for 6 hours/day, three days per week for 10 weeks at a concentration of 350 µg/m^3, while mice from experiment 2 underwent UFP exposures for 5hr/day, three times per week for 10

weeks at 450 μg/m^3(Fig. 14A). The PM exposure setup was as described in Chapters 1 and 2 (Fig. 14B). The greatest fraction of extracted PM for the exposures from the first experiment was total carbon (~52%), followed by inorganic ions (~28%), and metal elements (~52%) (Fig. 14C). In the second experiment, the chemical analysis showed total carbon (~51%), followed by inorganic ions (~27%), and metal elements (~22%) (Fig. 14C). In total, 21 mice were exposed to PM vs FA (n=10-11/group), and 42 mice were exposed in the second experiment (n=20-22/group).

We conducted two experiments exposing IL-10$^{-/-}$ mice to re-aerosolized PM 3/wk for 10 wks. In the first experiment, 10-11 mice were exposed to 6 hr sessions at PM concentrations of 350μg/m^3, while in the second experiment, 20-22 mice were exposed at 5 hr sessions at PM concentrations of 450 μg/m^3. performed double-blind histological scoring of the colons collected after 10 weeks of UFP inhalation exposure and found that while there was no significant difference seen in inflammation severity between the PM and FA groups in experiment one (Fig. 15A,C), colons in the PM group from experiment two showed a significant increase in histologic severity compared to their FA counterparts (Fig. 16A,C). Likewise, colon weight/length ratio showed a borderline significant difference (*p=0.074*) between PM and FA groups in the second experiment (Fig 17B), a change which was not observed in the first experiment (Fig. 16B). The mRNA levels of proinflammatory cytokines (IL-1β, IFNγ, TFNα) were similar between the PM and FA-exposed mice in the colons of mice from both experiments (Fig. 16D).

Longitudinal changes in the fecal microbiome of IL-10$^{-/-}$ mice after subchronic inhalation exposure to PM

In both experiments, fecal samples were collected at baseline and weeks 1, 5, and 10 of exposures to assess the kinetics of PM effects on the microbiome, with the addition of a

timepoint at week 3 in the second experiment. All samples underwent microbiome characterization by 16S rRNA gene sequencing. Longitudinal analysis of fecal samples from experiment 2 *IL-10*$^{-/-}$ mice showed that subchronic exposure to UFPs did not significantly alter alpha diversity (Fig. 17A, Fig. 18A) and while no beta diversity changes were seen between PM and FA in the first experiment (Fig. 17B), changes in microbiome composition were observed in experiment 2(Fig. 18B). Microbial beta diversity was significantly altered in the UFP-exposed group compared to the FA group at week 3 ($p=0.032$), week 5 ($p=0.013$), and week 10 ($p=0.026$) in experiment 2, but not in experiment 1 (Fig. 18B). There were significant differences in microbial abundances at all time points by testing of differential abundance at the level of amplicon sequence variants (ASVs), which roughly corresponds to species (Fig. 17C, Fig. 18C). Similar to the differential abundance results seen in Chapter 2, there was an increase in the number of ASVs with an increasing duration of exposures in the first experiment. Thus, while there was enrichment of only 2-5 ASVs at weeks 1 and 5 (Fig.17C), there was enrichment of 10 ASVs at week 10 in experiment 1. In the 2nd experiment, differentially abundant taxa were found at each tested time point (week 1, 3, 5, and 10) (Fig. 18C). This includes several members of the family *Muribaculaceae* and *Lachnospiraceae*.

Cross-sectional changes in the cecal and colonic microbiomes

Cecum and colon samples were collected after euthanasia and underwent 16S rRNA gene sequencing to characterize the microbiome. *Il-10*$^{-/-}$ mice showed a significant difference in beta diversity in the cecum microbiota ($p<10^{-5}$, Fig. 19A, Fig 20A) and colon microbiota ($p<10^{-5}$, Fig. 19B, Fig. 20B) of mice from both experiments. While there were no differences in alpha diversity in the first experiment, there was a significant difference in the Shannon index in the colon microbiome of mice from experiment 2 ($p=0.013$, Fig 20B). In addition, PM induced

significant changes in microbial abundance in both experiments. In the first experiment, the *RF39* ASV was significantly decreased in both the cecum and the colon (Fig 19A,B). In the second experiment the *Muribaculaceae* ASV was upregulated in both the cecum and in the colon, a *Desulfovibrio* ASV was downregulated in both regions (Fig. 20A,B), while a *Lachnospiraceae* ASV and a *[Eubacterium] ventriosum* ASV were downregulated in the colon.

Discussion

This study is the first to report on the effects of ultrafine PM inhalation on the IL-10$^{-/-}$ mouse model. Here we use PM collected from 2 different methods, and showed that PMs collected from both methods were bioactive to alter the microbiome of IL-10$^{-/-}$ after 10 weeks of subchronic exposure. We furthermore found changes in histological severity after exposure to PM collected via gel cascade impactor, combined with a larger sample size of IL-10$^{-/-}$ mice in experiment 2.

While there is epidemiological evidence to link air pollution to IBD, the mechanism of this association is unknown. It has been shown that orogastric exposure of IL-10$^{-/-}$ mice to pollution particles via gavage or food induces onset of intestinal inflammation (Salim et al. 2014; Kish et al. 2013). Inhalation of air particulate matter, which is the most physiologically relevant route of exposure, remained yet to be studied to our knowledge in any experimental, chronic model of IBD. Our study involves UFP that had been collected from the I-110 freeway in Los Angeles, re-aerosolized with a nebulizer and pumped to whole-body animal chambers. UFP is a subset of particulate matter that has been gaining recognition for its toxicity (Volk et al. 2013; Schraufnagel 2020), as the high specific area of UFP allows it to absorb and react with more organic compounds and toxic chemicals, promoting oxidative stress.

Currently, there is no data to support a causative connection between air pollution and intestinal inflammation via the microbiome, and scientific knowledge on the role of PM-modulated gut commensal bacteria in colitis is limited. The high prevalence in IBD of loss of therapeutic response and development of disease complications such as infections and strictures that require bowel resection highlights the importance of understanding the factors contributing to the development and treatment of this disease (San Román and Muñoz 2011). A closer analysis of the genetic transcripts may be necessary to identify cytokines involved in driving the inflammation we observe, beyond the cytokines we tested by RT-qPCR (IL-1β, IFNγ, TFNα).

This study is the first to research inhaled UFP in IL-10$^{-/-}$ mice and provide relevant insight into the effects of the urban pollution encountered in the United States on IBD. The IL-10 gene plays an important role in maintaining homeostasis in the gut via mucosal immune regulation. Not only does it suppress production of proinflammatory cytokines, it also scavenges inflammatory chemokines (D'amico et al. 2000). The IL-10$^{-/-}$ model is well-suited for investigating the role of an environmental factor on IBD pathogenesis due to data showing that germ-free IL-10$^{-/-}$ mice do not develop colitis (Sellon et al. 1998). Furthermore, the development of spontaneous inflammation in IL-10$^{-/-}$ mice strictly correlated to their microbiota composition. Although the role of the intestinal microbiome in IBD has been extensively studied and candidate mediators of inflammation such as *Enterobacteriaceae* (Zuo and Ng 2018) have been identified, it is unknown which environmental risk factors promote the development of dysbiosis in IBD and can explain the rising incidence of disease worldwide. This study is not only the first to assess whether inhaled air pollutants exacerbate an experimental, chronic model of IBD, but also surveys microbiome changes over time to UFP inhalation. Future microbiome transfer

experiments are necessary to establish a cause-and-effect relationship between microbiome change after air pollution exposure and inflammation.

Additionally, experiments with other chronic models of colitis mice and chronic PM inhalation exposure are needed to further investigate the impact of air pollution on IBD. Conducting experiments of inhaled UFP in other chronic mouse models may be useful to elucidate the roles of PM in various pathways of IBD pathogenesis. These may include the chronic DSS model, which focuses on effect of impaired barrier function and mucin in IBD development. The T cell transfer model can be also used to delineate whether PM inhalation is involved in immunological processes of IBD development. It modulated by the microbiome, making it suitable to investigate whether UFP alters intestinal T-cell driven inflammation via the microbiome (Britton et al. 2020). C57BL/6 donor mice could be exposed to inhaled UFP and an adoptive transfer of their naïve T cells ($CD4^{+}CD45RB^{high}$) into immune-deficient $Rag^{-/-}$ mice (recombinase activating gene-1 deficient mouse). Lastly, as discussed in previous chapters, the length of exposure or dosage of PM may lend to more significant results, had the exposure been prolonged. A dose-response study may also provide insight to the range of PM toxicity in terms of IBD.

In this chapter, we have demonstrated that subchronic UFP inhalation induces microbiome changes and increases histological markers of inflammation in the $IL\text{-}10^{-/-}$ mouse model.

Figures

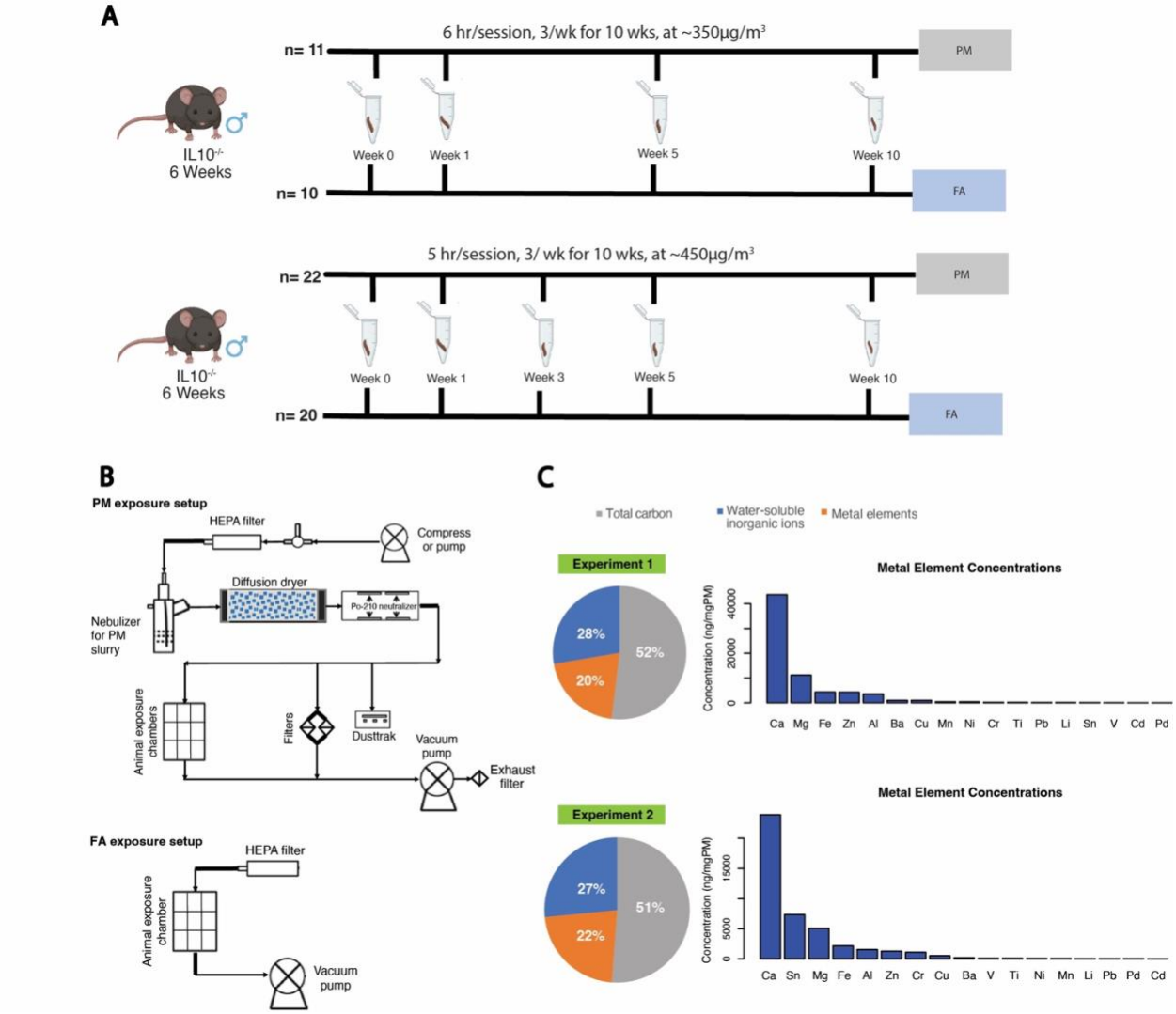

Figure 14. Exposure protocol and PM characterization. (A) Experimental design for the first (TOP) and second (BOTTOM) experiments, where male IL-10$^{-/-}$ mice were exposed to UFPs by inhalation 3 times per week for 10 weeks. Fecal pellet samples were collected at weeks 0 (baseline), 1, 5, and 10 to evaluate longitudinal changes in both experiments, and week 3 was included as an additional time point in the second experiment. Cecal and colon samples were collected following euthanasia. Figure1A was created with Biorender.com. (B) Schematic of aerosol generation and exposure system (C) Chemical profile of the PM aerosol in Experiments 1 and 2.

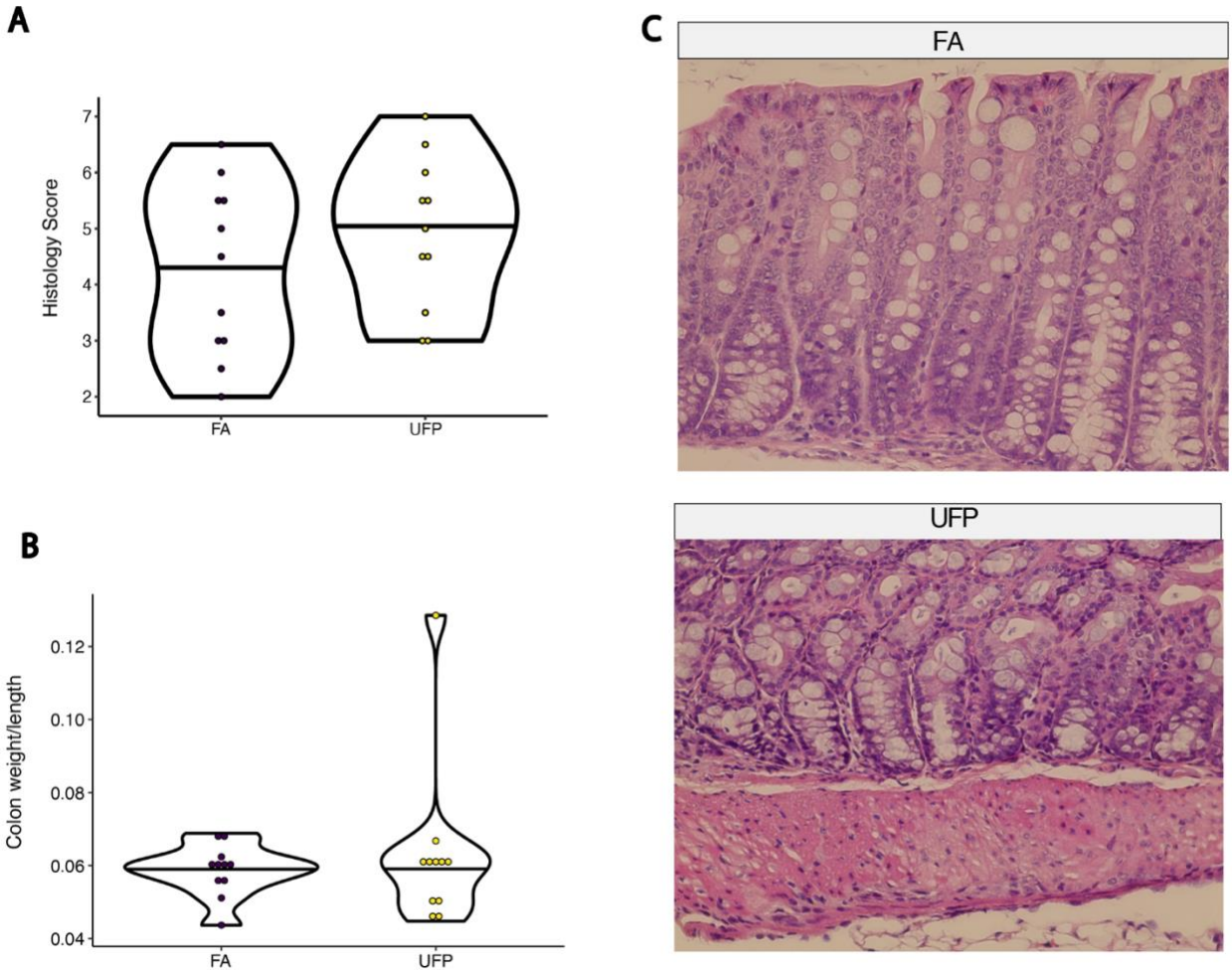

Figure 15. UFP inhalation exposure did not alter histological severity or colon weight/length in the first experiment. (A) Histology scores visualized by violin plot. (B) Colon weight/length with weight measured in miligrams and length measured in centimeters. (C) Representative median colon histology images from the UFP and FA groups.

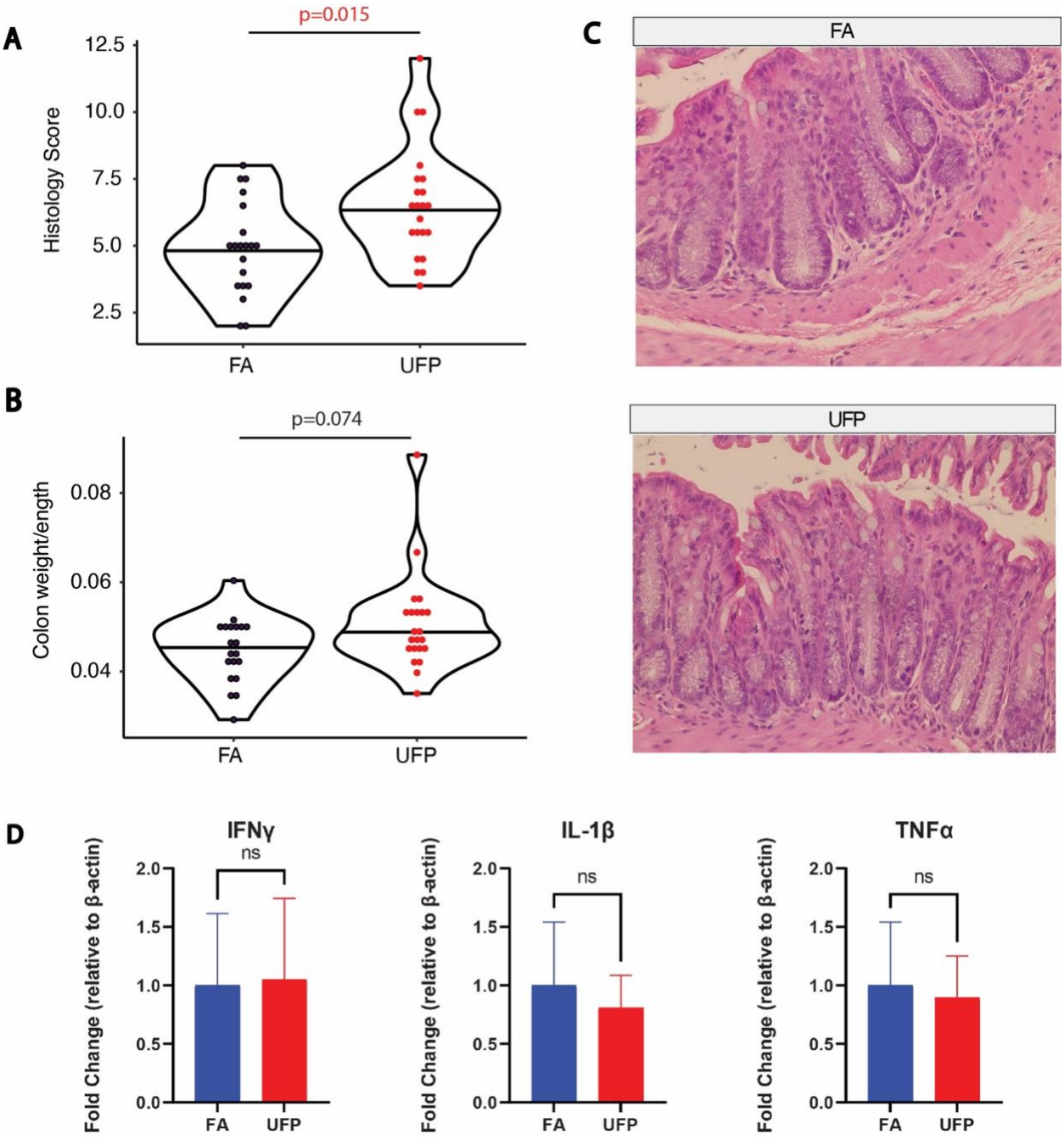

Figure 16. UFP inhalation exposure increased inflammatory cell infiltrates in the colon.
(A) Histology scores visualized as violin plot. (B) Colon weight/length with weight measured in milligrams and length measured in centimeters. (C) Representative median colon histology images from the UFP and FA groups. (D) mRNA levels of proinflammatory cytokines IL-1β, IFNγ, and TNF-α measured by RT-qPCR. ns= not significant.

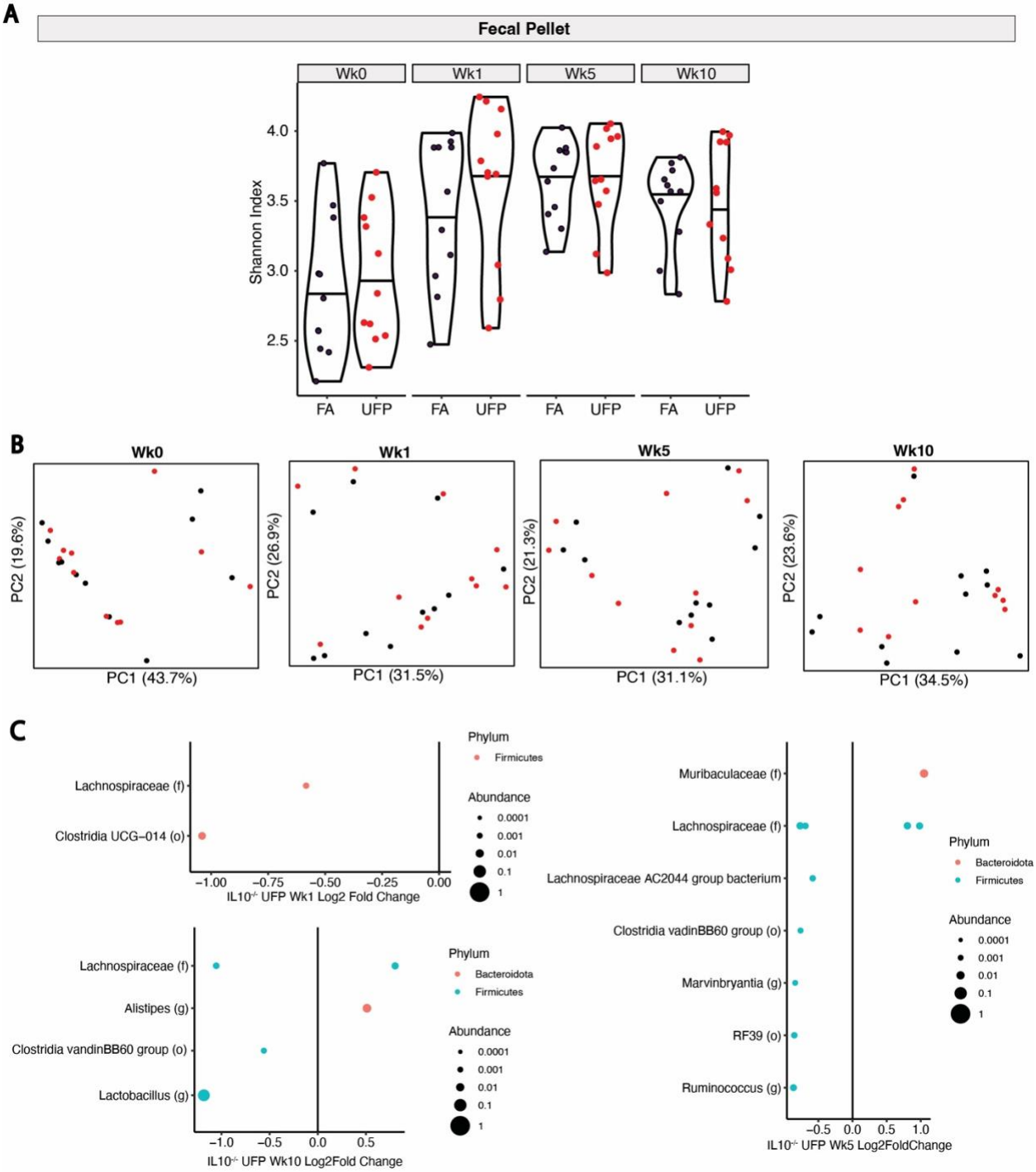

Figure 17. Differentially abundant taxa identified in IL-10$^{-/-}$ mice following subchronic UFP exposure from experiment 1. (A) Violin plots of fecal microbial alpha diversity *IL-10*$^{-/-}$ mice, measured by the Shannon index at weeks 0, 1, 5, and 10. (B) PCoA plots of Bray-Curtis dissimilarity, showing microbial composition of UFP and FA groups. Significance determined by PERMANOVA. (C) Differentially abundant fecal taxa between UFP and FA are also shown.

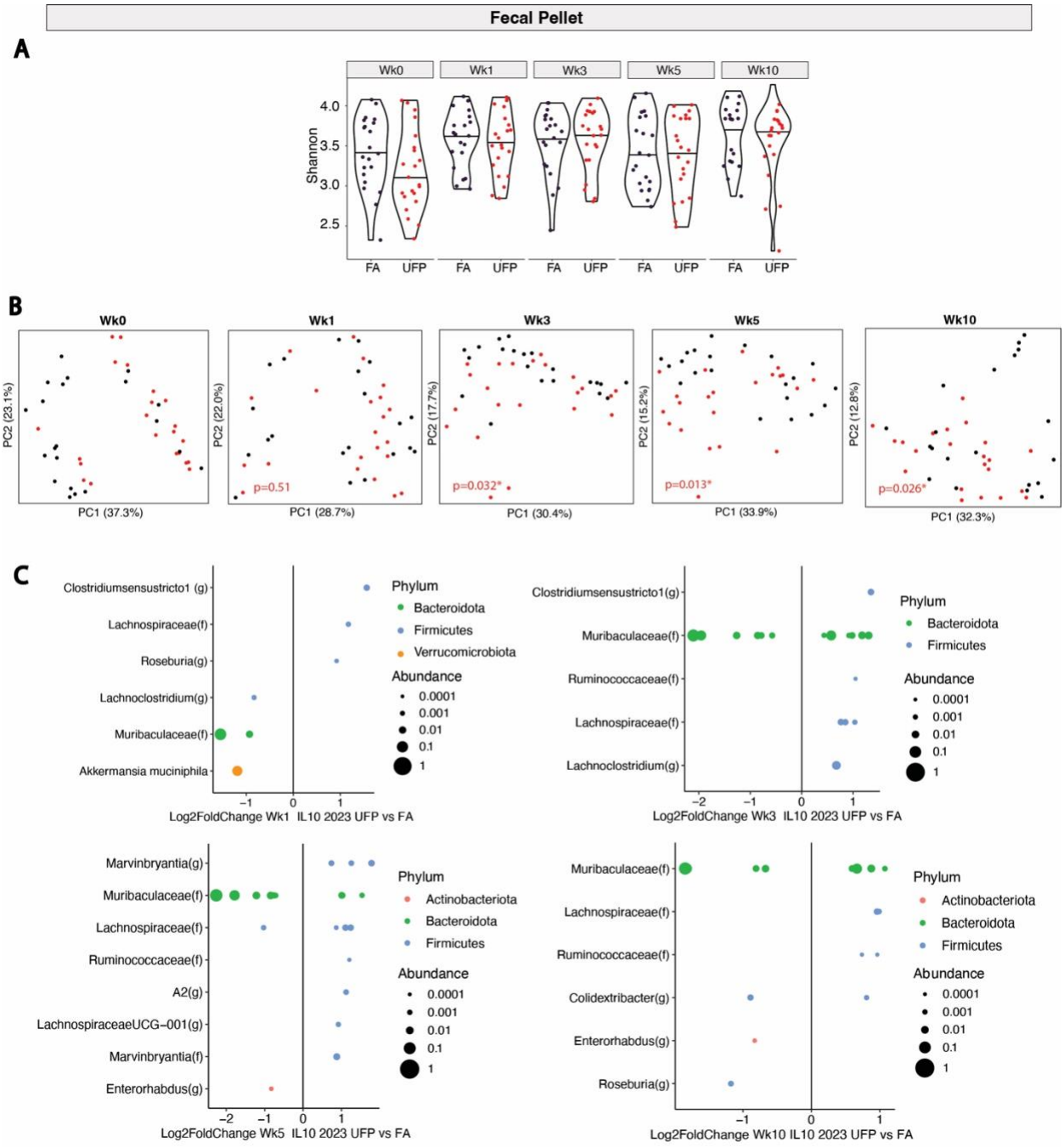

Figure 18. Subchronic UFP exposure induces shifts in fecal microbial composition in IL-10$^{-/-}$ from experiment 2. (A) Violin plots of fecal microbial alpha diversity *IL-10*$^{-/-}$ mice, measured by the Shannon index at weeks 0, 1, 3, 5, and 10. (B) PCoA plots of Bray-Curtis dissimilarity, showing microbial composition of UFP and FA groups. Significance determined by PERMANOVA. (C) Differentially abundant fecal taxa between UFP and FA are also shown.

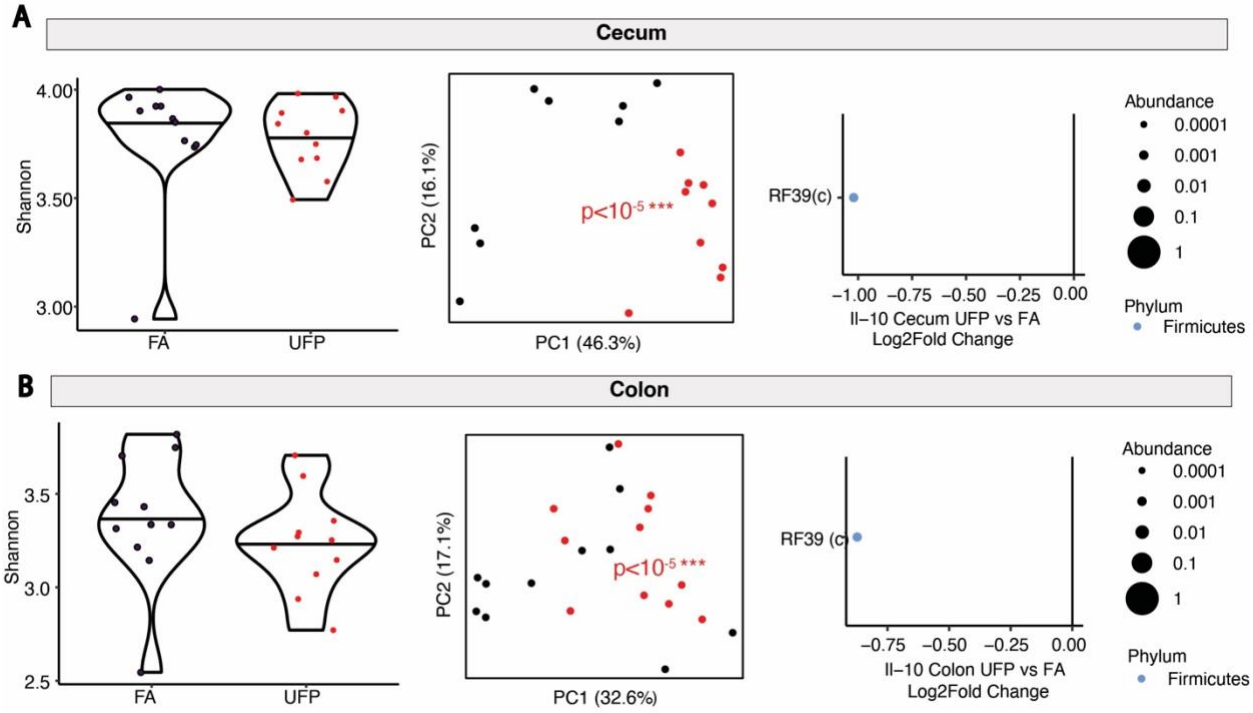

Figure 19. Subchronic UFP exposure alters cecal and colonic microbial composition in IL-10$^{-/-}$ mice from the 1st experiment. (A) Cecal and (B) colonic microbiome data, from left to right: (left)Violin plot displaying alpha diversity (Shannon index), (middle) PCoA plots showing microbial compositional differences between the UFP and FA groups after 10 weeks, and (right) Log2FoldChange plots showing differential taxa in the UFP group compared to FA group. Each dot represents one ASV, displayed with its lowest taxonomic classification which could be at the species, genus (g), family (f), or order (o) level, when species was not available.

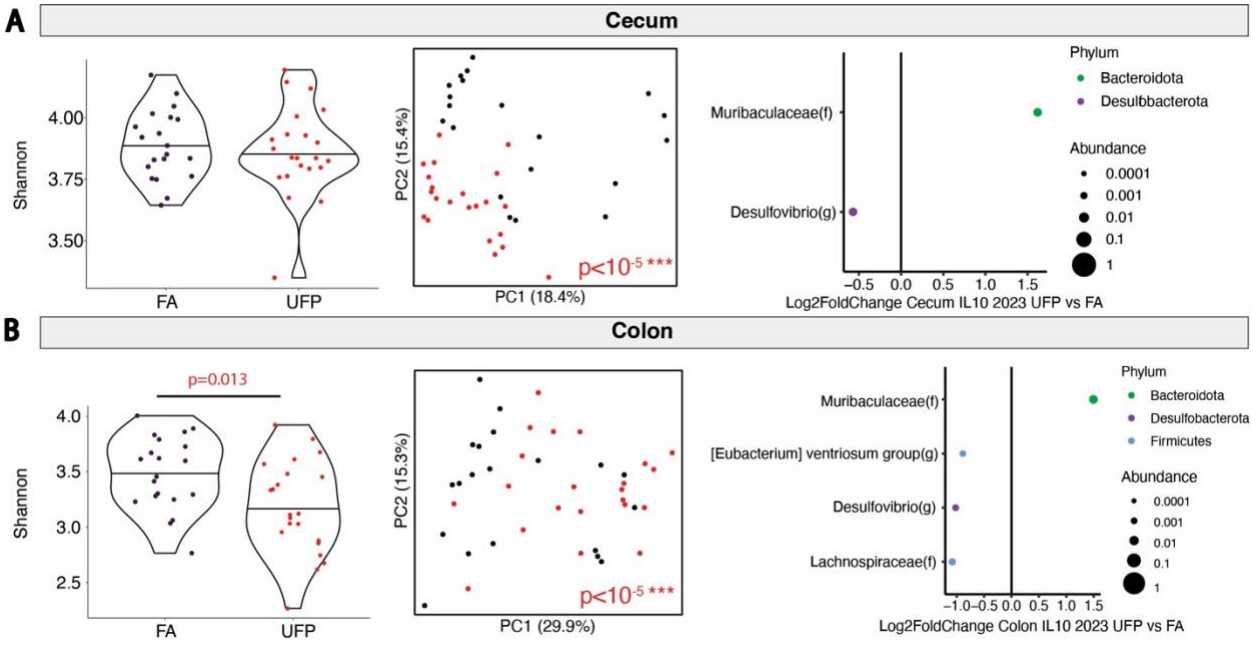

Figure 20. Subchronic UFP exposure induces shifts in fecal microbial composition in the cecum and colons of experiment 2 IL-10$^{-/-}$ mice. (A) Cecal and (B) colonic microbiome changes from left to right: (left) Violin plots of fecal microbial alpha diversity *IL-10*$^{-/-}$ mice, measured by the Shannon index, (middle) PCoA plots of Bray-Curtis dissimilarity, showing microbial composition of UFP and FA groups, Significance determined by PERMANOVA, (right) Log2FoldChange plots showing differential taxa in the UFP group compared to FA group. Each dot represents one ASV, displayed with its lowest taxonomic classification which could be at the species, genus (g), family (f), or order (o) level, when species was not available.

References

Alatab, Sudabeh, Sadaf G Sepanlou, Kevin Ikuta, Homayoon Vahedi, Catherine Bisignano, Saeid Safiri, Anahita Sadeghi, Molly R Nixon, Amir Abdoli, and Hassan Abolhassani. 2020. 'The global, regional, and national burden of inflammatory bowel disease in 195 countries and territories, 1990–2017: a systematic analysis for the Global Burden of Disease Study 2017', *The Lancet gastroenterology & hepatology*, 5: 17-30.

Aldekheel, Mohammad, Vahid Jalali Farahani, Ramin Tohidi, Abdulmalik Altuwayjiri, and Constantinos Sioutas. 2023. 'Development and performance evaluation of a two-stage cascade impactor equipped with gelatin filter substrates for the collection of multi-sized particulate matter', *Atmospheric Environment*, 294: 119493.

Berg, Daniel J, Natalie Davidson, Ralf Kühn, Werner Müller, Satish Menon, Gina Holland, LuAnn Thompson-Snipes, Michael W Leach, and Donna Rennick. 1996. 'Enterocolitis and colon cancer in interleukin-10-deficient mice are associated with aberrant cytokine production and CD4 (+) TH1-like responses', *The Journal of clinical investigation*, 98: 1010-20.

Britton, Graham J, Eduardo J Contijoch, Matthew P Spindler, Varun Aggarwala, Belgin Dogan, Gerold Bongers, Lani San Mateo, Andrew Baltus, Anuk Das, and Dirk Gevers. 2020. 'Defined microbiota transplant restores Th17/RORγt+ regulatory T cell balance in mice colonized with inflammatory bowel disease microbiotas', *Proceedings of the National Academy of Sciences*, 117: 21536-45.

Callahan, Benjamin J, Paul J McMurdie, Michael J Rosen, Andrew W Han, Amy Jo A Johnson, and Susan P Holmes. 2016. 'DADA2: High-resolution sample inference from Illumina amplicon data', *Nature methods*, 13: 581-83.

D'amico, G, G Frascaroli, G Bianchi, P Transidico, A Doni, A Vecchi, S Sozzani, P Allavena, and A Mantovani. 2000. 'Uncoupling of inflammatory chemokine receptors by IL-10: generation of functional decoys', *Nature immunology*, 1: 387-91.

Jacob, Noam, Jonathan P Jacobs, Kotaro Kumagai, Connie WY Ha, Yoshitake Kanazawa, Venu Lagishetty, Katherine Altmayer, Ariel M Hamill, Aimee Von Arx, and R Balfour Sartor. 2018. 'Inflammation-independent TL1A-mediated intestinal fibrosis is dependent on the gut microbiome', *Mucosal immunology*, 11: 1466-76.

Jacobs, Jonathan P, Maryam Goudarzi, Namita Singh, Maomeng Tong, Ian H McHardy, Paul Ruegger, Miro Asadourian, Bo-Hyun Moon, Allyson Ayson, and James Borneman. 2016. 'A disease-associated microbial and metabolomics state in relatives of pediatric inflammatory bowel disease patients', *Cellular and molecular gastroenterology and hepatology*, 2: 750-66.

Jacobs, Jonathan P, Lin Lin, Maryam Goudarzi, Paul Ruegger, Dermot PB McGovern, Albert J Fornace Jr, James Borneman, Lijun Xia, and Jonathan Braun. 2017. 'Microbial, metabolomic, and immunologic dynamics in a relapsing genetic mouse model of colitis induced by T-synthase deficiency', *Gut microbes*, 8: 1-16.

Katakura, Kyoko, Jongdae Lee, Daniel Rachmilewitz, Gloria Li, Lars Eckmann, and Eyal Raz. 2005. 'Toll-like receptor 9–induced type I IFN protects mice from experimental colitis', *The Journal of clinical investigation*, 115: 695-702.

Keubler, Lydia M, Manuela Buettner, Christine Häger, and André Bleich. 2015. 'A multihit model: colitis lessons from the interleukin-10–deficient mouse', *Inflammatory bowel diseases*, 21: 1967-75.

Kish, Lisa, Naomi Hotte, Gilaad G Kaplan, Renaud Vincent, Robert Tso, Michael Gänzle, Kevin P Rioux, Aducio Thiesen, Herman W Barkema, and Eytan Wine. 2013.

'Environmental particulate matter induces murine intestinal inflammatory responses and alters the gut microbiome', *PloS one*, 8: e62220.

Li, Bofeng, Prajwal Gurung, RK Subbarao Malireddi, Peter Vogel, Thirumala-Devi Kanneganti, and Terrence L Geiger. 2015. 'IL-10 engages macrophages to shift Th17 cytokine dependency and pathogenicity during T-cell-mediated colitis', *Nature communications*, 6: 1-13.

Mallick, Himel, Ali Rahnavard, Lauren J McIver, Siyuan Ma, Yancong Zhang, Long H Nguyen, Timothy L Tickle, George Weingart, Boyu Ren, and Emma H Schwager. 2021. 'Multivariable association discovery in population-scale meta-omics studies', *PLoS computational biology*, 17: e1009442.

Salim, Saad Y, Juan Jovel, Eytan Wine, Gilaad G Kaplan, Renaud Vincent, Aducio Thiesen, Herman W Barkema, and Karen L Madsen. 2014. 'Exposure to Ingested Airborne Pollutant Particulate Matter Increases Mucosal Exposure to Bacteria and Induces Early Onset of Inflammation in Neonatal IL-10–Deficient Mice', *Inflammatory bowel diseases*, 20: 1129-38.

San Román, Antonio López, and Fernando Muñoz. 2011. 'Comorbidity in inflammatory bowel disease', *World journal of gastroenterology: WJG*, 17: 2723.

Schraufnagel, Dean E. 2020. 'The health effects of ultrafine particles', *Experimental & molecular medicine*, 52: 311-17.

Sellon, Rance K, Susan Tonkonogy, Michael Schultz, Levinus A Dieleman, Wetonia Grenther, ED Balish, Donna M Rennick, and R Balfour Sartor. 1998. 'Resident enteric bacteria are necessary for development of spontaneous colitis and immune system activation in interleukin-10-deficient mice', *Infection and immunity*, 66: 5224-31.

Skapenko, Alla, Jan Leipe, Peter E Lipsky, and Hendrik Schulze-Koops. 2005. 'The role of the T cell in autoimmune inflammation', *Arthritis research & therapy*, 7: 1-11.

Taghvaee, Sina, Amirhosein Mousavi, Mohammad H Sowlat, and Constantinos Sioutas. 2019. 'Development of a novel aerosol generation system for conducting inhalation exposures to ambient particulate matter (PM)', *Science of the Total Environment*, 665: 1035-45.

Volk, Heather E, Fred Lurmann, Bryan Penfold, Irva Hertz-Picciotto, and Rob McConnell. 2013. 'Traffic-related air pollution, particulate matter, and autism', *JAMA psychiatry*, 70: 71-77.

Wang, Huaijun, Jose G Vilches-Moure, Samir Cherkaoui, Isabelle Tardy, Charline Alleaume, Thierry Bettinger, Amelie Lutz, and Ramasamy Paulmurugan. 2019. 'Chronic Model of Inflammatory Bowel Disease in IL-10-/-Transgenic Mice: Evaluation with Ultrasound Molecular Imaging', *Theranostics*, 9: 6031.

Wang, Shaoxuan, JinXuan Wang, Ran Ma, Shaofeng Yang, Tingting Fan, Jing Cao, Yang Wang, Wenbin Ma, Wenxiu Yang, and Fulai Wang. 2020. 'IL-10 enhances T cell survival and is associated with faster relapse in patients with inactive ulcerative colitis', *Molecular immunology*, 121: 92-98.

Zuo, Tao, and Siew C Ng. 2018. 'The gut microbiota in the pathogenesis and therapeutics of inflammatory bowel disease', *Frontiers in microbiology*, 9: 2247.

Chapter 5-Conclusions and Future Directions

Our research demonstrated that inhalation of UFPs induced changes in the gut microbiome, in a manner independent of measured inflammatory markers. Furthermore, we showed that subchronic UFP inhalation increases inflammation in the intestine in a model predisposed to inflammation. The kinetics of microbiome change is first discussed in the context of subchronic exposure in hyperlipidemic and normolipidemic models in Chapter 2. To our knowledge, the kinetics of the fecal microbiome change caused by UFP inhalation over time has not been reported before. There were strain specific changes reflected by alterations in different regions of the gut across the three types of mice. Longitudinal microbiome changes were also confirmed in the IL-10$^{-/-}$ mice as reported in Chapter 4.

In Chapter 3, we found that short term exposures to UFP inhalation did not affect severity of two acute mouse models of colitis. In both the DSS and TNBS models, there was no significant decrease in percent weight after exposure to PM, nor were there any differences in histological markers of inflammation. In the acute DSS model exposed to PM, we detected no differences from the FA group in terms of the DAI, a clinical assessment which considers percent weight change, stool consistency, and occult blood in the stool. Higher doses of PM may be required to detect changes in a shorter length of time.

Finally, in Chapter 4, we showed that UFP inhalation exacerbates inflammation in the context of predisposition to chronic IBD, specifically in the IL-10$^{-/-}$ model. A microbiome transfer experiment would be necessary to ascertain the role of the microbiome in the development of inflammation in IL-10$^{-/-}$ mice, and future UFPs experiments using other chronic models of chronic colitis would be informative to understand the how UFP inhalation affects the varied pathogeneses of IBD.

This dissertation addressed the effects of UFP inhalation across various animal models and lengths of time. As global incidence of IBD continues to rise, it is necessary to consider regulation of airborne particles, keeping in mind the far-reaching effects that PM on the many diseases related to inflammatory processes. While our study did not prove that the UFP-exposed microbiome is a mechanistic factor contributing to IBD, our findings support the necessity to conduct additional studies to decipher the relationship between UFP, the microbiome, and its effect on inflammation. The high prevalence in IBD of loss of therapeutic response and development of disease complications such as infections and strictures that require bowel resection highlights the importance of understanding the factors contributing to the development and treatment of this disease. As current antibacterial therapies and fecal microbial transplants have variable outcome, physiologically relevant therapies are necessary. Identifying clearer microbial targets of UFP-induced intestinal inflammation will progress development of microbiome-directed therapeutic strategies such as faux-biotics or small molecule treatment. Studies on specific microbes that worsen disease severity following exposure to PM may provide a basis for biotherapies of the future.